

R  
O

ADIOLOGY  
AND  
NCOLOGY



June 2008  
Vol. 42 No. 2  
Ljubljana

ISSN 1318-2099



# PRAVI TRENUTEK ZA NOV ZAČETEK

Odobrena indikacija za prehod  
med adjuvantnim zdravljenjem

**AROMASIN<sup>®</sup>**  
eksemestan

#### BISTVENE INFORMACIJE IZ POVZETKA GLAVNIH ZNAČILNOSTI ZDRAVILA

##### AROMASIN<sup>®</sup> 25 mg obložene tablete

**Sestava in oblika zdravila:** obložena tableta vsebuje 25 mg eksemestana. **Indikacije:** adjuvantno zdravljenje žensk po menopavzi, ki imajo invazivnega zgodnjega raka dojke s pozitivnimi estrogenskimi receptorji in so se uvodoma vsaj 2 leti zdravile s tamoksifenom. Zdravljenje napredovalega raka dojke pri ženskah z naravno ali umetno povzročeno menopavzo, pri katerih je bolezen napredovala po antiestrogenski terapiji. Učinkovitost še ni bila dokazana pri bolnicah, pri katerih tumorske celice nimajo estrogenskih receptorjev. **Odmerjanje in način uporabe:** 25 mg enkrat na dan, najbolje po jedi. Pri bolnicah z zgodnjim rakom dojke je treba zdravljenje nadaljevati do dopolnjenega petega leta adjuvantnega hormonskega zdravljenja oz. do recidiva tumorja. Pri bolnicah z napredovalim rakom dojke je treba zdravljenje nadaljevati, dokler ni razvidno napredovanje tumorja. **Kontraindikacije:** znana preobčutljivost na učinkovino zdravila ali na katero od pomožnih snovi, ženske pred menopavzo, nosečnice in doječe matere. **Posebna opozorila in previdnostni ukrepi:** predmenopavzni endokrini status, jetrna ali ledvična okvara, bolniki z redkimi prirojenimi motnjami, kot so fruktozna intoleranca, malabsorpcija glukoze-galaktoze ali insuficienca saharoze-izomaltaze. Lahko povzročijo alergijske reakcije ali zmanjšanje mineralne gostote kosti. Ženskam z osteoporozo ali tveganjem zanjo je treba izrecno izmeriti gostoto kosti s kostno densitometrijo, in sicer na začetku zdravljenja in nato redno med zdravljenjem. **Medsebojno delovanje z drugimi zdravili:** sočasna uporaba zdravil - npr. rifampicina, antiepileptikov (npr. fenitoina ali karbamazepina) ali zeliščnih pripravkov s šentjaževko - ki inducirajo CYP 3A4, lahko zmanjša učinkovitost Aromasina. Uporabljati ga je treba previdno z zdravili, ki se presnavljajo s pomočjo CYP 3A4 in ki imajo ozek terapevtski interval. Kliničnih izkušenj s sočasno uporabo zdravila Aromasin in drugih zdravil proti raku ni. Ne sme se jemati sočasno z zdravili, ki vsebujejo estrogen, saj bi ta izničila njegovo farmakološko delovanje. **Vpliv na sposobnost vožnje in upravljanja s stroji:** po uporabi zdravila je lahko psihofizična sposobnost za upravljanje s stroji ali vožnjo avtomobila zmanjšana. **Neželeni učinki:** neželeni učinki so bili v študijah ponavadi blagi do zmerni. **Zelo pogosti (> 10 %):** vročinski oblivi, bolečine v sklepih, utrujenost, slabost, nespečnost, glavobol, močnejše znojenje, blago zvišanje alkalne fosfataze. **Način in režim izdajanja:** zdravilo se izdaja le na recept, uporablja pa se po navodilu in pod posebnim nadzorom zdravnika specialista ali od njega pooblaščenega zdravnika. **Imetnik dovoljenja za promet:** Pfizer Luxembourg SARL, 283, route d'Arlon, L-8011 Strassen, Luksemburg. **Datum zadnje revizije besedila:** 9.12.2005

Pred predpisovanjem se seznanite s celotnim povzetkom glavnih značilnosti zdravila.

Podrobnejše informacije o zdravilu so na voljo pri:  
Pfizer, podružnica za svetovanje s področja farmacevtske dejavnosti, Ljubljana, Letališka cesta 3c, 1000 Ljubljana

**Pfizer**

ARO-03-06

# RADIOLOGY AND ONCOLOGY



Editorial office

**Radiology and Oncology**

Institute of Oncology

Zaloška 2

SI-1000 Ljubljana

Slovenia

Phone: +386 1 5879 369

Phone/Fax: +386 1 5879 434

E-mail: [gserša@onko-i.si](mailto:gserša@onko-i.si)

June 2008

Vol. 42 No. 2

Pages 51-113

ISSN 1318-2099

UDC 616-006

CODEN: RONCEM

Aims and scope

*Radiology and Oncology is a journal devoted to publication of original contributions in diagnostic and interventional radiology, computerized tomography, ultrasound, magnetic resonance, nuclear medicine, radiotherapy, clinical and experimental oncology, radiobiology, radiophysics and radiation protection.*

Editor-in-Chief

**Gregor Serša**

Ljubljana, Slovenia

Deputy Editors

**Andrej Čör**

Ljubljana, Slovenia

Executive Editor

**Viljem Kovač**

Ljubljana, Slovenia

**Igor Kocijančič**

Ljubljana, Slovenia

Editorial Board

**Karl H. Bohuslavizki**

Hamburg, Germany

**Maja Čemažar**

Ljubljana, Slovenia

**Christian Dittrich**

Vienna, Austria

**Metka Filipič**

Ljubljana, Slovenia

**Tullio Giraldi**

Trieste, Italy

**Maria Gódeény**

Budapest, Hungary

**Vassil Hadjidekov**

Sofia, Bulgaria

**Marko Hočevar**

Ljubljana, Slovenia

**Maksimilijan Kadivec**

Ljubljana, Slovenia

**Miklós Kásler**

Budapest, Hungary

**Michael Kirschfink**

Heidelberg, Germany

**Janko Kos**

Ljubljana, Slovenia

**Tamara Lah Turnšek**

Ljubljana, Slovenia

**Damijan Miklavčič**

Ljubljana, Slovenia

**Luka Milas**

Houston, USA

**Damir Miletic**

Rijeka, Croatia

**Maja Osmak**

Zagreb, Croatia

**Branko Palčič**

Vancouver, Canada

**Dušan Pavčnik**

Portland, USA

**Geoffrey J Pilkington**

Portsmouth, UK

**Ervin B. Podgoršak**

Montreal, Canada

**Uroš Smrdel**

Ljubljana, Slovenia

**Primož Strojjan**

Ljubljana, Slovenia

**Borut Štabuc**

Ljubljana, Slovenia

**Ranka Štern-Padovan**

Zagreb, Croatia

**Justin Teissié**

Toulouse, France

**Sándor Tóth**

Orosháza, Hungary

**Gillian M. Tozer**

Sheffield, UK

**Andrea Veronesi**

Aviano, Italy

**Branko Zakotnik**

Ljubljana, Slovenia

Advisory Committee

**Marija Auersperg** Ljubljana, Slovenia; **Tomaž Benulič** Ljubljana, Slovenia; **Jure Fettich** Ljubljana;

**Valentin Fidler** Ljubljana, Slovenia; **Berta Jereb** Ljubljana, Slovenia; **Vladimir Jevtič** Ljubljana, Slovenia;

**Stojan Plesničar** Ljubljana, Slovenia; **Živa Zupančič** Ljubljana, Slovenia

Publisher  
*Association of Radiology and Oncology*

Affiliated with  
*Slovenian Medical Association – Slovenian Association of Radiology, Nuclear Medicine Society,  
Slovenian Society for Radiotherapy and Oncology, and Slovenian Cancer Society  
Croatian Medical Association – Croatian Society of Radiology  
Societas Radiologorum Hungarorum  
Friuli-Venezia Giulia regional groups of S.I.R.M.  
(Italian Society of Medical Radiology)*

*Copyright © Radiology and Oncology. All rights reserved.*

Reader for English  
***Vida Kološa***

Key words  
***Eva Klemenčič***

Secretary  
***Mira Klemenčič***

Design  
***Monika Fink-Serša***

Printed by  
*Imprint d.o.o., Ljubljana, Slovenia*

*Published quarterly in 600 copies*

*Beneficiary name: DRUŠTVO RADIOLOGIJE IN ONKOLOGIJE  
Zaloška cesta 2,  
1000 Ljubljana  
Slovenia*

*Beneficiary bank account number: SI56 02010-0090006751  
IBAN: SI56020100090006751*

*Our bank name: Nova Ljubljanska banka, d.d.,  
Ljubljana, Trg republike 2,  
1520 Ljubljana; Slovenia*

*SWIFT: LJBAS12X*

*Subscription fee for institutions EUR 100, individuals EUR 50*

*The publication of this journal is subsidized by the Slovenian Research Agency.*

Indexed and abstracted by:  
*BIOMEDICINA SLOVENICA  
CHEMICAL ABSTRACTS  
EMBASE / Excerpta Medica  
Sci Base  
Scopus*

*This journal is printed on acid-free paper*

*Radiology and Oncology is available on the internet at: <http://www.onko-i.si/radioloncol> and <http://www.versita.com>*

ISSN 1581-3207



## CONTENTS

### RADIOLOGY

---

- MRI diagnosis of Baker cyst and significance of associated medial compartment knee osteoarthritis** 51  
*Vasilevska V, Szeimies U, Staebler A*
- The ovine jugular vein as a model for interventional radiology procedures** 59  
*Lu W, Park W K, Uchida B, Timmermans H A, Pavcnik D, Keller F S, Rösch J*
- Lateral ventricle epidermoid** 66  
*Franko A, Holjar-Erlič I, Miletić D*

### ONCOLOGY

---

- Cysteine cathepsins and stefins in head and neck cancer: an update of clinical studies** 69  
*Strojan P*
- Evaluation of shRNA-mediated gene silencing by electroporation in LPB fibrosarcoma cells** 82  
*Mesojednik S, Kamenšek U, Čemažar M*

<b>Optimization of electrode position and electric pulse amplitude in electrochemotherapy</b>	<b>93</b>
<i>Županič A, Čorović S and Miklavčič S</i>	
<b>Ecotoxicologically relevant cyclic peptides from cyanobacterial bloom (<i>Planktothrix rubescens</i>) – a threat to human and environmental health</b>	<b>102</b>
<i>Sedmak B, Eleršek T, Grach-Pogrebinsky O, Carmeli S, Sever N, T. Lah T</i>	
<b>SLOVENIAN ABSTRACTS</b>	<b>I</b>
<b>NOTICES</b>	<b>VII</b>

# MRI diagnosis of Baker cyst and significance of associated medial compartment knee osteoarthritis

Violeta Vasilevska<sup>1</sup>, Urlike Szeimies<sup>2</sup>, Axel Staebler<sup>2</sup>

<sup>1</sup>City Surgical Clinic "St.Naum Ohridski" Skopje, Republic of Macedonia;

<sup>2</sup>Radiology in Munchen Harlaching, Orthopaedic Clinic Harlaching, Munchen Germany

**Background.** The purpose was to evaluate the enlargement of the Baker cyst and the significance of medial compartment knee osteoarthritis.

**Patients and methods.** In a period of two years we evaluated 66 patients with MRI signs of the Baker cyst and medial compartment knee osteoarthritis (median age 56 years, age range 34-84 years, 23 males and 43 females). One group was with MRI signs of the large Baker cyst and the other one with the small Baker cyst. Following graded criteria for medial compartment were used: cartilage thickness, meniscus degeneration, bone marrow oedema, effusion. Lateral compartment was normal.

**Results.** In the group with the large Baker cyst, 26/31 cases (84%) had medial compartment cartilage loss. Eighteen from them had associated 3<sup>rd</sup> degree meniscal degeneration. Five/31 (16%) cases had only medial meniscus involvement. In the second group, 17/35 (48%) cases had cartilage loss, with 3<sup>rd</sup> degree meniscal degeneration was 14 (82%). In 18/35 (52%) cases only meniscus degeneration was present, 67% had 1<sup>st</sup> degree of meniscus degeneration. There was a statistically significant difference in the group with the distended Baker cyst between different degrees of medial meniscus degeneration.

**Conclusion.** The size of the Baker cyst, as a soft tissue tumour, is strongly correlated with degenerative changes of the cartilage and with the degree of meniscus degeneration on the medial compartment of the knee joint.

*Key words:* Baker cyst; medial compartment knee osteoarthritis; MRI

## Introduction

The popliteal (Baker) cyst is the most frequent encountered lesion around the knee. Cystic lesions around the knee may present as a painless palpable mass,<sup>1</sup> with pain or

to be detected during the routine MR imaging of the knee with suspected internal joint derangement.<sup>2</sup>

Multiple studies confirmed that the intraarticular derangement plays an important role in pathogenesis of the popliteal cyst. MR studies of the popliteal cyst demonstrated a connection to one or more intraarticular lesions in 87-98% of the cases, like osteoarthritis or inflammatory arthritis; often joint effusion, meniscus tear and degenerative disease of the joint are found.<sup>3</sup>

Received 15 February 2008

Accepted 29 February 2008

Correspondence to: Violeta Vasilevska, MD, Radiology Department, City Surgical Clinic "St.Naum Ohridski", Ul."11 Oktomvri" br.53, 1000 Skopje, Republic of Macedonia; Phone: +389 2 2773068; + 389 70 254 830; Fax: +389 2 3113986; E mail: v\_vasilevska@yahoo.com



**Figure 1a.** The large Baker's cyst in a 67-year-old man on a sagittal PDw fatsat image; complete cartilage lose on the femoral condyle and the tibial plateau of the medial compartment, with 3<sup>th</sup> degree of medial meniscus degeneration.



**Figure 1b.** The large Baker's cyst in a 67-year-old man on a coronal PDw fatsat image; complete cartilage lose on the femoral condyle and the tibial plateau of the medial compartment, with 3<sup>th</sup> degree of medial meniscus degeneration. Bone marrow edema and effusion is present.

The correlation between sizes of the Baker cyst in patients suffering from medial compartment osteoarthritis of the knee was recognized and evaluated. The purpose of our study of patients with MRI signs of the Baker cyst was to describe the significance of the associated medial compartment knee osteoarthritis: cartilage degeneration, different degree of medial meniscus degeneration, bone oedema and knee effusion.

### Patients and methods

In the period of two years (2005-2007) 66 cases were retrospectively evaluated with MR study of the knee and MR signs of the Baker cyst and medial compartment knee osteoarthritis. The median age was 56.42 years, with age range from 34-84 years, 23 males, 43 females.

We selected two groups according to the size of the Baker cyst on MRI. The first group was with palpable soft tissue mass on medial aspect of popliteal fossa large Baker

cyst and in the other group the Baker cyst was small and detected only on MRI.

Out of a total of 66 patients, the group with MRI signs of the large Baker cyst consisted of 31 (47%) cases, with a median age of 53.92 year, with an age range from 37 to 78 years. The group with the small Baker cyst encountered 35 (53%) patients with a mean age of 58.92 year, with the age range from 34 to 84 years.

MR images were obtained with a cp or 8-channel dedicated knee coil at 1.5 T (Magnetom Symphony; Siemens Medical Systems) with a standard protocol including PD-weighted frequency selective fat suppressed fast SE-sequences in coronal, sagittal and axial plane and T1-weighted coronal SE sequence with a slice thickness of 2.3 to 3.0 mm respectively.

On MRI the Baker cyst was presented as a circumscribed mass with low signal on T1-weighted image, intermedial signal intensity on proton density (PD) image and high signal intensity comparing with skeletal muscle on PD-weighted fatsat image. In

**Table 1.** Sex and age distribution of the large and small Baker cysts

	Number of cases	Sex	Age(age rengo)
		Male/Female	
Large Baker cyst	31	11/20	54(37-78)
Small Baker cyst	35	12/23	59(34-84)
Total	66	23/43	56(34-84)

both groups the size of the Baker cyst was assessed by measuring the distension of the cyst, and large cysts were distended more than 1 cm.

The following graded criteria for medial compartment osteoarthritis were used: cartilage thickness measured on the weight bearing zone, degeneration of the meniscus, bone marrow oedema, and knee effusion. On lateral compartment in both groups cartilage was also measured on weight bearing zone and meniscus was assed, they were normal.

We measured the thickness on residual cartilage in cases of subtotal loss, separately on femur and tibia. Degeneration of the meniscus was graded as following: 0-nor-

mal meniscus, 1- moderate degeneration with function, 2- severe degeneration with some residual tissue and 3-complete disintegration without functional meniscus. Additionally were assessed: bone marrow oedema (0-negative; 1-positive) and knee effusion (0-negative, 1-moderate, 2-intermediate and 3-severe). Lateral compartment had to be without meniscal lesion and with (measured) normal cartilage.

## Results

The large Baker cyst was found in 31 cases (47%) and 35 cases (53%) had small cysts (Table 1).



**Figure 2 a.** The large Baker's cyst in a 59-year-old woman; a coronal PDw fatsat image shows complete cartilage lose on the medial knee compartment with 3rd degree medial meniscus degeneration with degenerative disintegration, the lateral compartment is normal including the hyaline cartilage and the lateral meniscus.

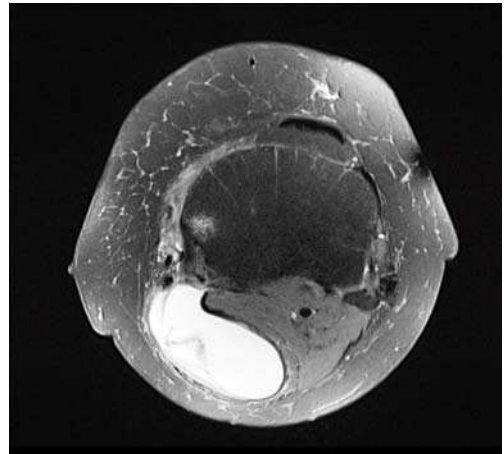


**Figure 2 b.** The large Baker's cyst in a 59-year-old woman; an axial PDw fatsat image demonstrates a the large Baker's cyst, with septum within the cyst.

**Table 2.** Internal derangement of the knee in the both groups, with the large and small Baker cyst

	Large Baker cyst – cartilage and meniscus degeneration	Large Baker cyst – meniscus degeneration	Small Baker cyst – cartilage and meniscus degeneration	Small Baker cyst – meniscus degeneration
Cartilage degeneration complete/subtotal	15 / 11	/	10 / 7	/
Meniscal degeneration 1 <sup>st</sup> degree	3	3 (60%)	1	12
Meniscal degeneration 2 <sup>nd</sup> degree	5	2 (40%)	2	6
Meniscal degeneration 3 <sup>th</sup> degree	18 (69.23%)	/	14 (82%)	/
Effusion 1 <sup>st</sup> degree	15	5	7	16
Effusion 2 <sup>nd</sup> degree	8	/	8	/
Effusion 3 <sup>th</sup> degree	3	/	2	/
Bone oedema absent	6	5	4	18
Bone oedema present	20 (64.51%)	/	13 (37%)	/
Total of each groups	26 (83.87%)	5 (16.12%)	17 (48.35%)	18 (51.65%)

In the group with the large Baker cyst, in 26/31 cases (83.9%), medial compartment cartilage loss was present complete (15 cases) or subtotal (11 cases) with different degree of medial meniscus degeneration (Figure 1). Eighteen cases (69.2%) had 3<sup>rd</sup> degree of medial meniscus degeneration. Of 31, five patients (16.1%) had degeneration of medial meniscus, without cartilage degeneration. From them 60% had 1<sup>st</sup> degree medial meniscus degeneration (Table 2, Figure 2).

In the group with small Baker cysts in 17/35 (48.4%) cases, medial compartment cartilage loss was present (complete-10 cases and subtotal-7cases), with different degree of medial meniscus degeneration (Figure 3). Out of these 14 (82%) were with 3<sup>rd</sup> degree of meniscus degeneration. In the group with the small Baker cyst, 51.42% (18 cases) had only degeneration of medial meniscus, from them 66.7% had 1<sup>st</sup> degree of meniscal degeneration (Table 2, Figure 4).

In the group with the large Baker cyst the Chi-square test showed statistically significant difference between different degree of medial meniscus degeneration and distension of the Baker cyst (Chi-square = 8.6; df = 2, p<0.01). Statistically, a significant difference was not present between different degree of medial meniscus degeneration in the group with the small Baker cyst (Chi-square=1.8; df = 2; p = 0.4)

There was no statistically significant difference between both groups for the presence of medial compartment cartilage loss with p<0.05 (Mann-Whitney U test).

Statistically, a significant difference was not present between both groups for the different degree of medial meniscus degeneration p>0.05 (Mann-Whitney U test).

In the group with large Baker cysts, 1<sup>st</sup> degree of knee effusion was present in 15/26 (57.7%) cases, and 2<sup>nd</sup> degree in 8/26 (30.8%) cases when there was a medial compartment cartilage loss and meniscal degeneration.

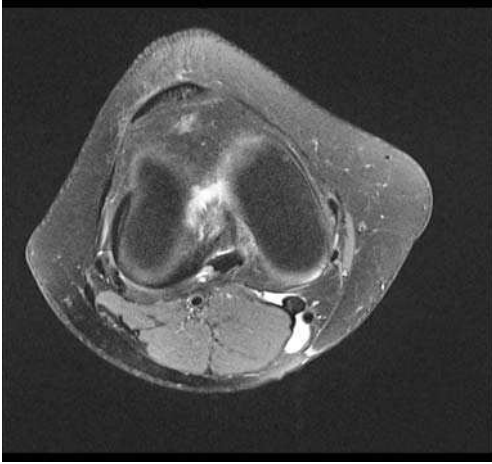


**Figure 3 a.** The small Baker's cyst in a 35-year-old women; an axial fatsat PDw images. The small Baker cyst is shown with its subgastrocnemius bursa and gastrocnemius-semimembranosus bursa connected by a tin neck.



**Figure 3 b.** The small Baker's cyst in a 35-year-old women; a coronal PD fatsat image of the same patient exhibits normal hyaline cartilage thickness without defects. Minor mucoid degeneration is shown of posterior horn of the medial meniscus at its base without tear.

Knee effusion in the cases with the small Baker cyst, associated with medial compartment cartilage loss and meniscal degeneration, 1<sup>st</sup> 7/17 (41.2%) and 2<sup>nd</sup> 8/17 (47.1%) degree was almost equal in frequency. Two cases had no effusion. Third degree effusion, the same like in the group with the large Baker cyst, was present in 11%.

In both groups all cases with isolated medial meniscus degeneration had first degree of effusion.

There was no statistically significant difference between both groups for the different degree of joint effusion  $p > 0.05$  (Mann-Whitney U test).

Bone oedema on medial compartment was present in 65% of the cases with the large Baker cyst and in the group with the small cyst in 37% of the cases. All cases with bone oedema were exhibited cartilage and meniscal degeneration in the medial compartment.

There was a statistically significant difference between both groups for the presence of bone oedema ( $p < 0.05$ ).

## Discussion

On MR imaging popliteal cysts are usually well defined, extending between the tendon of semimembranosus and the medial head of gastrocnemius into the gastrocnemius-semimembranosus bursa, situated superficial to the medial gastrocnemius muscle, along the medial side of the popliteal fosa.<sup>4,5</sup> As the cyst enlarges, the cystic fluid may extend in any direction. Inferomedial expansion is relatively common with a superficial location, which results in cysts becoming palpable.<sup>4,5</sup> In our series as palpable soft tissue masses on the medial aspect of the popliteal fossa was presented in all cases with the distended, large Baker cyst.

There is a statistically significant correlation between the Baker cyst and internal derangement of the joint without joint effusion. Internal derangement results from disturbed biomechanics with the increased pressure to shift normal joint fluid into the bursa.<sup>3</sup> The intraarticular pressure of the

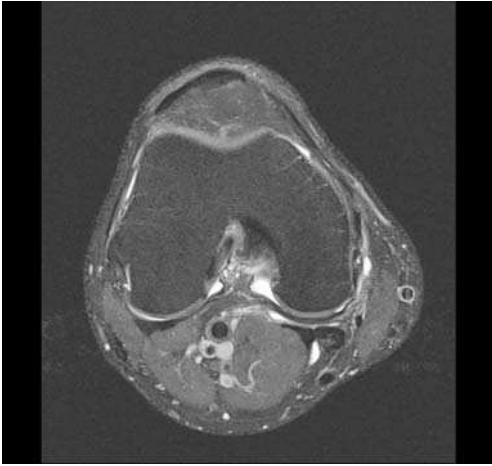


**Figure 4a.** The small Baker's cyst in a 55-years-old man; an axial PDw fatsat image presents small, not distended cyst, with small effusion.



**Figure 4b.** The small Baker's cyst in a 55-years-old man; on a sagittal PDw fatsat image intermediate cartilage lose corresponding to an instable horizontal tear of the posterior horn of the medial meniscus at the surface is seen. Otherwise the hyaline cartilage is preserved.

knee is increased with abnormal meniscus compared to healthy knees.<sup>3</sup> In our study joint effusion had no statistically significant influence on the distension of the Baker cyst in both groups.

Some studies report an incidence of Baker cysts on MR images done for the internal derangement of the knee of 5-58% with an increase in the prevalence with age, presence of arthritis, internal derangement and/or effusion.<sup>3,6</sup> Sansone *et al.* noted that Baker cysts were associated with one or more disorders detected by MRI in 94% of cases.<sup>7</sup>

The results confirmed a strong association between popliteal cysts and intra-articular pathology.<sup>7,8</sup>

Almost all popliteal cysts are secondary cysts and degenerative cartilage lesions are responsible in 30-60% of the cases.<sup>3,8</sup> Rupp *et al.* reported a connection of Baker cysts with intraarticular derangement in 100 patients. They found that the articular cartilage lesion was the most frequent accompanying lesion with popliteal cysts and suggested an influence in pathogenesis of the

popliteal cyst.<sup>9</sup> Sansone *et al.* reported that an isolated degenerative alteration of the cartilage was present in 43% of the cases, associated with Baker cyst.<sup>7,8</sup>

Although in other series there was a relationship between cartilage damage and Baker cysts,<sup>3</sup> Marti-Bonmati *et al.* reported that they have not observed any statistically significant relation with presence and degree of the cartilage lesions.<sup>10</sup> Cartilage lesion, inflammatory and degenerative arthropathy are pathologically associated with the Baker cyst.<sup>3,4,6,11</sup>

In the referred study of 30 patients with the popliteal cyst in 90% had lesion of the posterior horn of medial meniscus.<sup>8</sup> Meniscal lesions were also directly related to the presence and quantity of fluid inside the Baker cyst.<sup>10</sup> Although Baker cysts are more frequent with meniscus tear, their presence is also associated with menisci degeneration, especially of the posterior horn.<sup>3,10</sup>

Sansone *et al.* reported that the commonest lesions associated with the Baker

cyst were meniscal in 83%.<sup>7</sup> Later the same author reports that in a majority of cases with the Baker cyst the medial meniscus was usually involved (90%) and less frequently both menisci (17%).<sup>8</sup> The medial meniscus lesion was isolated in 33% of the cases.<sup>8</sup>

For fluid filled bursa have two etiological factors, knee joint effusion and persistence of one way valvular mechanism.<sup>12</sup> Vahlensieck *et al.* mention that there is a communication with the joint in half of all cases, according to the anatomy literature. Therefore, a joint effusion may increase the size of the gastrocnemius bursae.<sup>13</sup>

Marti-Bonmati L. *et al.* reported that the volume of the Baker cyst was statistically related with the presence of joint effusion in 70%.<sup>10</sup> The presence and volume of the cyst is directly related with the quantity of the joint effusion, and the presence and type of the meniscal lesion but not to the cartilage lesion.<sup>10</sup>

Bone oedema on medial compartment was present in 65% of the cases with the large Baker cyst but in the group with the small cyst in 37% of the cases. In our study bone oedema was present in 64% of the patients with the large Baker cyst and only when cartilage degeneration was present.

The popliteal cyst is almost never an isolated pathology in an adult knee.<sup>14</sup> The probability of popliteal cysts increase with the increasing number of associated knee conditions.<sup>3</sup> Of 77 MRI-observed cysts, a statistical correlation existed with effusion, meniscus tears or "degenerative" arthropathy, or combination of these 3 maladies.<sup>3</sup>

The combination of medial compartment cartilage degeneration and medial meniscus degeneration was associated with the large Baker cyst in 84%, but only 48% with the small Baker cyst. In the group with the large Baker cyst, isolated medial meniscus degeneration was present in 16%, comparing with the association of medial meniscus

degeneration in 52% from the cases with the small cyst.

In our study in the group with the large Baker cyst, there was a statistically significant difference between different degree of medial meniscus degeneration and distension of the Baker cyst. There was no statistically significant difference between both groups for the different degree of medial meniscus degeneration. The degree of medial meniscus degeneration has no influence on the distension of the Baker cyst generally but an influence was found, when there is cartilage degeneration.

There was no statistically significant difference between both groups for the different degree of joint effusion. In our study both groups, when there was a degeneration of cartilage and medial meniscus, equally were associated with moderate and intermediate joint effusion in 88% of cases.

Our results confirmed the strong association between popliteal cysts and the severity of the medial compartment osteoarthritis, emphasizing the importance of cartilage degeneration for the distension of Baker cysts.

## Conclusions

The baker cyst, as a soft tissue tumour in a popliteal fosa, is not a single joint lesion but it is associated with cartilage and meniscus degeneration on the medial compartment of the knee joint. Its size is strongly correlated with degenerative changes of the cartilage on the medial compartment and medial meniscus degeneration. In our study the distension of the cyst was not connected with a joint effusion.

## References

1. Kornaat PR, Bloem JL, Ceulemans RY, Riyazi N, Rosendaal FR, Nelissen RG, et al. Osteoarthritis of the knee: association between clinical features and MR imaging findings. *Radiology* 2006; **239**: 811-7.
2. Mc Carthy CL, Mc Nally EG. The MRI appearance of cystic lesions around the knee. *Skeletal Radiol* 2004; **33**: 187-209.
3. Miller TT, Staron RB, Koenigsberg T, Levin TL, Feldman F. MR imaging of Baker cysts: association with internal derangement, effusion and degenerative arthropathy. *Radiology* 1996; **201**: 247-450.
4. Torreggiani WC, Al-Ismail K, Munk PL, Roche C, Keogh C, Nicolaou S, et al. The imaging spectrum of Baker's (popliteal) cysts. *Clin Radiol* 2002; **57**: 681-91.
5. Steiner E, Steinbach LS, Schnarkowski P, Tirman PFJ, Ganant HK. Ganglia and cysts around joints. *Radiol Clin North Am* 1996; **34**: 400-10.
6. Ward EE, Jacobson JA, Fessel DP, Hayes CW, Van Holsbeeck M. Sonographic detection of Baker's cysts: comparison with MR imaging. *AJR Am J Roentgenol* 2001; **176**: 373-80.
7. Sansone V, de Ponti GM, del Maschio A. Popliteal cyst and associated disorder of the knee: critical review with MR imaging. *Int Orthop* 1995; **19**: 275-9.
8. Sansone V, De Ponti A. Arthroscopic treatment of popliteal cyst and associated intra-articular knee disorders in adults. *Arthroscopy* 1999; **15**: 368-72.
9. Rupp S, Seil R, Jochum P, Kohn D. Popliteal cyst in adults. Prevalence, associated intra-articular lesions and results after arthroscopic treatment. *Am J Sport Med* 2002; **30**: 112-5.
10. Marti-Bonmati L, Molla E, Dosda R, Casillas C, Ferrer P. MR imaging of Baker cyst-prevalence and relation to internal derangement of the knee. *MAGMA* 2000; **10**: 205-10.
11. Handy JR. Popliteal cysts in adults: a review. *Semin Arthritis Rheum* 2001; **31**: 108-18.
12. Takahashi M, Nagano A. Arthroscopic treatment of popliteal cyst and visualization of its cavity through the posterior portal of the knee. *Arthroscopy* 2005; **21**: 638.
13. Vahlensieck M, Linneborn G, Schild HH, Schmidt HM. Magnetic resonance imaging(MRI) of the bursa around the knee joint[in German]. *Rofo Fortschr Geb Rontgenstr Neuen Bildgeb Verfahr* 2001; **173**: 195-9.
14. Fritschy D, Fasel J, Umberto JC, Bianchi S, Verdonk R, Wirth CJ. The popliteal cyst. *Knee Surg Sport Traumatol Arthrosc* 2006; **14**: 623-8.

# The ovine jugular vein as a model for interventional radiology procedures

Wei Lu<sup>1,2</sup>, Won Kyu Park<sup>1,3</sup>, Barry Uchida<sup>1</sup>, Hans A. Timmermans<sup>1</sup>,  
Dusan Pavcnik<sup>1</sup>, Frederick S. Keller<sup>1</sup>, Josef Rösch<sup>1</sup>

<sup>1</sup>Dotter Interventional Institute, Oregon Health Sciences University, 3181 SW Sam Jackson Park Road, L-342, Portland, OR 97239-3098, <sup>2</sup>Department of Interventional Radiology, Nanfang Hospital, Southern Medical University, Guangzhou, Guangdong 510515, China, <sup>3</sup>Department of Radiology, College of Medicine, Yeungnam University, 317-1 Daemyung-dong, Nam-gu, Daegu, 705-717, Korea

**Background.** Detailed knowledge of the ovine jugular vein anatomy and physiology is a prerequisite for proper use of sheep as teaching or an experimental model in interventional radiology.

**Material and methods.** Ascending and descending jugular venograms in tilted position were done in 25 sheep to evaluate the jugular vein (JV) size and anatomy of its valves.

**Results.** The average maximal diameter of 50 JVs was  $13.34 \pm 1.18$  mm. Each vein contained an average of  $4.36 \pm 0.98$  valves. All valves were competent and 96.3% were bicuspid.

**Conclusions.** Because of similarities between ovine JV and human femoral vein in regards to diameters, number and type of valves and function of their valves with increased central and hydrostatic pressure, the ovine JV is a good model for evaluation of creation of JV valve incompetence, percutaneous valve transplantation and evaluation of prosthetic valve devices.

*Key words:* jugular vein; experimental model, ovine; interventional radiology

## Introduction

Percutaneous techniques have emerged as minimally invasive options in the treatment of chronic venous insufficiency. For replacement of diseased or absent venous valves,

several artificial percutaneously implanted valves have been developed over the last 10 years.<sup>1-5</sup> The ovine jugular vein (JV) has been often used for testing of the new valve devices because of its similar size to human femoral vein.<sup>3,5-10</sup> However, to our knowledge, there has not been a detailed study on the ovine JV angiographic anatomy, particularly regarding the number, distribution and type of its valves. The purpose of this study is to describe the angiographic anatomy of the ovine JV and its valves as a suitable model for interventional radiology procedures.

Received 29 February 2008

Accepted 12 March 2008

Correspondence to: Dusan Pavcnik, M.D., Ph.D., Dotter Interventional Institute, Oregon Health Sciences University, 3181 SW Sam Jackson Park Road, L-342, Portland, OR 97239-3098, U.S.A.; Phone: +1 503 494 3669; Fax: +1 503 494 4258; Email: pavcnikd@ohsu.edu

## Materials and methods

The study involved 25 adult female sheep weighing 53-74 kg (mean 64 kg) and was a part of the following studies: testing a new bioprosthetic valve testing (7 sheep), attempts of creation of primary venous insufficiency (8 sheep) and testing new IVC filters (10 sheep). The Institutional Animal Care and Use Committee of Oregon Health & Science University approved the protocols of these studies.

Animals fasted overnight with water available and were tranquilized intravenously with 7.5-10 mg (0.05 mg/lb) of Diazepam (Midazolam; Ben Venue Labs, Bedford, OH) and 400-800 mg (2.0 mg/lb) of Ketamine (Ketaset; Ft. Dodge Animal Health, Ft. Dodge, IA). Animals were then intubated. Inhalation anesthesia was maintained with 2-2.5% Isoflurane (IsoFlo; Abbott Laboratories, Chicago, IL) and 2 L/min of oxygen. To reduce salivation, 5 mg Atropine sulfate (American Regent Laboratories, Shirley, NY) was administered intravenously. Antibiotics (10 mg/kg cefazolin) were given intramuscularly as single dose at the beginning of procedures. Respiratory rhythm and carbon dioxide saturation were monitored during procedure. A GE/OEC 9800 cardiac mobile system with digital imaging (GE Medical Systems/OEC, Salt Lake City, UT) was used for imaging.

Both JVs were percutaneously entered just below the jaw and 7 cm long 6.0 FR Check-Flo vascular sheaths (Cook Medical, Bloomington, IN) were introduced and used to obtain venograms. A graduate measuring 0.035-inch wire guide (Cook Medical) was introduced into each sheath for calibration during venography. The right femoral vein was percutaneously entered and a 110 cm long 5FH1 Torcon Advantage catheter (Cook Medical) was introduced and advanced into the JV below its most central valve for descending venograms. Both ascending and

descending venograms were performed with the sheep in approximately 30 degrees tilted position (head down) using hand injections of 10-20 ml of contrast medium. Filming of each vein was performed in two projections and was prolonged to visualize the residual contrast in the valvular cusps. Simultaneous venograms of both JVs were also performed in antero-posterior projection for visualization their anatomical relation. In 10 animals evaluated for IVC filters placement, the descending venograms of each JV valve were performed after the H1 catheter was passed through the competent central valves.

After venographic study of the JV anatomy, the animals underwent further testing according to the protocols. Four animals were terminated immediately after these studies and specimens of their JVs were obtained for comparison with their venograms. The other 21 animals were used for long-term evaluation.

The diameters of JVs were measured on the venograms and the number of venous valves, the type of valves (number of their cusps), and their distribution were carefully studied. The JVs were divided into thirds, the peripheral (distal), the middle and the central (proximal) segments.

## Results

On the tilted ascending venograms, the JVs were well filled, distended and circular in shape. Their filling extended peripherally above the access site to the most peripheral competent valve. Some venous tributaries were also filled to their first venous valve. The JV diameters ranged from 9.8 mm to 15.2 mm with an average of  $13.34 \pm 1.18$  mm. The JV diameters in the peripheral segment ranged from 12.5 mm to 15.2 mm with an average of  $14.28 \pm 1.06$  mm. In the middle segment vein diameters ranged

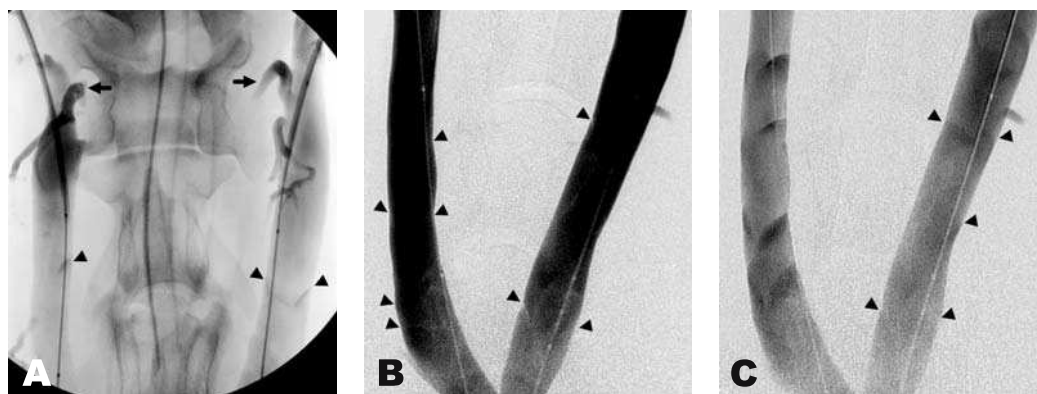
**Table 1.** Jugular vein diameters, valve distribution and frequency

Segments	Diameter (mm)	Valve Distribution	Valve Frequency
Peripheral	14.28±1.06	58 (26.6%)	92%
Middle	12.68±1.14	41 (18.8%)	76%
Central	12.92±1.03	119 (54.6%)	100%

from 10.6 mm to 13.7 mm with an average of 12.68±1.14 mm. The JV diameters in the central third ranged from 9.8 mm to 13.2 mm with an average of 12.92±1.03 mm (Table 1). The distended venograms often displayed the venous valves as faint linear defects inside sinuses, extending from the wall into lumen (Figure 1b). In the later phase of venograms valves were better visualized as their cusps contained some residual of contrast material and it was possible to define the number of cusps as well (Figures 1a, 1c). Altogether 218 valves were found in 50 JVs, with a range from 3-7 (4.36±0.98) valves in each JV. Most valves (210) were bicuspid (96.3%). Five valves had one cusp (monocusp - 2.3%) and three had three cusps (tricuspid - 1.4%). The major-

ity of valves 119 (54.6%) were distributed in the central venous segment that always contained at least two valves. In the middle segment, there were 41 (18.8%) valves with 3 JVs containing two valves. Twelve middle segments were without valves. In the peripheral segment, there were 58 (26.6%) valves. Four JVs peripheral segments were without valves.

The descending venograms displayed the valves and their types, whether they had one, two or three cusps well (Figure 2). The valves were competent and the hand injections filled the venous branches central to the valve. The axillary veins were always filled during injection below the central positioned valves. A perforating vein between the jugular and vertebral vein was filled

**Figure 1 a-c.** Ascending venograms of the jugular veins done in a titled position.

(a) Late phase venogram of the peripheral segment of the jugular vein demonstrates a monocusp valve on the right side (arrowhead) and bicuspid valve on the left side (arrowheads). There is filling of jugular vein tributaries and perforators vein (arrows).

(b) Early phase subtraction venograms of the middle and central segments of the jugular veins demonstrate valves as linear defects inside the vessel filled venous sinuses.

(c) Late phase subtraction venogram of the middle and central segments of the jugular veins demonstrates valves as residual filling in the valve cusps. Five bicuspid valves are seen on the right side and three on the left side (arrowheads).

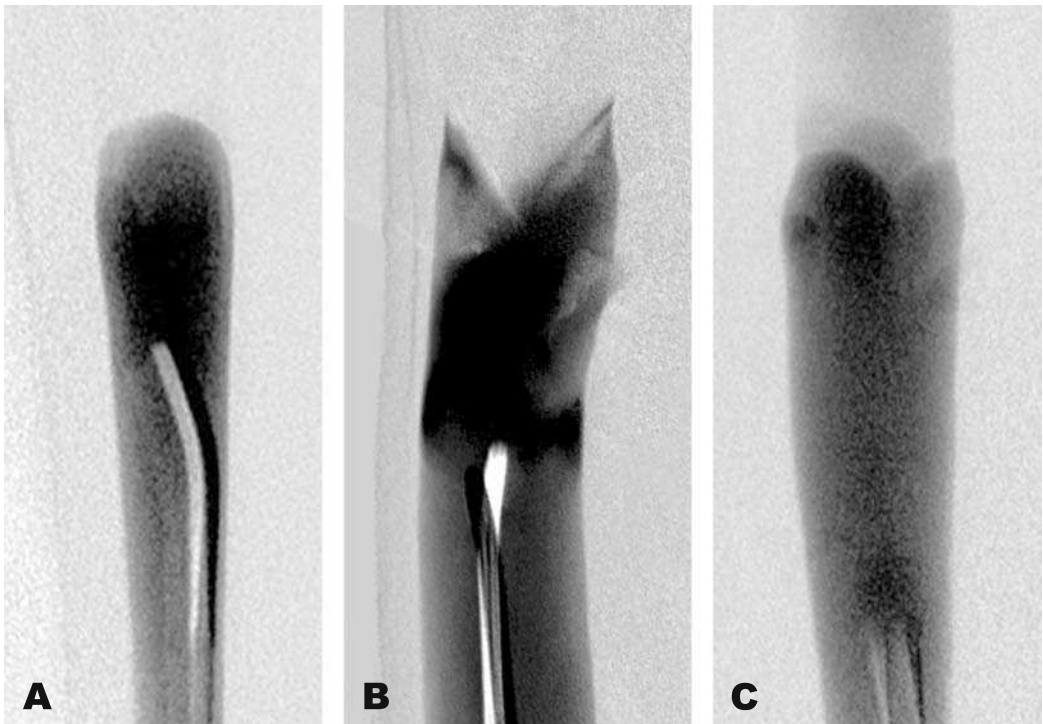


**Figure 2 a-c.** Descending venograms done in tilted position with injections central to valves demonstrate three types of valves. (a) Monocusp valve (b) Bicusps Valve (c) Tricusps valve.

when injection occurred below the most peripheral valve.

The specimens of 8 JVs removed at the autopsies in four animals showed the same number, distribution and type of valves. All were bicuspid as seen on their venograms (Figure 3).

### Discussion

Detailed knowledge of the ovine jugular vein anatomy and physiology is a prerequisite for proper use of sheep as teaching or an experimental model in interventional radiology. The ovine JV, also called the external JV, is the largest vein in the neck and drains most blood from the head and neck. The internal JV in sheep is small and often absent.<sup>11</sup> The JV originates near

the ventral border of the parotid gland at the angle of the mandible by the union of the external and internal maxillary veins. Traversing in the neck in the muscle groove, the JV accepts small tributary veins from thyroid, trachea, esophagus and muscles. Two axillary veins join the JV in its central segment at its entrance into the thorax.<sup>11</sup> The right and left JVs then unite to form the superior vena cava. The JVs are thin-walled vessels and at surgery were found to have a mean diameter of approximately 9 mm.<sup>8</sup> During ascending venography in tilted position, the JVs distend and their mean diameter was  $13.34 \pm 1.18$  in the presented series. The measurement of the maximal JV diameter during distention is important for selection of proper size of the valvular devices that we were testing. To prevent migration,



**Figure 3.** Longitudinally cut open specimen of both jugular veins 26 cm in length shows 5 bicuspid valves (arrow heads) on the right and four bicuspid valves on the left side (arrowheads).



**Figure 4.** A pentacusps valve. Venoscopy shows five well functioning cusps.

the device should have a diameter about 15 to 20% larger than the vein diameter.<sup>3</sup>

The valves in veins are located peripherally to the entrance of large venous tributaries or junction of two veins of equal diameter.<sup>12</sup> The valves close during increased central or hydrostatic pressure and prevent blood reflux and venous hypertension peripherally. Ascending venography demonstrated that the ovine JV contains one valve constant at its origin and two constant valves in its central segment at the entrance of two axillary veins. The number of valves in the middle segment was variable and ranged from zero to two. Venographic documentation of the presence and number of valves in the JV that compared well with the specimen studies is more accurate than their surgical identification. With valve identification by white semi-lunar lines formed by the attachment of the valve cusp to the vein wall, Jessup and Lane found only one to three valves in the jugular vein and in 3 of 32 veins (9.4%) found no valves.<sup>8</sup> The JV valves are mostly bicuspid, 96.3% in our series. JV valves are rarely monocuspid or tricuspid type. We found 2.3% and 1.4%, respectively in our se-

ries. However, valves with more than three cusps can also occur. In our previous experience with venoscopy of JV specimens, we found a (quintacusp) valve containing 5 well functioning cusps (Figure 4). In our series all JV valves evaluated by venography exhibited good function. All were competent and no venous reflux was seen during descending venography in tilted position. We consider venographic evaluation of valve competency more physiologic and accurate than the milking technique used by surgeons during open surgery. Using this technique, Jessup and Lane found that 18 of 32 JVs (56.3%) in normal sheep had partially or completely incompetent valves.<sup>8</sup>

The ovine JV is a good model for evaluation of new percutaneously placed venous devices because of its similarities with the human femoral vein (FV).<sup>3</sup> These similarities include their diameters, number, and type of valves and function of their valves with increased central and hydrostatic pressures. The diameter of the ovine JV is around 13.34 mm in the tilted position and compares well with the diameter of the normal standing human FV of  $10.0 \pm 0.21$  mm.<sup>13</sup> The number and distribution of valves are also similar. The ovine JV contains a mean of 4.6 valves in a vein length of about 25 cm to 30 cm. The human FV contains an average of 5 valves from the knee to the inguinal ligament including the constant valves at its central and peripheral end.<sup>14</sup> Most of the valves in the ovine JV and the human FV are of bicuspid type and function similarly. They are open during relaxation and with muscle contraction. An increased central venous pressure causes the competent valves to close and prevent venous reflux and peripheral venous hypertension. In humans, the competent FV valves close with increase hydrostatic pressure in the

upright position, and episodically pressure increases during deep breathing, straining and coughing. The function of JV valves in quadrupeds is to maintain the direction of the blood flow toward the heart and to protect the capillary beds of the head from the high venous pressure pulses caused by chest compressions and during eating and drinking with their heads down.<sup>15</sup>

Venographic studies are essential for both the evaluation of JV anatomy prior to prosthetic valve device placement and for following-up their function. Ascending venograms in the tilted position gives information about the JV size and position of their valves, particularly the central valve. As mentioned above, a prosthetic valve should be 15 to 20% larger than the JV diameter. The experimental prosthetic valves have been always placed across the central valve to replace its function.<sup>3,7,9</sup> Because placement of one prosthetic valve will probably not solve chronic venous insufficiency, placement of two or more prosthetic valves will need to be evaluated in the ovine JV. Therefore, determination of position of other JV valves will be necessary. Descending venography can be done as a part of the preplacement evaluation, particularly if there is a question regarding the type and competency of the central valve. For follow-up studies, however, descending venography is the main procedure to evaluate valve competency.<sup>16,17</sup> Ascending venography must also be done at that time to visualize the entire JV and evaluate any changes related to the prosthetic valve placement.

### Acknowledgements

The authors thank Sheri Imai-Swiggart for her contribution.

## References

1. Gomez-Jorge J, Venbrux AC, Magee C. Percutaneous deployment of a valved bovine jugular vein in the swine venous system: a potential treatment for venous insufficiency. *J Vasc Interv Radiol* 2000; **11**: 931-6.
2. Dalsing MC, Sawchuk AP, Lalka SG, Crikrit DF. An early experience with endovascular venous valve transplantation. *J Vasc Surg* 1996; **24**: 903-5.
3. Pavcnik D, Uchida B, Timmermans HA, Corless CL, O'Hara M, Toyota N, et al. Percutaneous bioprosthetic venous valve: a long-term study in sheep. *J Vasc Surg* 2002; **35**: 598-602.
4. de Borst GJ, Teijink JA, Patterson M, Quijano TC, Moll FL. A percutaneous approach to deep venous valve insufficiency with a new self-expanding venous frame valve. *J Endovasc Ther* 2003; **10**: 341-9.
5. Teebken OE, Puschmann C, Apert T, Haverich A, Mertsching H. Tissue-engineered bioprosthetic venous valve: a long-term study in sheep. *Eur J Vasc Endovasc Surg* 2003; **25**: 305-12.
6. Pavcnik D, Uchida B, Timmermans HA, Keller FS, Rösch J. Square stent: a new self-expandable endoluminal device and its applications. *Cardiovasc Intervent Radiol* 2001; **24**: 207-17.
7. Pavcnik D, Kaufman J, Uchida B, Correa L, Hiraki T, Kyu SC, et al. Second-generation percutaneous bioprosthetic valve: a short-term study in sheep. *J Vasc Surg* 2004; **40**: 1223-7.
8. Jessup G, Lane RJ. Repair of incompetent venous valves: a new technique. *J Vasc Surg* 1988; **8**: 569-75.
9. Pavcnik D, Kaufman JA, Uchida BT, Case B, Correa LO, Goktay AY, et al. Significance of spatial orientation of percutaneously placed bioprosthetic venous valves in an ovine model. *J Vasc Interv Radiol* 2005; **16**: 1511-6.
10. Brountzos E, Pavcnik D, Uchida B, Corless C, Uchida BT, Nihsen ES, et al. Remodeling of suspended small intestinal submucosa venous valve: an experimental study in sheep to assess the host cells' origin. *J Vasc Interv Radiol* 2003; **14**: 349-56.
11. May N. *The Anatomy of the Sheep*. 3rd ed. Queensland, Australia: University of Queensland, Press; 1970. p. 133-4.
12. Gottlob R, May R. *Venous valves*. New York: Springer-Verlag Wien; 1986. p. 15-6.
13. van Bemmelen, PS: Evaluation of the patient with chronic venous insufficiency: old and emerging technologies. In *Vascular Diseases. Surgical and Interventional Therapy*, Churchill Livingstone Inc., New York 1994, 941-949.
14. Strandness DE: Applied Physiology of the Venous System. In *Vascular Diseases. Surgical and Interventional Therapy*, Churchill Livingstone Inc., New York 1994, 103-117.
15. Voorhees WD 3rd, Ralston SH, Babbs CF. Regional blood flow during cardiopulmonary resuscitation with abdominal counter pulsation in dogs. *Am J Emerg Med* 1984; **2**: 123-8.
16. Pavcnik D, Yin Q, Uchida B, Park WK, Kim MD, Hoppe H, et al: Percutaneous autologous venous valve transplantation: feasibility study in and ovine model. *J Vasc Surg* 2007; **46**: 338-45.
17. Pavcnik D, Uchida B, Kaufman JA, Hinds M, Keller FS, Rösch J. Percutaneous management of chronic deep venous reflux: review of experimental work and early clinical experience with bioprosthetic valve. *J Vasc Med* 2008; **13**: 75-84.

case report

## Lateral ventricle epidermoid

Artur Franko, Izidora Holjar-Erlić, Damir Miletić

Department of Radiology, Clinical Hospital Rijeka, Croatia

**Background.** Epidermoids occurring within the lateral ventricles are rare. They are slow growing benign tumours, usually presented with non-specific signs of deterioration of mental functions.

**Case report.** Authors present a case of 49-year-old woman with epidermoid located in the frontal part of lateral ventricle. She underwent magnetic resonance imaging before the surgical treatment and the final pathohistological diagnosis.

**Conclusions.** Suprasellar and intraventricular epidermoids are rare, but must be included in differential diagnoses as well as meningiomas, ependimomas, subependimomas and papillomas of the choroid plexus.

*Key words:* epidermoid; intraventricular; arteriovenous malformation (AVM)

### Introduction

Epidermoid tumours represent 0.2% to 1% of all primary intracranial tumours.<sup>1</sup>

Intracranial epidermoid tumours are histologically benign, slow-growing, congenital neoplasms of the central nervous system.<sup>2</sup> They usually present in adults and are commonest in the cerebellopontine angle or suprasellar region protruding in the subarachnoid space.<sup>3</sup> Epidermoids occurring within the lateral ventricles are very rare. They are slow growing, and the clinical presentation is non-specific like deterioration of mental functions.<sup>4</sup>

To our knowledge, there were only 7 reports of epidermoids located in lateral ventricles.<sup>2,4-6</sup> We report a case of bulky lateral

ventricle epidermoid with mass effect on adjacent structures.

### Case report

A 49-year-old woman was admitted to the Clinic of Neurology due to progressive mnemonic deterioration, mild headache and right limbs paresthesia. The neurologist found discrete right limb paresis, disorientation and psychomotor deceleration. The score of mini-mental test was low (17/30) and after testing the psychologist concluded that her dysfunctions had an organic cause. The neurologist suspected on the brain tumour but also on the progressive demyelinating disorder and sent the patient directly to the magnetic resonance imaging (MRI) of the brain without previous computed tomography (CT).

Within the frontal part of the left lateral ventricle on T1-weighted images a large formation with heterogeneous signal and

Received 7 January 2008

Accepted 21 January 2008

Correspondence to: Izidora Holjar-Erlić, MD, Department of Radiology, Clinical Hospital Rijeka, Krešimirova 42, 51000 Rijeka, Croatia; Phone/Fax: +385 51 651 386; E-mail: izidora.holjar@ri.htnet.hr



**Figure 1.** Axial T1-weighted MRI scan reveals a large, bulky mass within the left lateral ventricle containing high-signal areas and low-signal foci.

significant hyperintense areas was obtained (Figure 1). After the contrast administration MRI showed a loose heterogeneous enhancement and sharp, well defined margins. This lesion had a spatiocompressive effect on surrounding structures, especially on foramen of Monro resulting with unilateral obstructive hydrocephalus (Figure 2).

The patient was restless during the MRI examination and T2-weighted sequences were undiagnostic. On FLAIR-weighted scans the MRI signal of the lesion was very similar to T1-weighted images. High signal areas were interpreted as subacute haemorrhage or fat inclusions (Figure 3).

The expansive neoplastic formation was interpreted as benign and the differential diagnosis was focused on central intraventricular meningioma, central neurocytoma, and subependymal giant cell astrocytoma.

The patient was transported to neurosurgery and underwent frontal craniotomy with a complete removal of brain tumour. Pathohistology confirmed the benign intraventricular tumour – epidermoid.

The control MRI was performed six months after the surgery revealing no recurrence.



**Figure 2.** Postgadolinium coronal section shows very discrete heterogeneous enhancement and huge mass-effect on adjacent structures including septum pellucidum and foramen of Monro.

## Discussion

Tumours are only rarely found in the lateral ventricles.<sup>7</sup> Although they are relatively easy to visualize, it is more difficult to narrow the differential diagnosis for a lesion in this location without knowledge of the tissue types that give rise to these tumours.<sup>8</sup> Epidermoid tumours are the most common fourth ventricular low density lesions and represent 5-10% of all intracranial epidermoids.<sup>9</sup> The location in the lateral ventricle, especially in the frontal horn, is very rare and that was the reason why authors initially did not think on it as a differential diagnosis.

The MRI usually demonstrated an irregularly but sharply demarcated mass with inhomogeneous density, variable enhancement with gadolinium, lack of invasion to adjacent normal structures, and extensive protrusion into cisternal and other cerebrospinal fluid with high-signal intensity on proton-weighted images.<sup>10</sup> In our case the lesion was inhomogeneous before and after the contrast administration with foci of

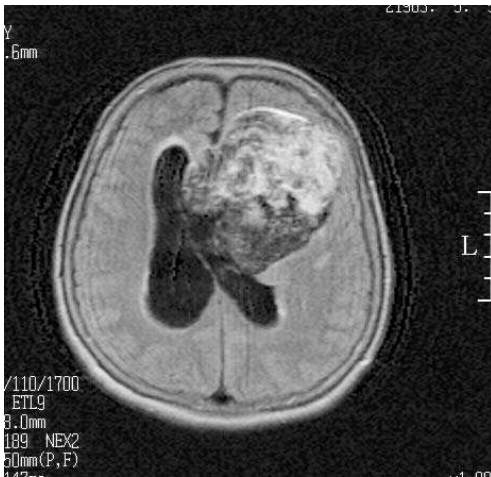


**Figure 3.** Despite significant movement artifacts FLAIR-weighted MRI shows hiperintense areas mostly corresponding to the same areas on T1-weighted image.

contrast enhancement. The patients would benefit if MRI spectroscopy would be done, but this was impossible due to patient's restlessness.

In histopathological specimens bone metaplasia and abundant lipoid detritus were found explaining signal heterogeneity. High-signal inclusions corresponded to fat. Because of the lack of mobile hydrogen, deposits of calcium appear on MR images as foci of diminished signal intensity within the tissue harbouring them. In our case CT was not performed and calcifications were missed.

Despite all imaging techniques the histopathological diagnosis was indispensable.

## References

1. Sener RN, Mechl M, Prokes B, Valek VA. Epidermoid tumor of the pons. *J Neuroradiol* 2004; **31**: 225-6.
2. Akar Z, Tanriover N, Tuzgen S, Kafadar AM, Kuday C. Surgical treatment of intracranial epidermoid tumors. *Neurol Med Chir* 2003; **43**: 275-81.
3. Sutton D, Stevens J, Miszkiel K. Intracranial lesions (1). In: Sutton D. *Textbook of Radiology and Imaging*. Edinburg: Churchill-Livingstone; 2003. p. 1763.
4. Bhatoe HS, Mukherji JD, Dutta V. Epidermoid tumour of the lateral ventricle. *Acta Neurochir* 2006; **148**: 339-42.
5. Koot RW, Jagtap AP, Akkerman EM, Den Heeten GJ, Majoie CB. Epidermoid of the lateral ventricle: evaluation with diffusion-weighted and diffusion tensor imaging. *Clin Neurol Neurosurg* 2003; **105**: 207-3.
6. Menq L, Yuqanq L, Shuqan Z, Xinqanq L, Chenqyuan W. Intraventricular epidermoids. *J Clin Neurosci* 2006; **13**: 428-30.
7. Delfini R, Acqui M, Oppoido PA, Capone R, Santoro A, Ferrante L. Tumors of the lateral ventricles. *Neurosurg Rev* 1991; **14**: 127-33.
8. Koeller KK, Sandberg GD. From the Archives of the AFIP: Cerebral intraventricular neoplasms: radiologic-pathologic correlation. *Radiographics* 2002; **22**: 1473-505.
9. Imamura Y, Ninchaji T, Nakajima S, Uemura K. Epidermoid tumor in the fourth ventricle with particular reference to metrizamide CT cisternography findings. *Surg Neurol* 1982; **18**: 444-7.
10. Panagopoulos KP, el-Azouzi M, Chisholm HL, Jolesz FA, Black PM. Intracranial epidermoid tumors. A continuing diagnostic challenge. *Arch Neurol* 1990; **47**: 813-6.

# Cysteine cathepsins and stefins in head and neck cancer: an update of clinical studies

Primož Strojjan

Department of Radiation Oncology, Institute of Oncology, Ljubljana, Slovenia

**Background.** Cancer of the head and neck represents a diverse group of malignant diseases; so far, no factor in a wide spectrum of biochemical and histological candidate-markers has yet been identified to predict reliably the natural course of the disease or its response to the therapy to be used in routine clinical practice. Among the factors that promote tumor growth and invasion, several protease systems, implemented in proteolytic degradation of extracellular matrix components, were studied, including papain-like lysosomal cysteine proteases (e.g. cathepsins B and L) and their physiological inhibitors cystatins (e.g. stefins A and B, cystatin C). The aim of the present report is to review the published studies on clinical applicability of cysteine cathepsins and their endogenous inhibitors stefins in squamous cell carcinoma of the head and neck and to present recent research results from this area conducted jointly by the Institute of Oncology Ljubljana and ENT Department of the University Medical Center Ljubljana, Slovenia.

**Conclusions.** According to our experience, immunohistochemical staining of cysteine cathepsins and stefins seems to be of limited value for predicting either treatment response or patients' survival. However, the results of studies on stefin A in tumor tissue cytosols should be considered hypothesis-generating and deserves further evaluation in the frame of prospective controlled multicentric clinical study.

*Key words:* head and neck cancer; cathepsins; stefins; prognosis

## Introduction

Cancer of the head and neck represents a diverse group of malignant diseases arising from mucosa of the upper aerodigestive

tract, major salivary glands and nodes from the neck. The majority of tumors is of squamous cell origin and alcohol and tobacco abuse are the two most important etiological factors. Surgery and radiotherapy are standard treatment options with systemic therapy being added to irradiation of the patients with increased risk for disease recurrence.<sup>1</sup>

To distinguish biologically more aggressive and less aggressive head and neck carcinomas within each traditional risk-category, numerous new prognostic factors were evaluated on genetic, mRNA or protein levels. Among the factors that promote tumor growth and invasion, several protease

Received 16 May 2008

Accepted 23 May 2008

Correspondence to: Assoc. Prof. Primož Strojjan, M.D., Ph.D., Department of Radiation Oncology, Institute of Oncology, Zaloška 2, SI-1000 Ljubljana, Slovenia; Phone: +386 1 5879 110; Fax: + 386 1 5879 400; E-mail: pstrojjan@onko-i.si

The research was supported by the Slovenian Research Agency Grant P3-0307. The article was presented at the 5<sup>th</sup> Conference on Experimental and Translational Oncology, Kranjska gora, Slovenia, March 26-30, 2008.

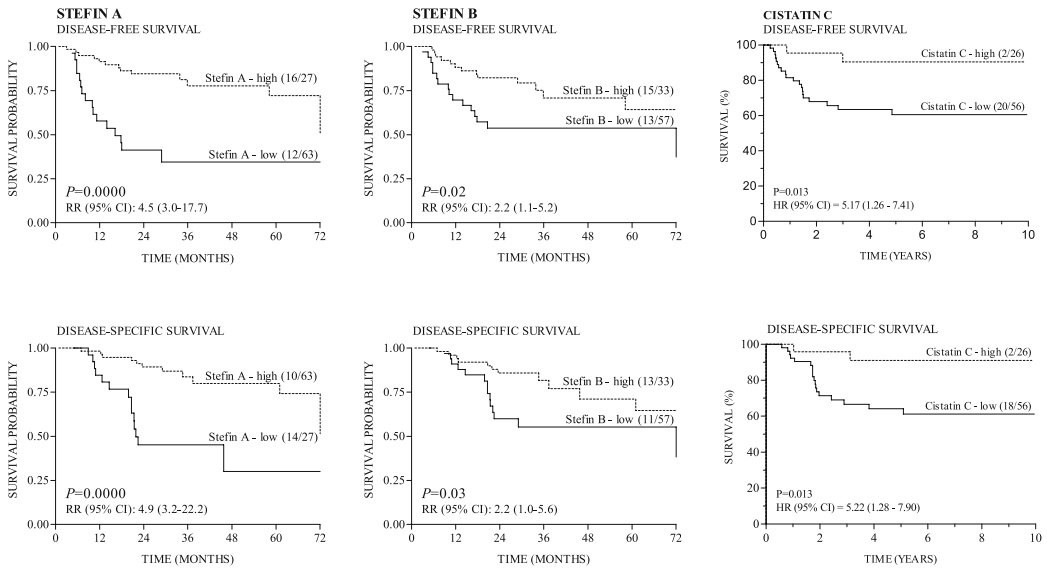


**Figure 1.** Actuarial disease-free survival and disease-specific survival as a function of stefin A, stefin B, and cystatin C status. The numbers in parentheses indicate the number of recurrences or deaths/total in each group.

systems, implemented in proteolytic degradation of extracellular matrix components, were studied, including papain-like lysosomal cysteine proteases, such as cathepsins B (CB) and L (CL), and their physiological inhibitors cystatins (e.g. stefins A [SA] and B [SB], cystatin C [CC]).<sup>2</sup> Recently, the involvement of cysteine cathepsins and stefins in apoptotic death of tumor cells, triggered also by irradiation and chemotherapeutics, was confirmed in several systems.<sup>3</sup>

The aim of the present report is to review the published studies on clinical applicability of cysteine cathepsins and their endogenous inhibitors stefins in squamous cell carcinoma of the head and neck and to present recent research results from this area collected jointly at the Institute of Oncology Ljubljana and ENT Department of the University Medical Center Ljubljana, Slovenia. In all our studies, the same kits of reagents were used for the determination of studied cathepsins and stefins, *i.e.* the commercially available ELISAs developed at the Jožef Stefan Institute.<sup>4</sup>

## What do we know?

At the moment, only cytosolic concentrations of cystatins from the tissue of operable head and neck carcinomas were found to correlate with the patients' survival. In our initial set of studies, high levels of SA, SB and CC in tissue homogenates from two independent, but smaller prospective cohorts of patients appeared prognostically advantageous (Table 1, Figure 1).<sup>5-7</sup> The issue of the protective role of high levels of cysteine protease inhibitors in tissue homogenates was raised also following the survival analysis of the patients with breast<sup>8</sup> and lung<sup>9,10</sup> carcinoma.

The results of the studies on the serine protease system inhibitor (plasminogen activator inhibitor type 1, PAI-1) in tumor tissue extracts of breast carcinoma,<sup>11</sup> SA immunohistochemistry in breast cancer sections,<sup>12</sup> and on various cystatins from the serum of patients with colorectal carcinoma,<sup>13</sup> lung carcinoma and non-Hodgkin's lymphomas<sup>14</sup> are contrary to the above hy-

**Table 1.** Clinical studies on cysteine cathepsins and their endogenous inhibitors in tissue cytosols conducted at the Institute of Oncology Ljubljana and ENT Department of the University Medical Center Ljubljana, Slovenia, 1995 – 2007

Study details	Study no., Year		
	I, 1995	II, 1998	III, 2006
No. of patients	45	49	92
Sex (female/male)	2/43	4/45	9/83
Age (in years) <sup>1</sup>	55 (40 – 69)	60 (37 – 72)	59 (37 – 80)
Primary tumor site			
Larynx	25	20	43
Nonlarynx <sup>2</sup>	20	29	49
T-stage			
pT <sub>1+2</sub>	14	23	33
pT <sub>3+4</sub>	31	26	59
N-Stage			
pN <sub>0</sub>	18	24	38
pN <sub>1-3</sub>	27	25	54
Overall TNM stage			
S <sub>I+II</sub>	7	10	18
S <sub>III+IV</sub>	38	39	74
Extranodal tumor spread <sup>3</sup>			
Negative	6	9	27
Positive	19	16	27
Unknown	2	0	0
Mode of therapy			
Surgery	2	7	8
Surgery + radiotherapy	39	42	84
Radiotherapy	4	0	0
Analytical method	ELISA	ELISA	ELISA
Reference(s) No.	5	6, 7	27

<sup>1</sup>Median (range).<sup>2</sup>Oral cavity, oropharynx, hypopharynx.<sup>3</sup>pN<sub>1-3</sub> patients only.<sup>4</sup>Sandwich ELISAs, KRKA dd & Institute Jožef Stefan Ljubljana, Slovenia.

pothesis. However, the observed variations in the relationship between the cystatin levels and survival probability could be attributed to the differences between the serine and cysteine proteases in regulatory mech-

anisms operating during tumor progression,<sup>15</sup> to the inherent variations between the biological samples of different types, and to the systemic response to malignant disease, which influence also the extracel-

lular (*i.e.* serum) levels of cystatins.<sup>13</sup> The importance of variations in methodology used for the preparation of biological samples of different types and of their inherent characteristics influencing quantitative (and most probably also qualitative) relations between individual enzymes and inhibitors were clearly exposed in a comparative study on pairs of different biological samples obtained from the same patients with breast carcinoma. For example, the authors identified CB cytosolic levels, but not also CB immunostaining in tumor cells, as prognostically important.<sup>16</sup>

Much less data exist on the clinical applicability of cysteine cathepsins and stefins determined in other types of biological samples. In the serum, alterations in activity and concentration levels of studied enzymes and inhibitors between patients and healthy controls were found to be highly variable and influenced by other non-malignant disease conditions, mainly inflammatory.<sup>17-22</sup> Thus, any interpretation of the results from pertinent studies would be only speculative. More convincing is the observation by a small but homogenous study group in regard to cancer type and treatment mode, reported by Kręcicki and Siewiński.<sup>17</sup> In 25 post-laryngectomy patients, serum CB-like activity was constantly declining, reaching normal values within four months post-surgery. In other 14 patients failing treatment, the mean serum values of CB activity dropped in the first month after surgery, but rapidly increased in the subsequent tests. The elevation had occurred at least two months before clinical evidence of metastases or recurrent tumor became apparent.<sup>17</sup> No persuasive evidence on the prognostic value of serum measurements of cysteine cathepsins and their inhibitors was provided so far.

The data on the immunohistochemically determined expression profile of cysteine cathepsins are available from a limited

number of rather small series and only for oral cavity tumors, but not also for pharyngeal or laryngeal carcinomas; the same finding was also referred to their possible prognostic significance.<sup>23-26</sup> So far, to the best of our knowledge, stefins have not been subjected to immunohistochemical evaluation in any of the studies conducted on head and neck carcinomas. The results on spatial distribution of CB and CL immunoreactivity, with perinuclear positivity mainly manifested intracellularly and on the membrane surface outside the tumor cells, reflect their physiological role and are consistent throughout the studies.<sup>23-26</sup>

### Clinical studies, 2006 – 2008

#### *Tissue homogenate (cytosol)*

With the aim to test prospectively the hypothesis about the protective role of high SA and SB levels in the patients with operable tumors, their concentrations were measured in tissue cytosols of non-tumorous mucosa and primary tumor from 92 patients.<sup>27</sup> All patients underwent curative surgery and 84 patients had postoperative radiotherapy. Fifty-nine (64%) tumors were staged as locally advanced pT3-T4, and nodal infiltration with tumor cells was determined in 54 (59%) cases, with extracapsular tumor spread in 27 of them.

Both stefins were found to be associated significantly with the disease-free survival probability only when exceeding a certain value. Thus, a flexible methodology for analyzing their effect – a “broken stick” model – was employed, with the advantage of avoiding arbitrary categorization and its subsequent loss of information.<sup>28</sup>

$$\beta(V - V_0)_+$$

(where  $V$  is the measured value,  $V_0$  is the cut-off value and the *plus* denotes that only

**Table 2.** Concentrations of stefin A and stefin B in tissue cytosols of match-pairs of tumor and adjacent non-tumorous mucosa

Patients	Stefin A (ng/mgp)				Stefin B (ng/mgp)			
	N	Median	Range	P-value	n	Median	Range	P-value
All								
Mucosa	92	759.5	7 – 4878	0.36	92	187.5	6 – 1736	0.98
Tumor	92	795	80 – 5320		92	203.5	28 – 1974	
Upregulated <sup>1</sup>								
Mucosa <sup>2</sup>	53	244	7 – 4878	<0.0001	49	54	6 – 703	<0.0001
Tumor <sup>3</sup>	53	1059	115 – 5320		49	294	57 – 1974	
Downregulated cases <sup>1</sup>								
Mucosa <sup>2</sup>	39	1690	196 – 4877	<0.0001	43	388	58 – 1736	<0.0001
Tumor <sup>3</sup>	39	468	80 – 2074		43	167	28 – 495	

<sup>1</sup>Patients with increased (upregulated cases) and decreased (downregulated cases) concentration of inhibitor

In tumor compared to mucosa.

<sup>2</sup>Mucosa, upregulated cases *vs.* downregulated cases: stefin A,  $P < 0.0001$ ; stefin B,  $P < 0.0001$ .

<sup>3</sup>Tumor, upregulated cases *vs.* downregulated cases: stefin A,  $P < 0.0001$ ; stefin B,  $P < 0.004$ .

N, Number of samples.

the part where  $V$  is greater than  $V_0$  is used). Both beta and  $V_0$  were estimated simultaneously by maximizing the Cox partial likelihood in a model using no additional covariates.<sup>28</sup> The model assumed no effect of the log of stefin A up to the cut-point value, which was calculated to be the 64<sup>th</sup> percentile in the group, and a linear effect afterwards. In the multivariate analysis, a significant decrease in the risk of disease re-appearance to only 3% (*i.e.* by 97%) of the reference value was observed after doubling the stefin a concentration above the calculated cut-off. In the case of SB, all patients with an inhibitor value exceeding the cut-off point (the 78<sup>th</sup> percentile in the group) were censored and no further calculations were performed.

These results were reconfirmed after pooling the data with two historical data sets<sup>5,6</sup> into a uniform series of 182 patients.

For each data set, we ranked the results of individual SA measurements; thus, the inhibitor levels were converted to fractional ranks (between 0 and 1) and the equal fractional ranks became comparable across the data sets.<sup>11</sup> Again, the optimal cut-off point for SA was found at the 63<sup>th</sup> percentile in the group, after which the risk of disease reappearance was reduced, reaching 53% of the reference value as the fractional rank of SA increased by 0.1 (Table 2).

The observed prognostic strength of SA forced us to study further the quantitative relationship between SA and SB and two cysteine cathepsins, which was simultaneously determined in the tissue homogenates from the same group of 92 patients, but had no impact on the patients' prognosis at all (Table 3). Analyzing the whole group of 92 samples, there was no differences observed in SA and SB concentrations between tu-

**Table 3.** Multivariate analysis on prognostic value of stefin A as determined in cytosols of tumor tissue: pooled analysis (N = 182)

Variable	Disease-free survival		
	HR	95% CI	P-value
Stefin A rank <sup>1, 2</sup>	0.53	0.35 – 0.82	0.004
Extracapsular extension			
Negative <sup>3</sup> vs. positive	2.44	1.31 – 4.52	0.005
pT-stage			
pT <sub>1+2+3</sub> vs. pT <sub>4</sub>	2.05	1.12 – 3.74	0.020
Primary tumor site			
Larynx vs. nonlarynx <sup>4</sup>	2.05	1.04 – 4.03	0.037

<sup>1</sup>After the threshold.

<sup>2</sup>The hazard ratio is given for a difference in 0.1 fractional rank.

<sup>3</sup>Patients without extension of tumor tissue beyond nodal capsule and those with pN<sub>0</sub>-stage of disease were included.

<sup>4</sup>Oral cavity, oropharynx, hypopharynx.

HR, Hazard ratio; CI, Confidence interval.

mor and mucosa. However, after stratifying the patients according to SA (and SB as well) differences as calculated in matched pairs of tumor tissue and non-tumorous mucosa, SA was found upregulated in 53 patients (higher concentrations were measured in tumor samples than in non-tumorous mucosa) and was downregulated in 39 patients; the corresponding numbers for SB were 49 and 43, respectively. The mucosal concentrations of either of the stefins were significantly higher in the patients with downregulated inhibitor concentration than in those with upregulated inhibitor concentration and the opposite was calculated for their tumor concentrations. Between SA and SB, a highly significant correlation was found when either mucosal ( $R_s=0.887$ ,  $P<0.0001$ ) or tumor ( $R_s=0.594$ ,  $P<0.0001$ ) concentrations were compared. The difference between tumor and mucosal SA and SB concentrations was congruent (*i.e.* both either positive or negative in the same pa-

tient) in 87% of patients. A significantly higher proportion of downregulated cases were found among the patients with disease re-appearance (70% vs. 35%,  $p=0.005$ ) who had significantly lower tumor concentrations of SA and SB compared to those experiencing successful treatment.<sup>27</sup>

The crucial observation from this study would be that, in the patients with inherently low SA concentrations in non-tumorous mucosa (upregulated ceases), the CB and CL mucosal concentrations were significantly lower compared to those patients with high mucosal concentrations of SA (downregulated cases) (Figure 2). It seems that, in normal tissue, the ability of inhibitory component (*i.e.* stefins) of cysteine proteolytic system is well adapted to the proteolytic capacity of proteases (*i.e.* CB and CL), suggesting an active buffer role of stefins.

Further, we hypothesized that, after malignant transformation of previously normal mucosal cells with inherently low cathepsin

and stefin levels (upregulated group), a significant and synchronous increase on both enzymatic and inhibitory side of proteolytic tandem occurred, gaining a more favorable prognosis of these patients. On the other hand, in the patients with originally high levels of cysteine cathepsins and stefins in normal mucosa (downregulated group), the malignant transformation resulted in an additional raise of the enzymes not being followed by an adequate adjustment of the inhibitors. The concentrations of the latter were found to be even depressed significantly compared to those of mucosa. Such pattern of quantitative relationships in cysteine proteolytic system contributes to a switch in cellular mechanisms at different levels toward more invasive cell phenotypes, resulting in an increased risk for disease recurrence or systemic failures. Furthermore, because in tumor tissue, no difference in concentrations of either CB or CL was observed between the down- and upregulated cases, it appears that the proteolytic balance after the malignant transformation is mainly determined by the changes on the stefin side (Figure 3).

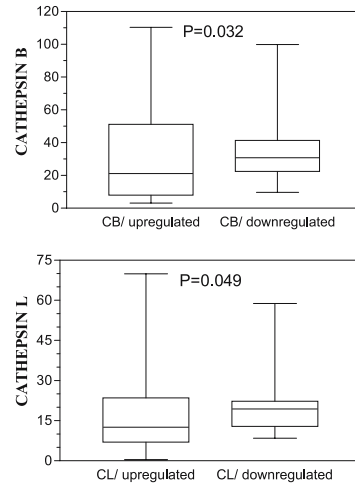


**Figure 2.** Cathepsin B and cathepsin L mucosal concentrations in patients grouped according to the stefin A difference as calculated in matched pairs of tumor tissue and non-tumorous mucosa.

*Immunohistochemistry*

Recently, we determined immunohistochemically the labeling pattern and expression profile of CB and CL and SA and SB in the tissue sections of 75 unresectable squamous cell carcinomas of the oropharynx treated with concomitant chemoradio-

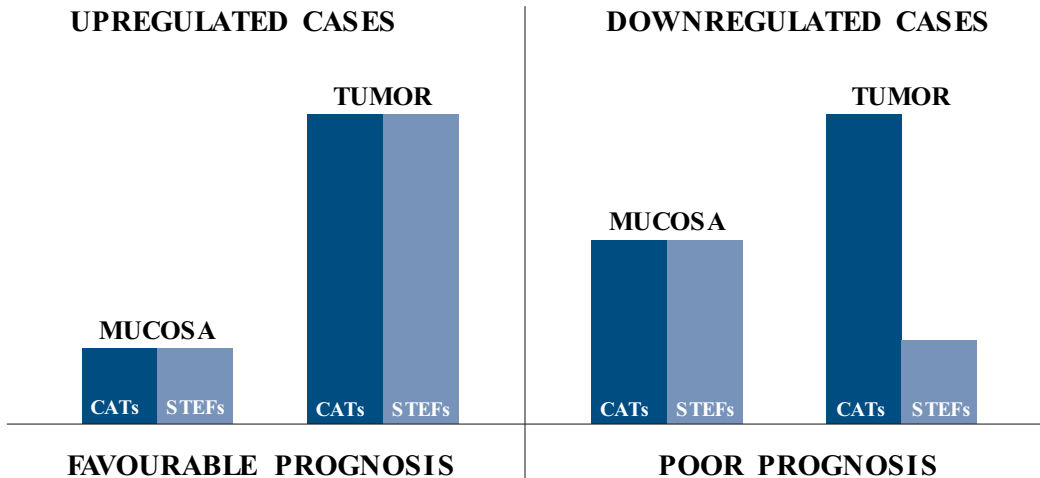


**Figure 3.** Relationship (schematic) between tumor and mucosal levels of cysteine cathepsins and stefins in down- and upregulated group of patients (in regard to the stefin A concentrations).

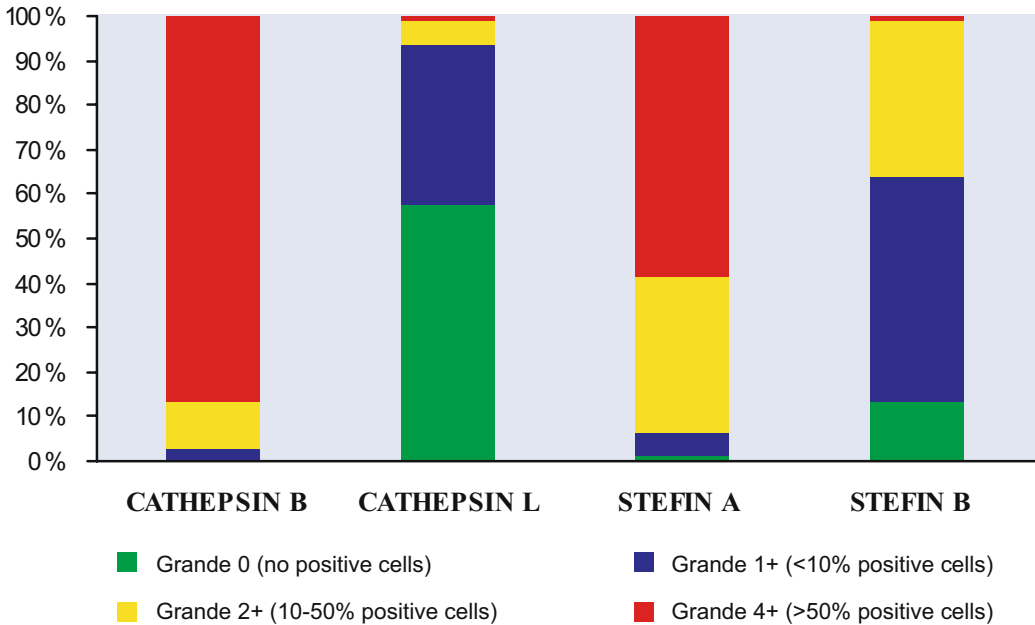


**Figure 4.** Immunohistochemical staining for cathepsins and stefins in tumor cells

therapy with mitomycin C and bleomycin. The secondary objective was to estimate the possible predictive and prognostic significance of the observed immunohistochemical reactions in this particular cancer type. The study population was intentionally homogenized by limiting the entry criteria to unresectable tumors of one subsite inside the upper aerodigestive tract, treated uniformly in order to minimize the impact of some well-established prognostic indicators on treatment results. According to the UICC TNM staging criteria, 67% of patients had stage IV disease. Because the intensity of immunohistochemical staining followed the variations in proportion of positively stained cells, as it was previously observed in breast (16) and rectal (29) carcinomas, a semiquantitative four grade (0–3+) scoring system was used for estimating the percentage of positively stained cells in tissue sections.

Tumor cells and stromal lymphocytes stained for all four studied parameters: in

tumor cells, the most extensive staining was observed for CB and SA, whereas CL and SB yielded much lower immunoreactivity scores (Figure 4). The comparable CB and CL immunohistochemical profiles were described in the study on oral cavity tumors by Vigneswaran *et al.*,<sup>23</sup> whereas conflicting results from some other studies could have resulted from the differences in analytical procedures used (antigens, reagents), low sample numbers in some series,<sup>24,25</sup> and from the inherent biological characteristics of the site of tissue sampling (oral cavity *vs.* oropharynx *vs.* other tumor types).<sup>6,7,27</sup> The observed perinuclear cathepsin positivity mainly manifested intracellularly and on the membrane surface outside the tumor cells, was more consistent throughout the studies (Figure 5a).<sup>23–26</sup> Exclusively intracellular immunostaining for stefins reflected the lack of secretory signal sequences on corresponding genes (Figure 5b).<sup>2</sup> Contrary to our observation, in the sections of breast carcinoma tissue and malignant brain tu-

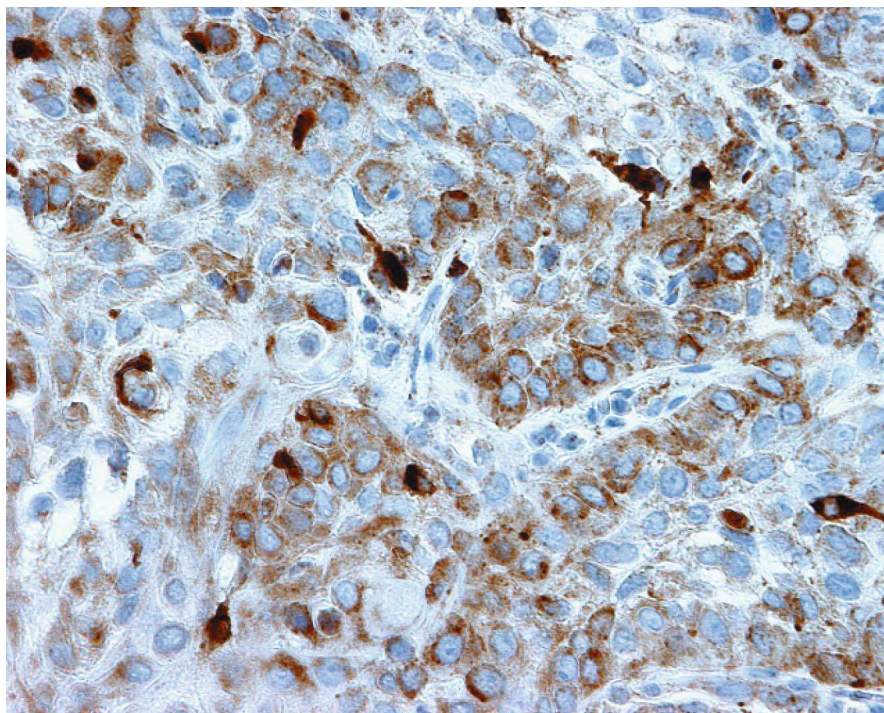


**Figure 5a.** Immunohistochemical staining for cathepsin B: predominant perinuclear pattern.

mors, SA and/or SB immunoreactivity was described in a minority of cases or was only sporadic.<sup>6,12,30</sup>

CB and SA scores were found to be predictive for the tumor origin within the oropharynx, and the balance in the tandem CB-SB inclined toward enzymatic component correlated with more advanced tumors ( $P=0.049$ ) and residual disease two months after therapy ( $P=0.024$ ). While the value of correlation observed between the CB and SA immunohistochemical scores and the origin of primary tumor is debatable, the domination of enzymatic over inhibitory component in the pair CB-SB linked to a more aggressive disease phenotype suggests a pivotal role of enzyme-to-inhibitor score ratio over the expression levels of individual parameters. The predictive significance of the cathepsin-stefin ratio for the incidence of pelvic metastases

has also been reported for the prostate carcinoma.<sup>31</sup>

Playing an important role in apoptosis, in one of the basic mechanisms of tumor cell killing with irradiation and chemotherapeutics,<sup>32</sup> the high expression level of cathepsins and stefins was hypothesized to predict a favourable response to chemoradiation. However, the observed association between strong immunostaining for CB (or CB-SB tandem) and locoregional treatment failure two months after therapy contradicts the proapoptotic role of cysteine cathepsins suggested in preclinical studies.<sup>3</sup> The opposing roles of cysteine cathepsins in oral squamous cell carcinoma apoptosis have been suggested recently by Johansson *et al.*<sup>33</sup> Intracellularly, they were recognized as promoters of apoptosis, whereas in extracellular compartments, cysteine cathepsins seem to be involved in shedding Fas

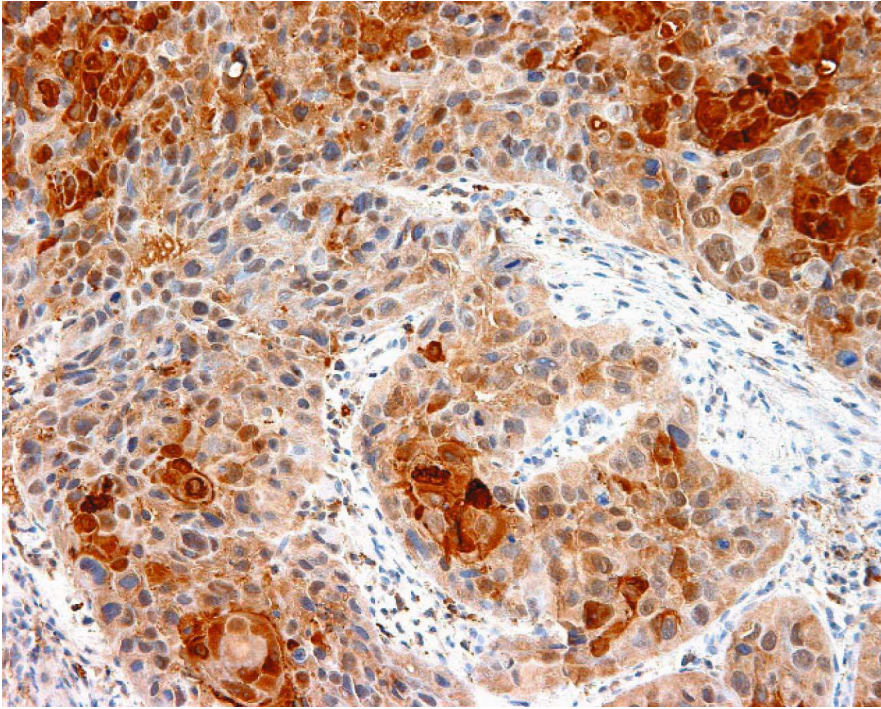


**Figure 5b.** Positive cytoplasmic immunohistochemical staining for stefin A.

death receptors on the cell surface and thus act to prevent apoptosis. The chemoresistance of laryngeal carcinoma cells with increased level of CB<sup>34</sup> and of glioblastoma cells with increased level of CL,<sup>35</sup> as well as unchanged TNF- $\alpha$  mediated apoptotic activity in HeLa cells after the transfection of CB and CL,<sup>36</sup> also support the hypothesis that high levels of cathepsin expression may not result in the enhanced response of tumor cells to proapoptotic stimuli.

Another reason for this discrepancy might be hypoxia mediated inhibition of TRIAL-induced apoptosis of tumor cells. The prevention of Bax activation and protection of mitochondrial stability with the inhibition of cathepsin translocation by hypoxia might be a mechanism by which tumor cells survive against tumor therapies.<sup>37</sup> On the other hand, hypoxia was demonstrated to increase CB expression and activity and to

down-regulate its inhibitors, SB and CC, resulting in an increased residual activity of CB and, consequently, enhanced invasive and /or metastatic potential of hypoxic tumor cells.<sup>38</sup> Thus, the relationship between tumor hypoxia, a frequent and prognostically unfavourable feature of advanced disease, as was the case in our patients, cathepsin and stefin expression levels or activity, and apoptosis is to be determined.<sup>39</sup>

Only CB immunostaining showed some prognostic potential on univariate survival analysis, with low scores being prognostically advantageous over more extensive immunoreactivity (Figure 6). However, after testing CB in multivariate model, it did not appear as an independent prognostic factor. In regard to other tumor types, immunohistochemical labeling for CB was found to be of prognostic value in malignant brain tumors and colorectal carcinoma,<sup>40,41</sup> but not

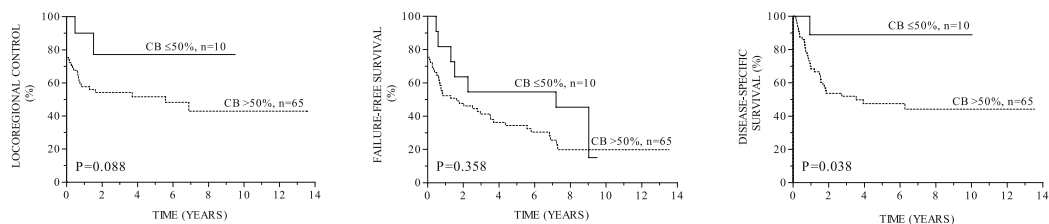


**Figure 6.** Actuarial survival of patients according to immunohistochemical staining for cathepsin B. **a)** locoregional control; **b)** failure-free survival; **c)** disease-specific survival.

in carcinomas of the breast and oral cavity.<sup>16,26</sup> In head and neck carcinomas, more convincing results were reported from biochemical studies (see above, Refs.<sup>6,7,27</sup>). The importance of complexity of interactions between individual enzymes and inhibitors in biological samples of different types for prediction of survival was clearly exposed in the study by Lah *et al.*<sup>16</sup> In the samples obtained from the same patients with breast carcinoma, the authors identified CB cytosolic levels, but not also CB immunostaining in tumor cells, as prognostically important, thereby suggesting the existence of inherent variations between biological samples of different types. Furthermore, the prognostic importance of individual parameters in a particular cancer type might vary across different patient subgroups, stratified according to well-established prognostic factors. For example, the prognostic reliability of SA immunostaining in breast cancer was reported to be N stage dependent,<sup>42</sup> whereas in prostate carcinoma, the CB-SA ratio reliably differentiated less aggressive from more aggressive subpopulations of tumors within an individual Gleason score.<sup>31</sup>

## Conclusions

The knowledge on predictive and prognostic value of cysteine proteases and their endogenous inhibitors in squamous cell carcinoma of the head and neck is scanty.

According to our experience, immunohistochemical staining of cysteine cathepsins and stefins seems to be of limited value in this respect. However, the determination of SA in tumor tissue cytosols certainly deserves further evaluation: (i) SA confirmed its prognostic value in three independent data sets, with high levels being prognostically advantageous; and (ii) considering the differences in inhibitor concentrations in matched pairs of tumor and mucosa samples, two populations of tumors were clearly identified. This observation has strong prognostic implications because downregulated cases are at an increased risk for disease recurrence. These results should be considered hypothesis-generating and should encourage a prospective controlled and multicentric evaluation of cytosolic SA as a promising prognostic indicator in head and neck cancer on sufficiently large number of patients and with standardized analytical method for SA determination.

## Acknowledgement

The author thanks to Professor Nina Gale for providing photographs on cathepsin B immunohistochemical staining and to all colleagues who actively participated in the presented studies: Professors Marjan Budihna, Janez Škrk, Lojze Šmid, Janko Kos, and colleagues Ivan Vrhovec, Branka Svetic, Irena Oblak and Aleksander Aničin.

## References

1. Vokes EE, Weichselbyum RR, Lippman SM, Hong WK. Head and neck cancer. *N Engl J Med* 1993; **328**:184-94.
2. Strojan P. Cathepsins and their endogenous inhibitors in clinical oncology. *Radiol Oncol* 1996; **30**: 120-33.
3. Stoka V, Turk B, Turk V. Lysosomal cysteine cathepsins: signaling pathways in apoptosis. *Biol Chem* 2007; **388**: 555-60.
4. Kos J, Šmid L, Krašovec M, Svetic B, Lenarcic B, Vrhovec I, et al. Lysosomal proteases cathepsins D, B, H, L and their inhibitors stefins A and B in head and neck cancer. *Biol Chem Hoppe Seyler* 1995; **376**: 401-5.
5. Budihna M, Strojan P, Šmid L, Skrk J, Vrhovec I, Zupevc A, et al. Prognostic value of cathepsins B, H, L, D and their endogenous inhibitors stefins A and B in head and neck carcinoma. *Biol Chem Hoppe Seyler* 1996; **377**: 385-90.
6. Strojan P, Budihna M, Šmid L, Vrhovec I, Skrk J. Prognostic significance of cysteine proteinases B and L and their endogenous inhibitors stefins A and B in patients with squamous cell carcinoma of the head and neck. *Clin Cancer Res* 2000; **6**: 1052-62.
7. Strojan P, Oblak I, Svetic N, Šmid L, Kos J. Cysteine proteinase inhibitor cystatin C in squamous cell carcinoma of the head and neck: relation to prognosis. *Br J Cancer* 2004; **90**: 1961-8.
8. Lah TT, Kos J, Blejec A, Frkovic-Georgio S, Golouh R, Vrhovec I, et al. The expression of lysosomal proteinases and their inhibitors in breast cancer: possible relationship to prognosis of the disease. *Pathol Oncol Res* 1997; **3**: 89-99.
9. Knoch H, Werle B, Ebert W, Spiess E. Imbalance between cathepsin B and cysteine proteinase inhibitors is of prognostic significance in human lung cancer. *Int J Oncol* 1994; **5**: 77-85.
10. Ebert E, Werle B, Jülke B, Kopitar-Jerala N, Kos J, Lah T, et al. Expression of cysteine proteinase inhibitors stefin A, stefin B, and cystatin C in human lung tumor tissue. *Adv Exp Med Biol* 1997; **421**: 259-65.
11. Look MP, van Putten WL, Duffy MJ, Harbeck N, Christensen IJ, Thomssen C, et al. Pooled analysis of prognostic impact of urokinase-type plasminogen activator and its inhibitor PAI-1 in 8377 breast cancer patients. *J Natl Cancer Inst* 2002; **94**: 116-28.
12. Kuopio T, Kankaanranta A, Jalava P, Kronqvist P, Kotkansalo T, Weber E, et al. Cysteine proteinase inhibitor cystatin A in breast cancer. *Cancer Res* 1998; **58**: 432-6.
13. Kos J, Krasovec M, Cimerman N, Nielsen HJ, Christensen IJ, Brunner N. Cysteine proteinase inhibitors stefin A, stefin B, and cystatin C in sera from patients with colorectal cancer: relation to prognosis. *Clin Cancer Res* 2000; **6**: 505-11.
14. Kos J, Lah T. Role of cystatins and stefins in cancer. In: Zerovnik E, Kopitar-Jerala N, Uversky V, editors. *Human stefins and cystatins*. New York: Nova Science Publishers, Inc; 2006. p. 233-6.
15. Levičar N, Kos J, Blejec A, Golouh R, Vrhovec I, Frkovic-Grazio S, et al. Comparison of potential biological markers cathepsin B, cathepsin L, stefin A and stefin B with urokinase and plasminogen activator inhibitor-1 and clinicopathological data of breast carcinoma patients. *Cancer Detect Prev* 2002; **26**: 42-9.
16. Lah TT, Kalman E, Najjar D, Gorodetsky E, Brennan P, Somers R, et al. Cells producing cathepsins D, B and L in human breast carcinoma and their association with prognosis. *Hum Pathol* 2000; **3**: 149-60.
17. Kręcicki T, Siewiński M. Serum cathepsin B-like activity as a potential marker of laryngeal carcinoma. *Eur Arch Otorhinolaryngol* 1992; **249**: 293-5.
18. Bongers V, Konings CH, Grijpma AM, Steen I, Braakhuis BJM, Snow GB. Serum proteinase activities in head and neck squamous cell carcinoma patients. *Anticancer Res* 1995; **15**: 2763-6.
19. Strojan P, Budihna M, Šmid L, Svetic B, Vrhovec I, Škrk J. Cathepsin B and L and stefin A and B levels as serum tumor markers in squamous cell carcinoma of the head and neck. *Neoplasma* 2001; **48**: 66-71.
20. Strojan P, Budihna M, Šmid L, Svetic B, Vrhovec I, Kos J, et al. Cathepsin H in squamous cell carcinoma of the head and neck. *Radiol Oncol* 1999; **33**: 143-51.
21. Siewiński M, Kręcicki T, Jarmułowicz J, Berdowska I. Cysteine proteinase inhibitors in serum of patients with head and neck tumors. *Diagn Oncol* 1992; **2**: 323-6.
22. Strojan P, Svetic B, Šmid L, Kos J. Serum cystatin C in patients with head and neck carcinoma. *Clin Chim Acta* 2004; **344**: 155-61.

23. Vigneswaran N, Zhao W, Dassanayake A, Muller S, Miller DM, Zacharias W. Variable expression of cathepsin B and D correlates with highly invasive and metastatic phenotype of oral cancer. *Hum Pathol* 2000; **31**: 931-7.
24. Macabeo-Ong M, Shiboski CH, Silverman S, Ginzinger DG, Dekker N, Wong DT, et al. Quantitative analysis of cathepsin L mRNA and protein expression during oral cancer progression. *Oral Oncol* 2003; **39**: 638-47.
25. Nikitakis NG, Rivera H, Lopes MA, Siavash H, Reynolds MA, Ord RA, et al. Immunohistochemical expression of angiogenesis-related markers in oral squamous cell carcinoma with multiple metastatic lymph nodes. *Am J Clin Pathol* 2003; **119**: 574-86.
26. Kawasaki G, Kato Y, Mizuno A. Cathepsin expression in oral squamous cell carcinoma: Relationship with clinicopathologic factors. *Oral Surg Oral Med Oral Patol Oral Radiol Endod* 2002; **93**: 446-54.
27. Strojan P, Aničin A, Svetic B, Pohar M, Šmid L, Kos J, Stefin A and stefin B: markers for prognosis in inoperable squamous cell carcinoma of the head and neck. *Int J Radiat Oncol Biol Phys* 2007; **68**: 1335-41.
28. Bossard N, Descotes F, Bremond AG, Bobin Y, De Saint Hilaire P, Golfier F, et al. Keeping data continuous when analyzing the prognostic impact of the tumor marker: an example with cathepsin D in breast cancer. *Breast Cancer Res Treat* 2003; **82**: 47-59.
29. Castiglioni T, Merino MJ, Elsner B, Lah TT, Sloane BF, Emmert-Buck MR. Immunohistochemical analysis of cathepsin D, B and L in human breast cancer. *Hum Pathol* 1994; **25**: 857-62.
30. Strojnik T, Židanik B, Kos J, Lah TT. Cathepsin B and L are markers for clinically invasive types of meningiomas. *Neurosurgery* 2001; **48**: 598-605.
31. Sinha AA, Quast BJ, Wilson MJ, Fernandes ET, Reddy PK, Ewing SL, et al. Prediction of pelvic lymph node metastasis by the ratio of cathepsin B to stefin A in patients with prostate carcinoma. *Cancer* 2002; **94**: 3141-9.
32. Kim R, Emi M, Tanabe K, Uchida Y, Arihiro K. The role of apoptotic or nonapoptotic cell death in determining cellular response to anticancer treatment. *Eur J Surg Oncol* 2006; **32**: 269-77.
33. Johansson AC, Norberg-Spaak L, Roberg K. Role of lysosomal cathepsins in naphthazarin- and Fas-induced apoptosis in oral squamous cell carcinoma cells. *Acta Oto-Laryngol* 2006; **126**: 70-81.
34. Osmak M, Svetic B, Gabrijelčič-Geiger, Skrk J. Drug-resistant human laryngeal carcinoma cells have increased levels of cathepsin B. *Anticancer Res* 2001; **21**: 481-4.
35. Zajc I, Hreljac I, Lah T. Cathepsin L affects apoptosis of glioblastoma cells: a potential implication in the design of cancer therapeutics. *Anticancer Res* 2006; **26**: 3357-64.
36. Gewies A, Grimm S. Cathepsin-B and cathepsin-L expression levels do not correlate with sensitivity of tumor cells to TNF-alpha-mediated apoptosis. *Br J Cancer* 2003; **89**: 1574-80.
37. Nagaraj NS, Vigneswaran N, Zacharias W. Hypoxia inhibits TRAIL-induced tumor cell apoptosis: involvement of lysosomal cathepsins. *Apoptosis* 2007; **12**: 125-39.
38. Wickramasinghe NS, Banerjee K, Nagaraj NS, Vigneswaran N, Zacharias W. Hypoxia alters cathepsin B/inhibitor profiles in oral carcinoma cell lines. *Anticancer Res* 2005; **25**: 2841-9.
39. Horsman MR. Measurement of tumor oxygenation. *Int J Radiat Oncol Biol Phys* 1998; **42**: 701-4.
40. Strojnik T, Kos J, Židanik B, Golouh R, Lah T. Cathepsin B immunohistochemical staining in tumor and endothelial cells is a new prognostic factor for survival in patients with brain tumors. *Clin Cancer Res* 1999; **5**: 559-67.
41. Campo E, Munoz J, Miquel R, Palacín A, Cardesa A, Sloane BF. Cathepsin B expression in colorectal carcinomas correlates with tumor progression and shortened patient survival. *Am J Pathol* 1994; **145**: 301-9.
42. Elzagheid A, Kuopio T, Pyrhönen S, Collan Y. Lymph node status as a guide to selection of available prognostic markers in breast cancer: the clinical practice of the future? *Diagn Pathol* 2006; **1**: 41.

# Evaluation of shRNA-mediated gene silencing by electroporation in LPB fibrosarcoma cells

Suzana Mesojednik, Urška Kamensek, Maja Čemažar

Department of Experimental Oncology, Institute of Oncology Ljubljana, Slovenia

**Background.** Silencing oncogenes or other genes that contribute to tumor malignancy and progression offers a promising approach to treating cancer. Specific and efficient silencing of gene expression can be achieved by RNA interference (RNAi) technology using small interfering RNA (siRNA) or short hairpin RNA (shRNA). However, a major challenge in RNAi technology is effective delivery of interfering molecules into target cells. The aim of our study was to evaluate electroporation as a perspective method for efficient *in vitro* transfection of LPB fibrosarcoma cells with plasmid DNA expressing shRNA.

**Methods.** Induction of shRNA-mediated gene silencing by electroporation was determined by fluorescence microscopy, flow cytometry and western blot analysis. The effect of electroporation conditions on cell survival and proliferation was determined by clonogenic assay.

**Results and conclusions.** Our results demonstrated that electroporation is a feasible and effective method for delivery of plasmid DNA expressing shRNA into cancer cells *in vitro*. Electrotransfection of murine LPB fibrosarcoma cells, continuously expressing green fluorescence protein - GFP (LPB<sub>GFP</sub>), with plasmid DNA encoding shRNA-GFP, reduced GFP expression, which was determined on the protein level, as well as by measurement of GFP fluorescence intensity. A pronounced reduction in GFP expression level was detected from the second to the fifth day after treatment. Moreover, the method is easy to perform and showed low cell damaging effects, which are the most important and preferential factors for further *in vivo* studies.

*Key words:* electroporation; plasmid DNA; shRNA; fibrosarcoma.

## Introduction

RNA interference (RNAi) is a newly described natural biological phenomenon mediated by short RNA molecules, which target complementary mRNA. The RNAi pathway is activated by a double-stranded RNA (dsRNA), which is then processed by

the cytoplasmatic enzyme Dicer (RNase III family) into short RNA fragments of 20-21 base pairs. One of the strands becomes incorporated into a RNA-induced silencing complex (RISC), where it serves as a guide for mRNA degradation or down-regulation of gene expression.<sup>1</sup> The process has evolved in eukaryotic organisms as a defense mechanism against viruses and a regulatory mechanism of cellular gene expression.<sup>2</sup> When the dsRNA is exogenous (viruses), the RNA is imported directly into cytoplasm and cleaved by Dicer to siRNA fragments. Endogenously expressed dsR-

Received 8 May 2008  
Accepted 22 May 2008

Correspondence to: Dr. Maja Čemažar, Department of Experimental Oncology, Institute of Oncology Ljubljana, SI-1000 Ljubljana, Slovenia. E-mail: mcemazar@onko-i.si

NAs are processed in the cell nucleus from primary transcripts called pri-miRNA to short, stem-loop structures called pre-miRNA. The dsRNA portion of this pre-miRNA is then bound and cleaved in the cytoplasm by Dicer to produce mature, short, single stranded miRNA that can be integrated into the RISC complex. Downstream of this initial processing, miRNA and siRNA share the same cellular mechanism.<sup>1</sup> RNAi triggered molecules can be easily synthesized in the lab and used as a research tool for studying gene function and biochemical pathways, as well as for application in gene therapy of human diseases such as viral infections, inflammations and cancer.<sup>2-8</sup> Different synthetic forms of short RNAs have already been used: siRNA (short interfering RNA)<sup>9-11</sup>, shRNA (short hairpin RNA)<sup>12-14</sup> and miRNA (microRNA).<sup>15</sup> The first can be delivered directly into the cytoplasm, where it mimics the natural Dicer product. Synthetic shRNA and miRNA mimic naturally occurring nuclear pre-miRNA molecules. In order to be delivered into the nucleus, they must be introduced by viral or non-viral vectors. Once in the nucleus, they can be amplified by transcription, thus allowing the gene silencing to be long-term.<sup>16</sup>

Since our understanding of deregulated genes in cancers has grown significantly, RNAi technology has been applied to this field with great promise and enthusiasm all over the world. It has been used to interfere with neoangiogenesis, cell division, inhibition of apoptosis, resistance to chemotherapy and inhibition of anticancer immune responses.<sup>4,6,17,18</sup> However, the efficiency and duration of siRNA mediated gene silencing in tumors depends to a large extent on the choice of gene delivery system.<sup>19</sup> In terms of patient safety, non-viral gene delivery systems (siRNA alone, plasmid DNA, liposome, polyplexes, nanoparticles) are superior to viral vectors. However, they have

proved to be less efficient, so they have been used in combination with physical methods such as electroporation, gene gun, ultrasound, hyperthermia or magnetofection.<sup>20</sup>

Electroporation has already been proven to be a feasible and effective method for delivering chemotherapeutic drugs and genes into tumor cells.<sup>21-23</sup> A variety of therapeutic genes have been delivered into tumor cells by this technique, including diphtheria toxin A (DT-A), interleukins (IL-12, IL-2, IL-15, IL-18), granulocyte-macrophage colony-stimulating factor (GM-CSF), transcription factor p53, tumor necrosis factor-related apoptosis-inducing ligand (TRAIL/Apo2L), interferon-alpha, endostatin and viral protein R (Vpr), and all have resulted in a therapeutic level of protein expression.<sup>22,24</sup> Intratumoral electrotransfer of plasmid DNA encoding the human IL-12, IL-2 or tumor antigens has already reached clinical trials.<sup>18,22</sup> The therapeutic potential of electrically assisted delivery of siRNA molecules into tumors has also been shown.<sup>25-28</sup> However, siRNA molecules can be rapidly degraded in the tumor tissue, so plasmids expressing shRNA and miRNA may be used for more prolonged and stable expression of RNAi effector molecules.<sup>10,14,29-31</sup>

In the present study, we tested whether electrically-assisted delivery of plasmid DNA expressing shRNA may result in efficient *in vitro* transfection of LPB fibrosarcoma cells and, consequently, in a reduction of target protein expression level. To test this hypothesis, we electrotransfected the murine LPB fibrosarcoma cell line that continuously expressed a green fluorescence protein (GFP) with plasmid DNA encoding shRNA directed against GFP. The use of reporter protein GFP allowed us to follow up the siRNA activity by three different methods: direct imaging of green fluorescence under an inverted fluorescence microscope, measuring GFP fluorescence intensity by flow cytometer and determin-

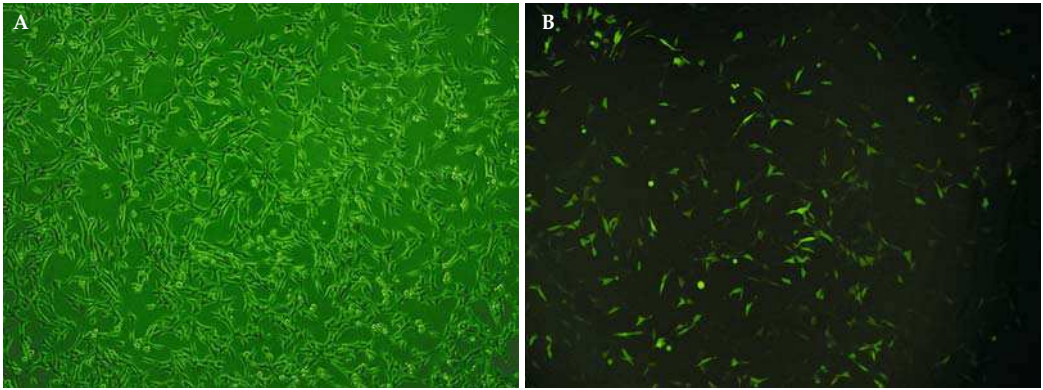


**Figure 1.** Construction of LPB<sub>GFP</sub> cell line. Light (A) and fluorescent (B) view of LPB<sub>GFP</sub> cells continuously expressing GFP under inverted fluorescence microscope. Magnification: 10×. LPB cells were electrotransfected with psiRNA-EGFP and selected for two months by using 800 µg/ml of geneticin to obtain a cell line that continuously expressed GFP.

ing the changes in protein level by western blot analysis.

### Material and methods

#### Construction of murine cell line LPB continuously expressing GFP

Murine fibrosarcoma cell line LPB was maintained in Eagle's minimum essential medium (EMEM, Sigma), supplemented with

10% fetal calf serum (FCS, Sigma), 2 mM L-glutamine, 1 mM sodium pyruvate, and 100 IU/ml penicillin/streptomycin (Pliva, Zagreb, Croatia) in a 5% CO<sub>2</sub> humidified incubator at 37 °C.

Plasmid DNA encoding green fluorescence protein (GFP) and neomycin-resistant gene (pEGFP-N1; Clontech, Basingstoke, UK) was used for construction of LPB cell line continuously expressing GFP. Plasmid DNA was amplified in the Top10 DH5α

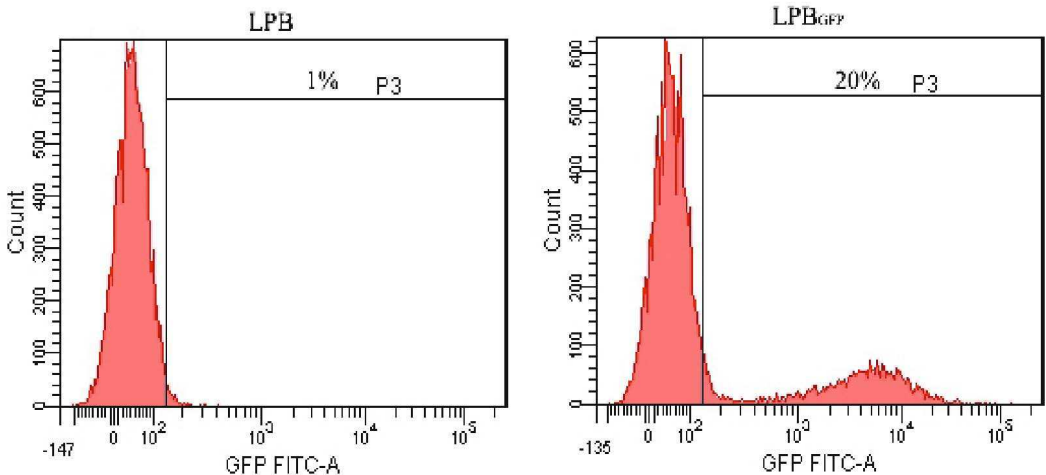


**Figure 2.** Flow cytometer histograms of GFP fluorescence in LPB<sub>GFP</sub> cells. Flow cytometer analysis showed that only 20% of cells in LPB<sub>GFP</sub> cell line stably expressed GFP.

strain of *Escherichia coli* under kanamycin selection and purified using a QIAGEN Endofree Plasmid Mega Kit (QIAGEN GmbH, Hilden, Germany).

*Electroporation* was used for introduction of pEGFP-N1 into LPB cells *in vitro*. Specifically, LPB cells grown as monolayers were harvested and a  $2.5 \times 10^7$  cells/ml cell suspension was prepared in electroporation buffer (125 mM sucrose, 10 mM  $K_2HPO_4$ , 2,5 mM  $KH_2PO_4$ , 2 mM  $MgCl_2 \times 6 H_2O$ ). A dense cell suspension with a concentration of  $1 \times 10^6$  cells and 10  $\mu$ g of pEGFP-N1 in 50  $\mu$ l of electroporation buffer was placed between two flat parallel stainless steel electrodes with a 2-mm gap connected to the GT-1 electroporator (Faculty of Electrical Engineering, Ljubljana, Slovenia) and subjected to eight square-wave electric pulses with an amplitude per distance 600 V/cm, 5 msec duration time and 1 Hz repetition frequency. After exposure to electric pulses, the cells were incubated for 5 min at room temperature. Electrotransfection of LPB cells with pEGFP-N1 and a further 2 months culturing of the treated cells under selectable marker geneticin (800 $\mu$ g/ml) resulted in continuous expression of GFP protein in 20% of the cells (Figure 1,2). The GFP expressing cell line was named LPB<sub>GFP</sub>. This cell line was further used in subsequent experiments of siRNA-mediated gene silencing after electrotransfection of cells with plasmid psiRNA-EGFP.

#### *Electrotransfection of LPB<sub>GFP</sub> cells with shRNA-expressing pDNA*

The above described electroporation protocol was used for the introduction of shRNA-expressing pDNAs, psiRNA-EGFP (Invivogen, San Diego, USA) and psiRNA-scramble (Invivogen, San Diego, USA), into LPB<sub>GFP</sub> cells *in vitro*.

psiRNA-EGFP transcribes a single-stranded RNA 5' - GCA AGC UGA CCC

UGA AGU UCA CCA CCU GAA CUU CAG GGU CAG CUU GCuu - 3', which forms stem-loop-structured siRNA, targeted to EGFP mRNA (targeted sequence: 5' GCA AGC TGA CCC TGA AGT TCA 3'), with a loop sequence of CACC.

psiRNA-scramble which transcribes the non related sequence RNA 5' - GCA UAU GUG CGU ACC UAG CAU UCA AGA GAU GCU AGG UAC GCA CAU AUG Cuu - 3' was used as control pDNA to psiRNA-EGFP throughout the study.

Both shRNA-expressing plasmid DNAs are driven by the CMV enhancer/promoter. Plasmid DNAs expressing shRNA were amplified in the GT116 strain of *Escherichia coli* under zeocin selection, and purified using a QIAGEN Endofree Plasmid Mega Kit.

#### *Determination of siRNA silencing effect*

*Fluorescence microscopy.* Electrotransfected cells were plated on 6-cm Petri dishes (Corning Costar, Acton, MA, USA). In LPB<sub>GFP</sub> fibrosarcoma cells, GFP fluorescence was detected by inverted fluorescence microscope. From the first to the fifth day after treatment visible and fluorescence images at 10 $\times$  magnifications were taken with a CCD Camera (Olympus, Germany) connected to fluorescence microscope.

*Flow cytometry.* Electrotransfected cells were plated on 10-cm Petri dishes (Corning Costar). From the first to the fifth day after treatment, cells were subjected to flow cytometry analysis. Twenty thousand cells were analyzed for each sample. The threshold for autofluorescence was set to a value at which 99% of the control cells (LPB cells without GFP) were included. The mean GFP fluorescence intensity of the cells expressing GFP was determined from histograms obtained by flow cytometer (Becton Dickinson, Calibur, Franklin Lakes, USA). The experiments were repeated three times.

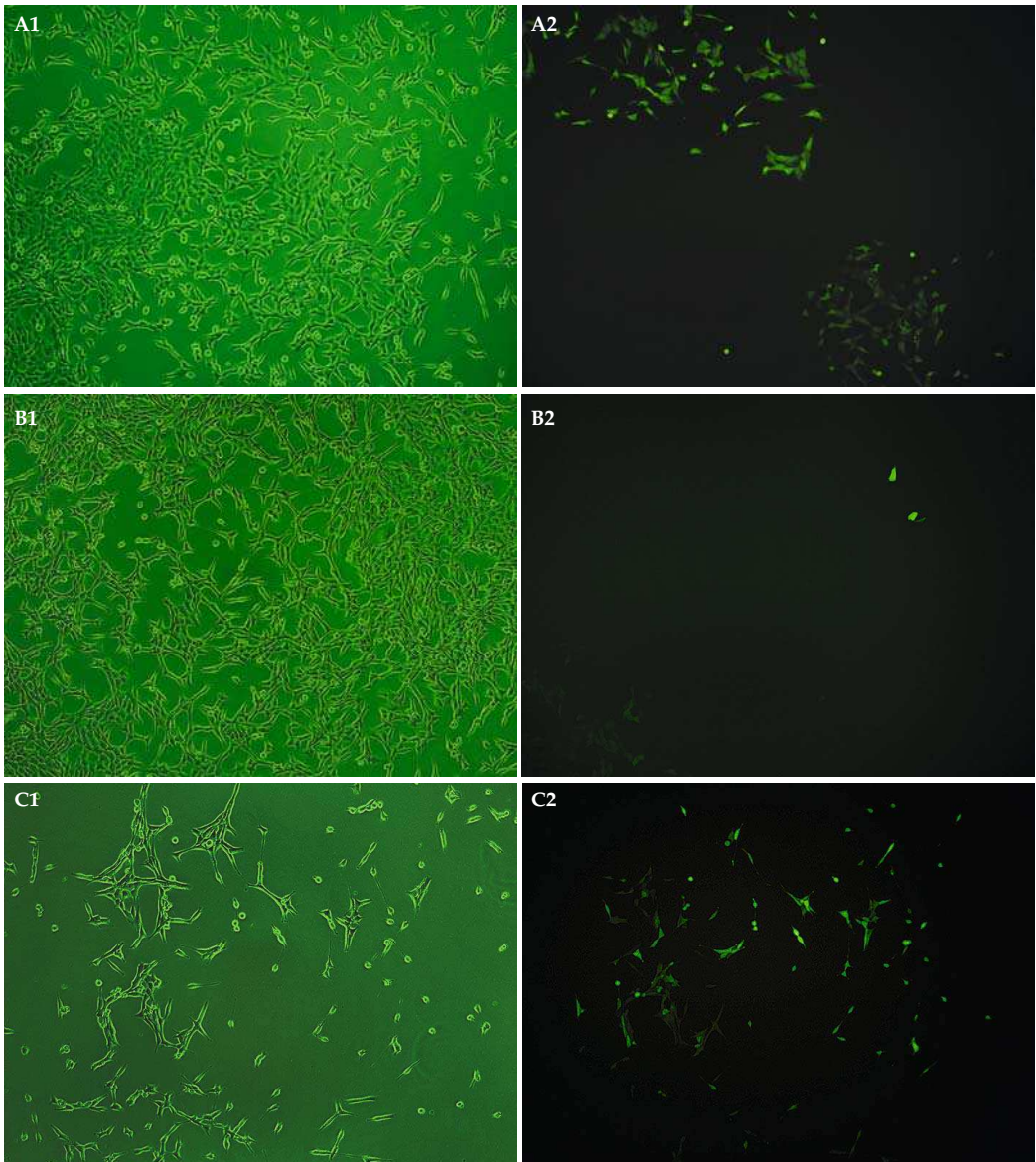


**Figure 3.** Imaging of GFP expressions in LPB<sub>GFP</sub> cells on the fifth day after treatment under inverted fluorescence microscope. Light (1) and fluorescent view (2) of experimental groups: A (LPB<sub>GFP</sub> + EP), B (LPB<sub>GFP</sub> + psiRNA-EGFP + EP), and C (LPB<sub>GFP</sub> + psiRNA-scr + EP). A pronounced reduction in the fraction of GFP positive cells was observed after electrotransfection of LPB<sub>GFP</sub> cells with psiRNA-EGFP (B2). Magnification 10 $\times$ .

**Western blot.** After electrotransfection, LPB<sub>GFP</sub> cells were plated on 10-cm Petri dishes. Cells were harvested by cell scraper 48 h after transfection, lysed in lysis buffer (20 mM Tris, mM NaCl, 0.1% Triton), sonificated for 15 s and centrifuged for 10 min (10000 × g, 4 °C). The obtained total protein suspension was stored at -20 °C for further western blot analysis. The protein concentration was determined by BCA Protein Assay Kit (Pierce, Rockford, USA). The amount of total protein extract from samples was adjusted to 50 µg/lane, followed by the transfer of protein samples to a nitrocellulose membrane sheet (Pierce, Rockford, USA). Antibodies against GFP (B-2) (sc-9996, 1: 1000, Santa Cruz Biotechnology INC, Santa Cruz, CA, USA) and HRP-conjugated goat anti-mouse antibodies IgG<sub>2a</sub>-HRP (sc-2061, Santa Cruz Biotechnology INC, Santa Cruz, CA, USA) were used. Protein bands were detected after incubation of the membrane with chemo-luminescent reagent (Santa Cruz Biotechnology INC, Santa Cruz, CA, USA) and 1 minute exposure to film. Optical densities of proteins were determined by the Image J software system (National Institute of Health, Research Services Branch, Bethesda, MD USA).

#### *Effect of treatment on cell survival and proliferation*

The sensitivity of the cell line to plasmid DNAs, electroporation conditions and the combination of them was determined by clonogenic assay. Cells (250 – 500) were plated on 6-cm Petri dishes with 4 ml of medium and incubated in a 5% CO<sub>2</sub> humidified incubator at 37 °C. After 10 to 12 days, colonies were stained with crystal violet and counted. Colonies containing less than 50 cells were ignored. Plating efficiency and the surviving fraction were then calculated. The experiments were performed in triplicate and repeated three times.

#### *Statistical analysis*

The data were tested for normality of distribution using the Kolmogorov-Smirnov test. Differences between experimental groups were statistically evaluated by one-way analysis of variance (ANOVA) followed by the Holm-Sidak test for multiple comparison. A p-value of less than 0.05 was considered to be statistically significant. Statistical analysis was done using Sigma Stat (Systat Software Inc., London, UK)

## **Results**

#### *Induction of RNAi after electrotransfection of psiRNA-EGFP into LPB<sub>GFP</sub> cells*

Fluorescence microscope imaging showed a markedly reduced level of GFP expression from the second to the fifth day in LPB<sub>GFP</sub> cells after electrotransfection with psiRNA-EGFP. No reduction in GFP expression level was observed in LPB<sub>GFP</sub> cells treated with electric pulses only or electrotransfected with control psiRNA-scr (Figure 3).

Flow cytometry measurements were also performed from the first to the fifth day after electrotransfection. The intensities of GFP fluorescence were diminished in LPB<sub>GFP</sub> cells electrotransfected with psiRNA-EGFP in comparison with the control group electrotransfected with psiRNA-scr. The second day after electrotransfection with psiRNA-EGFP, the mean fluorescence intensity of GFP was lower by 14±6.3% and from the third to the fifth day after electrotransfection it was around 30% lower than in the control group. However, the obtained mean fluorescence intensities did not show a statistically significant difference in GFP fluorescence intensities between the experimental and control group (Figure 4).

Western blot analysis of protein optical density showed a 20% reduction in GFP

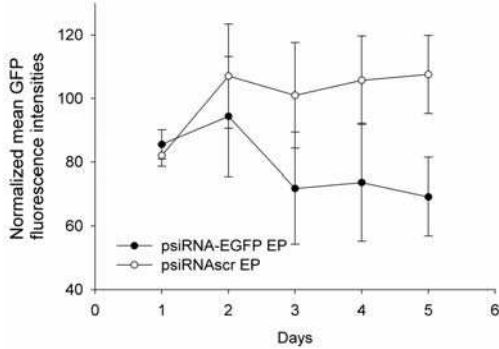


**Figure 4.** Flow cytometry measurements of GFP fluorescence intensity levels in LPB<sub>GFP</sub> cells after electrotransfection with psiRNA-EGFP or psiRNA-scr over time. Shown are GFP fluorescence intensities normalized for each day to GFP fluorescence intensities of the control group, which was treated with electric pulses only.

protein level on the second day after electrotransfection with psiRNA-EGFP compared to the control (psiRNA-scr) (Figure 5).

*Cell survival and proliferation after electrotransfection of psiRNA-EGFP into LPB<sub>GFP</sub> cells*

LPB<sub>GFP</sub> cells showed a 33±15% reduction in colony formation after treatment with electric pulses only. The introduction of psiRNA-EGFP or psiRNA-scr into LPB<sub>GFP</sub> cells by electrotransfection reduced colony formation even more, by 65±9.7% and 70±11.5% (Figure 6).

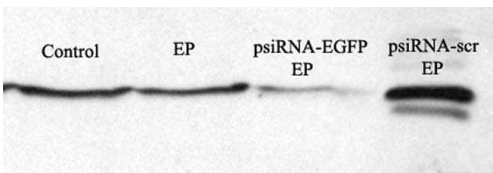


**Figure 5.** Western blot analyses of the changes in GFP protein level in LPB<sub>GFP</sub> cells after electrotransfection and electrotransfection with psiRNA-EGFP or pshRNAscr. On day 2 after electrotransfection of LPB<sub>GFP</sub> cells with psiRNA-EGFP, western blot analysis showed up to 20% lower GFP protein level in comparison with the control vector.

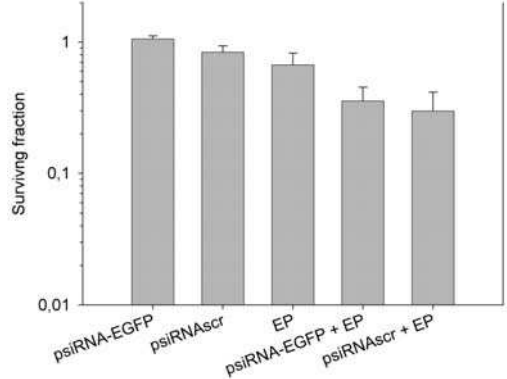


**Figure 6.** Cell survival after electrotransfection with psiRNA-EGFP or pshRNAscr. Values were normalized to the survival of untreated cells. Data present MEAN±SE, which were pooled from triplicates of three experiments.

**Discussion**

The study examined whether electroporation as a physical gene delivery method and plasmid DNA as a gene delivery vector could be used for the introduction of shRNA into murine LPB fibrosarcoma cells. The study was performed *in vitro* in a murine LPB fibrosarcoma cell line constructed in such a way as to continuously express GFP (LPB<sub>GFP</sub>). Reporter gene GFP was chosen due to the ease of imaging and measuring GFP gene expression levels in LPB<sub>GFP</sub> cells, which enabled the determination of siRNA activity directed against GFP.

Various delivery methods for *in vitro* gene silencing have been used to date, mostly transduction with adenoviral, retroviral and SV40 vectors, as well as chemical (lipoplexes, polyplexes) non-vector or vector based transfection methods, which have shown a good silencing effect of either reporter or therapeutic genes.<sup>9,32-35</sup> Among nonviral delivery methods, liposomes have proved to be a very suitable method for *in vitro* delivery of siRNA or shRNA.<sup>15,26,27,29-31</sup> In addition, a recent study has demonstrated that electroporation also results in effective

siRNA mediated gene silencing. Namely, in a study by Merkova *et al.* electroporation was used to introduce siRNA into chronic myeloid leukemia (CML) cells. Gene expression was reduced by 37%, which is comparable with our results using shRNA (35% at day 5). However, in both studies, electroporation was associated with higher cell death compared to other delivery methods.<sup>15,26,27,29-31,36</sup>

In our study, the siRNA silencing effect was measured quantitatively and temporally. Compared with the electrotransfected control vector psiRNA-scr, the psiRNA-EGFP reduced GFP expression after electrotransfection into LPB<sub>GFP</sub> cells, which was shown by flow cytometry analysis of GFP fluorescence intensity, by western blot analysis of GFP protein levels in cells and by fluorescence microscope imaging of cells expressing GFP. The second day after electrotransfection of LPB<sub>GFP</sub> cells with psiRNA-EGFP, a 14% decrease in GFP fluorescence intensity was related to a 20% reduction in GFP protein level. On the third day, siRNA activity decreased GFP fluorescence intensity by ~ 30% and this level remained stable for the next two measuring days. Since the duration of gene silencing by naked siRNA is usually less than 5 days in rapidly growing cell lines<sup>28,37</sup>, we assumed that plasmid DNA expressing shRNA had been transferred into the nucleus, where it was amplified by transcription and a prolonged silencing effect was therefore achieved in the rapidly dividing LPB<sub>GFP</sub> cell line (doubling time 24-30 h). No decrease in GFP intensities was determined on the first day after electrotransfection with psiRNA-EGFP, which could be explained by the more than 24 h half-life of the GFP protein.<sup>38</sup> An increased reduction in the fraction of cells expressing GFP was observed by fluorescence microscopy from the second to the fifth day after electrotransfection with psiRNA-EGFP, which

coincided with the mean GFP fluorescence intensity results. Nevertheless, the mean values of GFP fluorescence between the experimental (psiRNA-EGFP) and control groups (psiRNA-scr) did not show statistically significant differences. This may be because only 20% of cells in the LPB<sub>GFP</sub> cell line stably expressed GFP. Namely, the cells which did not express GFP and were possibly electrotransfected with psiRNA-EGFP contributed to the apparently lower GFP silencing effect. We believe that more convincing GFP silencing after electrotransfection with psiRNA-EGFP may therefore be achieved by using the LPB<sub>GFP</sub> cell line, in which all cells would express GFP. Another factor that could affect the GFP silencing effect is the CMV enhancer/promoter, which drives shRNA expressing plasmid DNA. It has been shown that CMV enhancer/promoter can be inactivated in cells by methylation, which inhibits transgene expression. Methylation of the promoter may thus be a critical event in gene transcription.<sup>39,40</sup>

The sensitivity of LPB<sub>GFP</sub> cells to electric pulse conditions did not exceed the critical level. Cell proliferation was reduced by only 33%. More concerning is the cytotoxicity of psiRNA-EGFP and even more of psiRNA-scr introduced into the cells by electroporation, which resulted in a 65% and 70% reduction of colony formation, respectively, in comparison with the untreated control group (LPB<sub>GFP</sub>). It is probable that LPB cells that had been previously transfected with pEGFP-N1 might have increased sensitivity to electrotransfection by default, since expression of exogenous GFP can affect cell viability.<sup>41</sup> However, cytotoxicity results are not so relevant in demonstrating the potentiality of electroporation as a technique for efficient delivery of plasmid DNA expressing shRNA into cancer cells, although they should be taken into account when the therapeutic shRNA molecules are tested.

However, the results of the present study showed that electroporation is feasible and effective method for the *in vitro* delivery of plasmid DNA expressing shRNA. Further studies should be extended to *in vivo* experiments examining whether electrically assisted delivery of plasmid DNA expressing shRNA-GFP into LPB<sub>GFP</sub> subcutaneous tumors may reduce GFP expression levels in tumor cells for a sufficient period of time. *In vivo* electrotransfection of plasmid DNA into tumors has been reported as an efficient gene delivery method, with great potential for cancer treatment.<sup>22,23</sup> On the other hand, low transfection efficiencies have been obtained in some tumor types with this delivery method, which may be a problem in its application for siRNA mediated cancer gene therapy.<sup>42-46</sup> However, only a few *in vivo* studies have demonstrated successful silencing of a target gene after electrotransfection of tumors with plasmid DNA expressing therapeutic shRNA.<sup>30,31</sup> Reporter genes should be used for validation of the method. Takahashi and coworkers used plasmid DNA expressing shRNA directed against luciferase, whereby luciferase activity was measured over time indirectly.<sup>29</sup> Namely, tumors were excised and homogenized, the homogenate was centrifuged, the supernatant was then mixed with luciferase assay buffer and the chemiluminescence produced was measured in a luminometer. The ability to image a reporter gene directly can save significant time and resources, especially in view of the high cost of siRNA molecules and the number of animals required for *in vivo* studies. Direct imaging of the GFP reporter gene expression profile after treatment would enable non-invasive monitoring of siRNA activity in mice over time. On the basis of GFP reporter gene imaging, we can predict whether electrically assisted delivery of plasmid DNA expressing GFP specific shRNA into tumors in mice is safe,

specific and effective, how much plasmid DNA transfer occurred, and whether and for how long the shRNA is expressed in a specific tumor type.

## Conclusion

Our *in vitro* results showed that electroporation is a feasible and effective method for delivering plasmid DNA expressing shRNA into tumor cells *in vitro*, which was shown through efficient silencing of the targeted reporter gene for GFP. Imaging and measurements of GFP expression levels over time *in vitro* showed that electroporation, in combination with plasmid DNA as the gene delivery vector, can induce a prolonged gene silencing effect in rapidly dividing LPB<sub>GFP</sub> cells. Moreover, electroporation proved to be reproducible, easy to perform and showed a low cell damaging effect, which are all important and preferential factors for *in vivo* experiments and, ultimately for clinical trials.

## Acknowledgement

The authors acknowledge financial support from the state budget by the Slovenian Research Agency (Projects No. P3-0003, J3-7044, J3-9580). We thank the Department of Cytopathology at the Institute of Oncology, Ljubljana, for help with flow cytometer analysis. We thank Prof. dr. Gregor Serša and Gregor Tevž for critically reading the manuscript and Mira Lavrič for help with experiments.

## References

- 1 Agami R. RNAi and related mechanisms and their potential use for therapy. *Curr Opin Chem Biol* 2002; **6(6)**: 829-34.
- 2 Caplen NJ. Gene therapy progress and prospects. Downregulating gene expression: the impact of RNA interference. *Gene Ther* 2004; **11(16)**: 1241-8.
- 3 Ryther RC, Flynt AS, Phillips JA, III, Patton JG. siRNA therapeutics: big potential from small RNAs. *Gene Ther* 2005; **12(1)**: 5-11.
- 4 Izquierdo M. Short interfering RNAs as a tool for cancer gene therapy. *Cancer Gene Ther* 2005; **12(3)**: 217-27.
- 5 Scherer L, Rossi JJ. Recent applications of RNAi in mammalian systems. *Curr Pharm Biotechnol* 2004; **5(4)**: 355-60.
- 6 Pai SI, Lin YY, Macaes B, Meneshian A, Hung CF, Wu TC. Prospects of RNA interference therapy for cancer. *Gene Ther* 2006; **13(6)**: 464-77.
- 7 Dykxhoorn DM, Palliser D, Lieberman J. The silent treatment: siRNAs as small molecule drugs. *Gene Ther* 2006; **13(6)**: 541-52.
- 8 Jana S, Chakraborty C, Nandi S, Deb JK. RNA interference: potential therapeutic targets. *Appl Microbiol Biotechnol* 2004; **65(6)**: 649-57.
- 9 Bantounas I, Phylactou LA, Uney JB. RNA interference and the use of small interfering RNA to study gene function in mammalian systems. *J Mol Endocrinol* 2004; **33(3)**: 545-57.
- 10 Behlke MA. Progress towards in vivo use of siRNAs. *Mol Ther* 2006; **13(4)**: 644-70.
- 11 Birmingham A, Anderson E, Sullivan K, Reynolds A, Boese Q, Leake D et al. A protocol for designing siRNAs with high functionality and specificity. *Nat Protoc* 2007; **2(9)**: 2068-78.
- 12 Paddison PJ, Caudy AA, Bernstein E, Hannon GJ, Conklin DS. Short hairpin RNAs (shRNAs) induce sequence-specific silencing in mammalian cells. *Genes Dev* 2002; **16(8)**: 948-58.
- 13 Brummelkamp TR, Bernards R, Agami R. A system for stable expression of short interfering RNAs in mammalian cells. *Science* 2002; **296(5567)**: 550-3.
- 14 Cullen BR. Induction of stable RNA interference in mammalian cells. *Gene Ther* 2006; **13(6)**: 503-8.
- 15 McManus MT, Petersen CP, Haines BB, Chen J, Sharp PA. Gene silencing using micro-RNA designed hairpins. *RNA* 2002; **8(6)**: 842-50.
- 16 McAnuff MA, Rettig GR, Rice KG. Potency of siRNA versus shRNA mediated knockdown in vivo. *J Pharm Sci* 2007; **96(11)**: 2922-30.
- 17 Gottesman MM. Cancer gene therapy: an awkward adolescence. *Cancer Gene Ther* 2003; **10(7)**: 501-8.
- 18 Meyer M, Wagner E. Recent developments in the application of plasmid DNA-based vectors and small interfering RNA therapeutics for cancer. *Hum Gene Ther* 2006; **17(11)**: 1062-76.
- 19 Xie FY, Woodle MC, Lu PY. Harnessing in vivo siRNA delivery for drug discovery and therapeutic development. *Drug Discov Today* 2006; **11(1-2)**: 67-73.
- 20 Russ V, Wagner E. Cell and tissue targeting of nucleic acids for cancer gene therapy. *Pharm Res* 2007; **24(6)**: 1047-57.
- 21 Sersa G, Cemazar M, Miklavcic D, Rudolf Z. Electrochemotherapy of tumours. *Radiol Oncol* 2006; **40(3)**: 163-74.
- 22 Heller LC, Heller R. In vivo electroporation for gene therapy. *Hum Gene Ther* 2006; **17(9)**: 890-7.
- 23 Tamura T, Sakata T. Application of in vivo electroporation to cancer gene therapy. *Curr Gene Ther* 2003; **3(1)**: 59-64.
- 24 Cemazar M, Sersa G. Electrotransfer of therapeutic molecules into tissues. *Curr Opin Mol Ther* 2007; **9(6)**: 554-62.
- 25 Fan Y, Xin XY, Chen BL, Ma X. Knockdown of RAB25 expression by RNAi inhibits growth of human epithelial ovarian cancer cells in vitro and in vivo. *Pathology* 2006; **38(6)**: 561-7.
- 26 Nakai N, Kishida T, Shin-Ya M, Imanishi J, Ueda Y, Kishimoto S et al. Therapeutic RNA interference of malignant melanoma by electrotransfer of small interfering RNA targeting Mitf. *Gene Ther* 2007; **14(4)**: 357-65.
- 27 Takei Y, Nemoto T, Mu P, Fujishima T, Ishimoto T, Hayakawa Y et al. In vivo silencing of a molecular target by short interfering RNA electroporation: tumor vascularization correlates to delivery efficiency. *Mol Cancer Ther* 2008; **7(1)**: 211-21.

- 28 Golzio M, Mazzolini L, Ledoux A, Paganin A, Izard M, Hellaudais L et al. In vivo gene silencing in solid tumors by targeted electrically mediated siRNA delivery. *Gene Ther* 2007; **14(9)**: 752-9.
- 29 Takahashi Y, Nishikawa M, Kobayashi N, Takakura Y. Gene silencing in primary and metastatic tumors by small interfering RNA delivery in mice: quantitative analysis using melanoma cells expressing firefly and sea pansy luciferases. *J Control Release* 2005; **105(3)**: 332-43.
- 30 Takahashi Y, Nishikawa M, Takakura Y. Suppression of tumor growth by intratumoral injection of short hairpin RNA-expressing plasmid DNA targeting beta-catenin or hypoxia-inducible factor 1alpha. *J Control Release* 2006; **116(1)**: 90-5.
- 31 Rejiba S, Wack S, Aprahamian M, Hajri A. K-ras oncogene silencing strategy reduces tumor growth and enhances gemcitabine chemotherapy efficacy for pancreatic cancer treatment. *Cancer Sci* 2007; **98(7)**: 1128-36.
- 32 Chiu YL, Rana TM. RNAi in human cells: basic structural and functional features of small interfering RNA. *Mol Cell* 2002; **10(3)**: 549-61.
- 33 Devi GR. siRNA-based approaches in cancer therapy. *Cancer Gene Ther* 2006; **13(9)**: 819-29.
- 34 Thomas M, Lu JJ, Ge Q, Zhang C, Chen J, Klivanov AM. Full deacylation of polyethylenimine dramatically boosts its gene delivery efficiency and specificity to mouse lung. *Proc Natl Acad Sci U S A* 2005; **102(16)**: 5679-84.
- 35 Grayson AC, Doody AM, Putnam D. Biophysical and structural characterization of polyethylenimine-mediated siRNA delivery in vitro. *Pharm Res* 2006; **23(8)**: 1868-76.
- 36 Merkerova M, Klamova H, Brdicka R, Bruchova H. Targeting of gene expression by siRNA in CML primary cells. *Mol Biol Rep* 2007; **34(1)**: 27-33.
- 37 Bartlett DW, Davis ME. Insights into the kinetics of siRNA-mediated gene silencing from live-cell and live-animal bioluminescent imaging. *Nucleic Acids Res* 2006; **34(1)**: 322-33.
- 38 Corish P, Tyler-Smith C. Attenuation of green fluorescent protein half-life in mammalian cells. *Protein Eng* 1999; **12(12)**: 1035-40.
- 39 Grassi G, Maccaroni P, Meyer R, Kaiser H, D'Ambrosio E, Pascale E et al. Inhibitors of DNA methylation and histone deacetylation activate cytomegalovirus promoter-controlled reporter gene expression in human glioblastoma cell line U87. *Carcinogenesis* 2003; **24(10)**: 1625-35.
- 40 Krishnan M, Park JM, Cao F, Wang D, Paulmurugan R, Tseng JR et al. Effects of epigenetic modulation on reporter gene expression: implications for stem cell imaging. *FASEB J* 2006; **20(1)**: 106-8.
- 41 Liu HS, Jan MS, Chou CK, Chen PH, Ke NJ. Is green fluorescent protein toxic to the living cells? *Biochem Biophys Res Commun* 1999; **260(3)**: 712-7.
- 42 Rols MP, Delteil C, Golzio M, Dumond P, Cros S, Teissie J. In vivo electrically mediated protein and gene transfer in murine melanoma. *Nat Biotechnol* 1998; **16(2)**: 168-71.
- 43 Wells JM, Li LH, Sen A, Jahreis GP, Hui SW. Electroporation-enhanced gene delivery in mammary tumors. *Gene Ther* 2000; **7(7)**: 541-7.
- 44 Bettan M, Ivanov MA, Mir LM, Boissiere F, Delaere P, Scherman D. Efficient DNA electrotransfer into tumors. *Bioelectrochemistry* 2000; **52(1)**: 83-90.
- 45 Cemazar M, Sersa G, Wilson J, Tozer GM, Hart SL, Grosel A et al. Effective gene transfer to solid tumors using different nonviral gene delivery techniques: electroporation, liposomes, and integrin-targeted vector. *Cancer Gene Ther* 2002; **9(4)**: 399-406.
- 46 Cemazar M, Wilson I, Dachs GU, Tozer GM, Sersa G. Direct visualization of electroporation-assisted in vivo gene delivery to tumors using intravital microscopy - spatial and time dependent distribution. *BMC Cancer* 2004; **4(81)**.

# Optimization of electrode position and electric pulse amplitude in electrochemotherapy

Anže Županič, Selma Čorović and Damijan Miklavčič

University of Ljubljana, Faculty of Electrical Engineering, Ljubljana, Slovenia

**Background.** In addition to the chemotherapeutic drug being present within the tumor during electric pulse delivery, successful electrochemotherapy requires the entire tumor volume to be subjected to a sufficiently high electric field, while the electric field in the surrounding healthy tissue is as low as possible to prevent damage. Both can be achieved with appropriate positioning of the electrodes and appropriate amplitude of electric pulses.

**Methods.** We used 3D finite element numerical models and a genetic optimization algorithm to determine the optimum electrode configuration and optimum amplitude of electric pulses for treatment of three subcutaneous tumor models of different shapes and sizes and a realistic brain tumor model acquired from medical images.

**Results.** In all four tumor cases, parallel needle electrode arrays were a better choice than hexagonal needle electrode arrays, since their utilization required less electric current and caused less healthy tissue damage. In addition, regardless of tumor geometry or needle electrode configuration, the optimum depth of electrode insertion was in all cases deeper than the deepest part of the tumor.

**Conclusions.** Our optimization algorithm was able to determine the best electrode configuration in all four presented models and with further improvement it could be a useful tool in clinical electrochemotherapy treatment planning.

*Key words:* electrochemotherapy; electroporation; subcutaneous tumor; finite element method; numerical modeling; optimization

## Introduction

Electrochemotherapy (ECT) is an effective local tumor therapy performed by the administration of chemotherapeutic drugs followed by the application of local high-voltage electric pulses.<sup>1, 2</sup> The electric

pulses cause transient structural changes (electroporation) of tumor cell membranes and thus increase the entrance of the chemotherapeutic drugs. This potentiates the chemotherapeutic effect and lowers the required drug dose.<sup>3</sup> Numerous studies have demonstrated ECT to be a very efficient treatment in various tumor types; in recent years, it has become a treatment of choice for cutaneous and subcutaneous tumor nodules of different histologies.<sup>4-9</sup>

Two conditions have to be met for ECT to be efficient: 1) a sufficient amount of chemotherapeutic drug has to be present in the

Received 19 May 2008

Accepted 29 May 2008

Correspondence to: Prof. Dr. Damijan Miklavčič, University of Ljubljana, Faculty of Electrical Engineering, Tržaška 25, SI-1000 Ljubljana, Slovenia, Phone: +386 1 4768 456, Fax: +386 1 4264 658, E-mail: damijan.miklavcic@fe.uni-lj.si

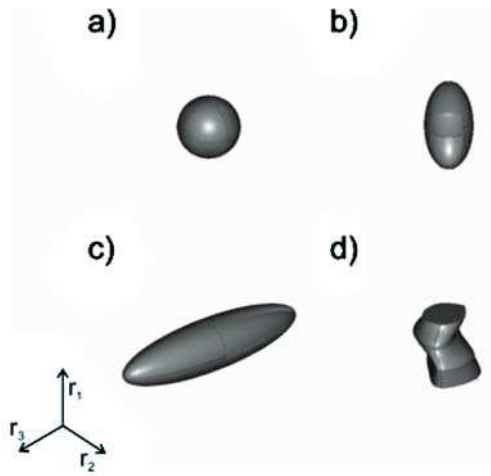


**Figure 1.** 3D subcutaneous tumor geometries. a) sphere ( $r_{1,3} = 2$  mm); b) ellipsoid positioned deeper in tissue ( $r_1 = 4$  mm,  $r_{2,3} = 2$  mm); c) ellipsoid ( $r_{1,2} = 2$  mm,  $r_3 = 8$  mm); d) realistic tumor geometry from medical images ( $r_1 = 3.8$  mm,  $r_2 = 2.4$  mm,  $r_3 = 2.6$  mm).

target tissue, when the electric pulses are applied; 2) the electric pulses have to reversibly electroporate the entire tumor volume, which means that the electric field established by the pulses should be of a magnitude between the reversible and irreversible electroporation threshold ( $E_{rev} < E < E_{irrev}$ ). The optimal ECT protocol should thus destroy all tumor cells, while minimising electrically induced damage to healthy tissue due to irreversible electroporation. This can be achieved by choosing the most suitable electrode configuration and the lowest amplitude of electric pulses that guarantees whole tumor electroporation.<sup>10,11</sup> Finding the optimum treatment parameters is often difficult, since it requires a complete understanding of the treatment mechanisms. Since the electric field is one of the most important factors in ECT efficiency, modeling the electric field distribution is not only necessary for understanding the treatment, but is also a crucial step towards treatment planning.<sup>12-14</sup> This study presents the first use of an ECT optimization algorithm on several different tumor geometries.

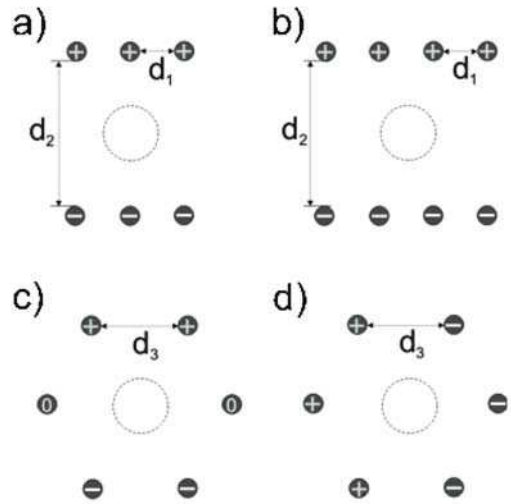


**Figure 2.** Electrode geometries and polarities: a) three needle electrode pairs (3 pairs); b) four needle electrode pairs (4 pairs); c) hexagonal needle electrode array with two electrodes on positive potential, two on negative and two neutral (2x2); d) hexagonal needle electrode array with three electrodes on positive potential and three on negative potential (3x3). Distances between electrodes  $d_{1-3}$  were among the optimized parameters in our optimization process. Diameter of all electrodes was 0.7 mm.

The goal of our study was to optimize the electric field distribution in four different 3D subcutaneous tumor models (Figure 1) by optimizing the electrode configuration around the tumor tissue and the amplitude of the electric pulses for each of the four different electrode geometries that have been used in clinics in recent years (Figure 2).<sup>1,15</sup> Optimization was performed using a combination of finite element numerical modeling and a genetic algorithm. All tumor/electrode cases were optimized for the following parameters: distances between electrodes (Figure 2), depth of electrode insertion and amplitude of electric pulses. Our optimization algorithm successfully found the best parameters in all cases and with some further improvement it could be a useful tool in clinical ECT treatment planning as well as in treatment planning of other electroporation based treatments.<sup>16-18</sup>

## Materials and methods

### Tissue properties and model geometry

Each model of a subcutaneous tumor consisted of two tissues: the target/tumor tissue and the surrounding healthy tissue. Four different tumor geometries were chosen, a small sphere, an ellipsoid positioned deeper in the tissue, an elongated ellipsoid and a realistic tumor geometry taken from a previous study and scaled for better comparison with the other tumor geometries (Figure 1).<sup>14</sup> All tissues were considered isotropic and homogeneous, the assigned conductivity values being 0.4 S/m for the tumors and 0.2 S/m for the healthy tissue. These values describe the conductivity at the end of the electroporation process.<sup>19</sup> The values were chosen in accordance with previous measurements of tumor and tissue conductivity and models of subcutaneous tumor and skin electroporation.<sup>13,16,20</sup> The electric field distribution was calculated for three different electrode geometries: two different parallel needle electrode arrays (Figure 2a,b) and a hexagonal electrode array with two different electrode polarities (Figure 2c,d). These geometries and polarities were chosen because they are frequently used in ECT research and therapy.

### Numerical modeling

Numerical calculations were performed with the commercial finite element software package COMSOL Multiphysics 3.4 (COMSOL AB, Sweden). The electric field distribution in the tissue, caused by the electroporative pulse, was determined by solving the Laplace equation for static electric currents:

$$-\nabla \cdot (\sigma \cdot \nabla \phi) = 0,$$

where  $\sigma$  and  $\phi$  are the conductivity of the tissue and electric potential, respectively. The boundary conditions used in our cal-

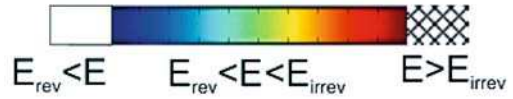


**Figure 3.** False color legend of Figs. 4, 5 indicating the degree of tissue permeabilization. The white region represents insufficiently permeabilized regions of tissue ( $E < E_{rev}$ ) and the patterned region represents irreversibly permeabilized regions of tissue ( $E \geq E_{irrev}$ ).

culations were a constant potential on the surface of the electrodes and electric insulation on all outer boundaries of the model.

The electric field distributions obtained in our models were displayed in the range from the reversible  $E_{rev} = 400$  V/cm to the irreversible electroporation threshold value  $E_{irrev} = 900$  V/cm (Figure 3). These values were taken from a previously published study, in which we estimated them by comparing *in vivo* measurements and numerical modeling of electroporation of a subcutaneous tumor.<sup>13,21</sup>

### Optimization

The genetic algorithm<sup>22</sup> was written in MATLAB 2007a (Mathworks, USA) and was run together with the finite element model using a link between MATLAB and COMSOL. The initial population of possible solutions was generated randomly, taking into account the following model constraints: range of distances between electrodes ( $d_1$ : 0.7-4.0 mm;  $d_2$ : 3.4-5.0 mm;  $d_3$ : 1.3-5.0 mm), range of depths of electrode insertion into tissue (-1.0-5.0 mm below the tumor) and range of amplitudes of electric pulses (1-1200 V). These constraints were chosen so that the calculation domain size, COMSOL meshing capabilities and oncology experts' demands for a safety margin<sup>23</sup> when treating solid tumors, were all respected. Solutions for reproduction were selected proportionally to their fitness, according to the fitness function:

**Table 1.** Optimized distances between electrodes ( $d_{1,3}$ ), depth of electrode insertion below the tumor and amplitude of electric pulse (U) are given for all analyzed tumor models and electrode geometries. Qualities of individual optimized solutions are described by the calculated values of total electric current through tissue (I), fraction of reversibly permeabilised target tissue ( $V_{Trev}/V_T$ ) and normalized volume of damaged healthy tissue ( $V_{Hirrev}/V_{sph}$ ).

Tumor	Electrode geometry	$d_1$ [mm]	$d_2$ [mm]	$d_3$ [mm]	Insertion depth [mm]	U [V]	I [A]	$V_{Trev}/V_T$	$V_{Hirrev}/V_{sph}$
	3 pairs	0.70	3.4		1.1	210	0.45	1	1.00
	4 pairs	0.70	3.4		0.9	210	0.52	1	1.03
	3x3			1.3	0.3	200	0.55	1	3.58
	2x2x2			1.3	0.3	220	0.32	1	1.77
	3 pairs	0.70	3.4		0.9	220	0.65	1	1.59
	4 pairs	0.70	3.6		0.9	220	0.75	1	1.39
	3x3			1.3	0.3	210	0.89	1	6.31
	2x2x2			1.3	0.7	220	0.47	1	2.51
	3 pairs	2.60	3.4		0.9	320	0.88	1	7.40
	4 pairs	1.60	3.4		0.7	320	0.96	1	7.08
	3x3			4.3	0.5	550	1.19	1	15.84
	2x2x2			4.6	0.1	1160	1.25	1	31.22
	3 pairs	0.75	3.4		0.9	270	0.65	1	3.17
	4 pairs	0.70	3.4		0.7	270	0.70	1	3.39
	3x3			1.8	1.1	320	1.07	1	11.44
	2x2x2			1.6	0.9	320	0.55	1	5.45

$$F = 12 + 100 \cdot V_{Trev} - 10 \cdot V_{Hirrev} - V_{Hrev} - V_{Tirrev},$$

where F stands for fitness,  $V_{Trev}$  and  $V_{Tirrev}$  stand for the tumor volume subjected to the local electric field above  $E_{rev}$  and above  $E_{irrev}$  and  $V_{Hrev}$  and  $V_{Hirrev}$  stand for the volume of healthy tissue subjected to the local electric field above  $E_{rev}$  and above  $E_{irrev}$  respectively. The weights in the fitness function were set according to the importance of the individual parameters for efficient ECT. Namely,  $V_{Trev}$  is crucial for efficient ECT, so its weight is largest (100) in comparison to the weight of  $V_{Hirrev}$  (10), which was in turn larger than the weights of  $V_{Hrev}$  and  $V_{Tirrev}$  since their significance for successful electrochemotherapy is still debated. Other weight values that kept a

similar ratio gave similar results. The integer 12 is present only to ensure that the fitness function is always positive.

The selected solutions reproduced by cross-over or by mutation. The genetic algorithm was terminated after 100 generations, when the fitness of the highest ranking solution usually reached a plateau. The average computation time of the algorithm was two hours on a standard desktop PC (Windows XP, 3.0 GHz, 1 GB RAM).

## Results

The optimized parameters of electrochemotherapy (ECT) for all tumor/electrode cases are given in Table 1. The optimum distance

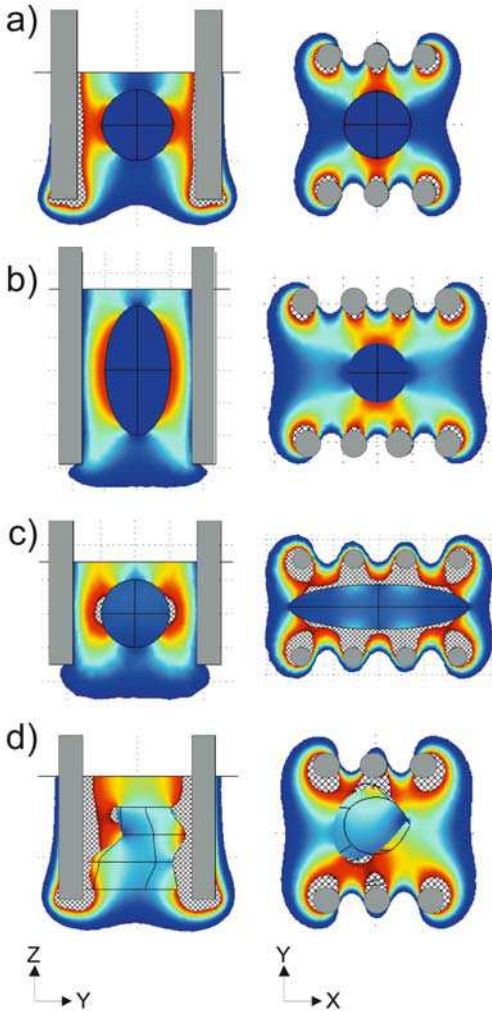


**Figure 4.** Electric field distribution for the optimized models of subcutaneous tumors is shown. In each case, only the best electrode configuration is given: a) three needle pairs for the spherical tumor; b) four needle pairs for the ellipsoid; c) four needle pairs for the ellipsoid deeper in tissue; d) three needle pairs for the realistic tumor. The electric distribution is shown in two central perpendicular planes: YZ and XY both passing through the center of the tumor. Corresponding values of parameters are given in Table 1.

between electrodes in a parallel row ( $d_1$ ) was similar for all tumor models, except, due to its size, for the elongated ellipsoid tumor geometry, for which successful electroporation required the electrodes to be

further apart. The electrodes were as close to each other as possible considering the parameter constraints, which guaranteed that the electric field distribution in the target tissue was homogeneous as possible (comparison of Figure 4b and Figure 4c). The optimum distance between electrode rows ( $d_2$ ) was also similar for all tumor geometries and as small as possible, the reason being that small inter-electrode distances required a lower voltage to ensure electroporation, thus also requiring less electric energy and causing less damage to tissue. The same is true for the distance between electrodes in a hexagonal array ( $d_3$ ), the reason this time being a combination of both homogeneity of the local electric field and lower required voltage. In contrast, the optimum depth of electrode insertion varied with the tumor and electrode geometry. Nevertheless, the optimum position for the electrodes was in all cases below the tumor. The optimum electric pulse amplitude did not differ much in cases of a spherical tumor and ellipsoid tumor deep in tissue but in other tumor geometries, parallel electrode arrays required considerably lower amplitudes than their hexagonal counterparts.

We compared the quality of the optimized solution in terms of total electric current through the tissue and extent of healthy tissue damage (Table 1 –  $V_{Hirrev}/V_{sph}$ ). We normalized the volumes of irreversibly electroporated tumor with the volume of a spherical tumor better to compare the amount of tissue damage between individual treatment cases. Parallel electrode arrays gave better results for all four tumor geometries. Three needle pairs always resulted in less total electric current. However, four needle pairs produced a more homogeneous field, which, in combination, caused three needle pairs to be a slightly better choice (less healthy tissue damage) for the spherical and the realistic

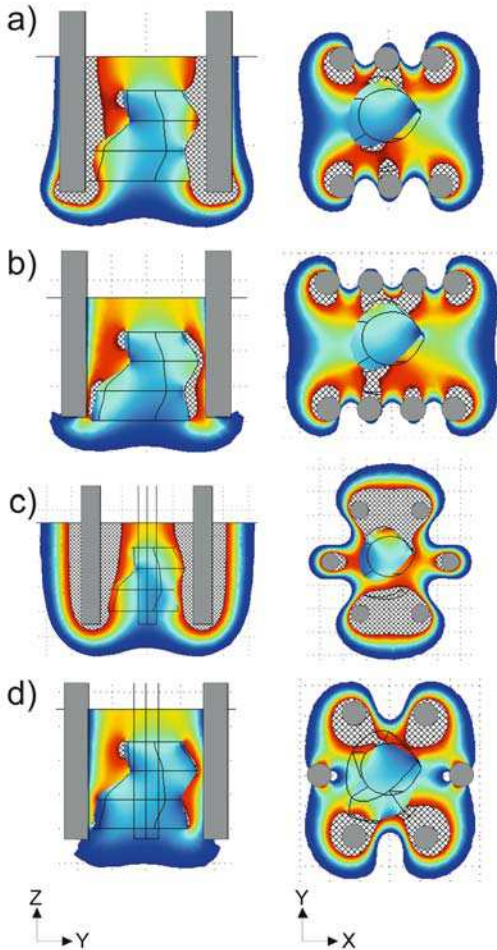


**Figure 5.** Electric field distribution for the optimized model of the realistic tumor with a) three needle pairs; b) four needle pairs; c) 3x3 hexagonal needle electrode array; d) 2x2x2 hexagonal needle electrode array is shown. The electric distribution is shown in two central perpendicular planes: YZ and XY both passing through the center of the tumor. Corresponding values of parameters are given in Table 1.

tumor geometry and four needle pairs to be slightly better for the other two geometries. The best electrode configurations for all tumor geometries and the corresponding electric field distributions are shown in Figure 4. Hexagonal electrodes caused considerably more healthy tissue damage ( $E > E_{\text{irrev}}$ ) than parallel electrodes, which can be seen

in Figure 5 for the realistic tumor geometry. The 3x3 hexagonal electrode array caused more healthy tissue damage than the other three geometries and also required the highest total electric current, mostly because the electric current ran between the closest positive and negative electrodes, instead of through the target tissue (Figure 5).

## Discussion

The aim of our study was to optimize the electrode configuration around the target tissue and electric pulse amplitude for ECT of four 3D models of subcutaneous tumors treated with four different needle electrode array geometries. In all 16 cases, the optimization resulted in reversible electroporation of the entire tumor (Table 1:  $V_{\text{Trev}}/V_{\text{T}} = 1$ ), which was the parameter with the highest weight in our fitness function. At the same time, the damage to healthy tissue was minimal. When treating a spherical tumor, only a volume of healthy tissue equal to the tumor volume was irreversibly electroporated (Table 1:  $V_{\text{Hirrev}}/V_{\text{sph}}$ ). Treatment of larger tumors caused more healthy tissue damage.

The usefulness of numerical modeling in predicting electroporation outcomes has already been demonstrated.<sup>14,15,19,24-26</sup> We examined the adequacy for ECT of needle electrode array geometries by calculating the values of total electric current through the model (must be as low as possible to avoid nerve stimulation<sup>27</sup> and not exceed the capacities of the electric pulse generator<sup>28</sup>) and volumes of reversibly and irreversibly electroporated tumor tissue and healthy tissue. Three-needle electrode pairs were best for the spherical and the realistic tumor geometry; they required the lowest total electric current and caused only a small volume of healthy tissue to be irreversibly electroporated (healthy tissue damage) (Figure 4).

Four-needle electrode pairs caused the least healthy tissue damage in the other tumor geometries, but they required more electric current (Figure 4), confirming previous results of our group - more electrodes mean a more invasive procedure, higher required current and lower required voltage to obtain the same target tissue coverage. Parallel electrode arrays gave much better results than the 2x2 and 3x3 hexagonal needle electrode arrays, mostly because they induced a much more homogeneous field and, consequently, a lower electric current density.

Our work built on a previous study by our group that optimized the distance and voltage between electrodes for a realistic brain tumor (the same tumor geometry that we used in a scaled form in this study).<sup>14</sup> Our present study took optimization one step further by optimizing for four different electrode geometries and for two additional parameters, *i.e.* distance between electrodes in a row and depth of electrode insertion, which lead to perhaps the most important practical result. It is very difficult to guess the best possible insertion depth, since it depends in complex ways on tumor geometry, electrode geometry, electroporation thresholds and the conductivities of tumor and healthy tissue. However, based on our results, electrodes should always be inserted deeper than the deepest part of the tumor (Table 1).

We chose a genetic algorithm as the optimization method, since different linear and non-linear constraints, such as the technical limitations of the high-voltage electric pulse generator (maximum output voltage and current) can be easily taken into account. A genetic algorithm also allows optimization of a large number of continuous, discrete and categorical parameters, *e.g.* type of electrodes and can give as a result many solutions of similar quality, which can nevertheless be topologically very different. This gives the treating physician more alterna-

tives for the positioning of electrodes, which can be very valuable if some of them are not easy to access. The major drawback of a genetic algorithm is the relatively long computation time. However, since it can be considerably shortened by using a more powerful computer or by making the optimization parameters discrete instead of continuous, we do not consider this to be a significant issue and believe that this approach is well suited to the problem being addressed.

Even though our algorithm gives good results, several challenges remain to be addressed before it can be used for treatment planning of ECT. We must determine the most appropriate level of complexity of our numerical models. In this study, we did not take into account changes to tissue conductivity due to electroporation, the possibility of several consecutive pulses being used, of changing the electric field orientation or of moving the electrodes during treatment of a larger tumor; all of which options must be considered in the future.<sup>13,15,25</sup> Another crucial development would be an algorithm that would convert medical images of the treatment area into 3D structures ready to import into numerical modeling software.

In conclusion, we demonstrated that numerical modeling and optimization can be efficiently combined to control the extent of tissue electroporation in ECT and to produce the optimum electrode configuration and amplitude of electric pulses. Our algorithm is a step towards effective treatment planning, not only in clinical ECT, but also in other electroporation based treatments, such as gene electrotransfer, transdermal drug delivery and irreversible tumor ablation.<sup>16-18</sup>

## Acknowledgements

This research was supported by the Slovenian Research Agency.

## References

1. Marty M, Sersa G, Garbay JR, et al. Electrochemotherapy - An easy, highly effective and safe treatment of cutaneous and subcutaneous metastases: Results of ESOPE (European Standard Operating Procedures of Electrochemotherapy) study. *Eur J Cancer Suppl* Nov 2006; **4**: 3-13.
2. Sersa G. The state-of-the-art of electrochemotherapy before the ESOPE study; advantages and clinical uses. *Eur J Cancer Suppl* 2006; **4**: 52-9.
3. Domenge C, Orlowski S, Luboinski B, DeBaere T, Schwaab G, Belehradek J, et al. Antitumor electrochemotherapy - New advances in the clinical protocol. *Cancer* 1996; **77**: 956-63.
4. Heller R, Gilbert R, Jaroszeski MJ. Clinical applications of electrochemotherapy. *Adv Drug Deliv Rev* 1999; **35**: 119-29.
5. Gothelf A, Mir LM, Gehl J. Electrochemotherapy: results of cancer treatment using enhanced delivery of bleomycin by electroporation. *Cancer Treat Rev* 2003; **29**: 371-87.
6. Tijink BM, De Bree R, Van D, Leemans CR. How we do it: Chemo-electroporation in the head and neck for otherwise untreatable patients. *Clin Otolaryngol* 2006; **31**: 447-51.
7. Mir LM, Gehl J, Sersa G, et al. Standard operating procedures of the electrochemotherapy: Instructions for the use of bleomycin or cisplatin administered either systemically or locally and electric pulses delivered by the Cliniporator (TM) by means of invasive or non-invasive electrodes. *Eur J Cancer Suppl* 2006; **4**: 14-25.
8. Snoj M, Rudolf Z, Cemazar M, Jancar B, Sersa G. Successful sphincter-saving treatment of anorectal malignant melanoma with electrochemotherapy, local excision and adjuvant brachytherapy. *AntiCancer Drugs* 2005; **16**: 345-8.
9. Sersa G, Cemazar M, Miklavcic D, Rudolf Z. Electrochemotherapy of tumours. *Radiol Oncol* 2006; **40**: 163-74.
10. Miklavcic D, Beravs K, Semrov D, Cemazar M, Demsar F, Sersa G. The importance of electric field distribution for effective in vivo electroporation of tissues. *Biophys J* 1998; **74**: 2152-8.
11. Miklavcic D, Semrov D, Mekid H, Mir LM. A validated model of in vivo electric field distribution in tissues for electrochemotherapy and for DNA electrotransfer for gene therapy. *Biochim Biophys Acta* 2000; **1523**: 73-83.
12. Miklavcic D, Corovic S, Pucihar G, Pavselj N. Importance of tumour coverage by sufficiently high local electric field for effective electrochemotherapy. *Eur J Cancer Suppl* 2006; **4**: 45-51.
13. Pavselj N, Bregar Z, Cukjati D, Batiuskaite D, Mir LM, Miklavcic D. The course of tissue permeabilization studied on a mathematical model of a subcutaneous tumor in small animals. *IEEE Trans Biomed Eng* 2005; **52**: 1373-81.
14. Sel D, Lebar AM, Miklavcic D. Feasibility of employing model-based optimization of pulse amplitude and electrode distance for effective tumor electroporomeabilization. *IEEE Trans Biomed Eng* 2007; **54**: 773-81.
15. Gilbert RA, Jaroszeski MJ, Heller R. Novel electrode designs for electrochemotherapy. *Biochim Biophys Acta* 1997; **1334**: 9-14.
16. Cukiati D, Batiuskaite D, Andre F, Miklavcic D, Mir LM. Real time electroporation control for accurate and safe in vivo non-viral gene therapy. *Bioelectrochemistry* 2007; **70**: 501-7.
17. Pliquett UF, Vanbever R, Preat V, Weaver JC. Local transport regions (LTRs) in human stratum corneum due to long and short 'high voltage' pulses. *Bioelectrochem Bioener* 1998; **47**: 151-61.
18. Al Sakere B, Bernat C, Connault E, Opolon O, Rubinsky B, Davalos R, et al. Tumour ablation with irreversible electroporation. *PLoS ONE* 2007; **11**.
19. Corovic S, Pavlin M, Miklavcic D. Analytical and numerical quantification and comparison of the local electric field in the tissue for different electrode configurations. *Biomed Eng Online* 2007; **6**.
20. Miklavcic D, Pavselj N, Hart FX. Electric properties of tissues. *Wiley Encyclopedia of Biomedical Engineering*. New York: John Wiley & Sons; 2006.
21. Semrov D, Miklavcic D. Calculation of the electrical parameters in electrochemotherapy of solid tumours in mice. *Comput Biol Med* 1998; **28**: 439-48.
22. Holland JH. *Adaptation in Natural and Artificial Systems: An Introductory Analysis with Applications to Biology, Control, and Artificial Intelligence*. Cambridge: MIT Press; 1992.
23. Gehl J, Geertsen PF. Palliation of haemorrhaging and ulcerated cutaneous tumours using electrochemotherapy. *Eur J Cancer Suppl* 2006; **4**: 35-7.
24. Gehl J, Sorensen TH, Nielsen K, Raskmark P, Nielsen SL, Skovsgaard T, et al. In vivo electroporation of skeletal muscle: threshold, efficacy and relation to electric field distribution. *Biochim Biophys Acta* 1999; **1428**: 233-40.

25. Sersa G, Cemazar M, Semrov D, Miklavcic D. Changing electrode orientation improves the efficacy of electrochemotherapy of solid tumors in mice. *Bioelectrochem Bioener* 1996; **39**: 61-6.
26. Sel D, Mazeres S, Teissie J, Miklavcic D. Finite-element modeling of needle electrodes in tissue from the perspective of frequent model computation. *IEEE Trans Biomed Eng* 2003; **50**: 1221-32.
27. Zupanic A, Ribaric S, Miklavcic D. Increasing the repetition frequency of electric pulse delivery reduces unpleasant sensations that occur in electrochemotherapy. *Neoplasma* 2007; **54**: 246-50.
28. Puc M, Corovic S, Flisar K, Petkovsek M, Nastran J, Miklavcic D. Techniques of signal generation required for electropermeabilization. Survey of electropermeabilization devices. *Bioelectrochemistry* 2004; **64**: 113-24.

# Ecotoxicologically relevant cyclic peptides from cyanobacterial bloom (*Planktothrix rubescens*) – a threat to human and environmental health

Bojan Sedmak<sup>1</sup>, Tina Eleršek<sup>1</sup>, Olga Grach-Pogrebinsky<sup>2</sup>, Shmuel Carmeli<sup>2</sup>,  
Nataša Sever<sup>1</sup>, Tamara T. Lah<sup>1</sup>

<sup>1</sup> National Institute of Biology, Ljubljana, Slovenia, <sup>2</sup> School of Chemistry, Raymond and Beverly Sackler Faculty of Exact Sciences, Tel Aviv University, Ramat Aviv Tel Aviv, Israel

**Background.** The information of the overall production of major cyanobacterial cyclic peptides in a water body is essential for risk assessment and for the prediction of future development of the bloom. A procedure that gives a review of both toxic and non-hepatotoxic hydrophilic cyclic peptide production is important to evaluate the ecological conditions in the water environment and to predict the release of dangerous toxic and tumour promoting substances.

**Methods.** The cyclic peptides were identified on the basis of their retention times, characteristic spectra, molecular masses and biological activity. The non-hepatotoxic cyclic peptides were characterised by their inhibition of porcine pancreatic elastase, while cytotoxicity to mammalian cells was tested with the MTT test on B16 cell line.

**Conclusions.** The method presented gives a rapid, simultaneous assessment, preliminary identification and estimation of bioactive cyclic peptides. The synthesis of non-hepatotoxic cyclic peptides can mediate the release various toxic and otherwise biologically active substances that induce systemic genotoxicity in mammals.

**Key words:** tumour promoters; microcystin; anabaenopeptin; planktopeptin; toxic cyanobacterial blooms; environmental health

## Introduction

Mass occurrence of cyanobacteria decreases the aesthetic value of recreational water bodies and diminishes the applicability of water resources, even for industrial purposes. It poses a serious risk to humans, live-

stock, wildlife, and consequently to overall environmental health especially during the blooms lysis. As a consequence, the World Health Organization has published provisional guidelines concerning the overall cyanobacterial cell density in environmental waters<sup>1</sup> and, more specifically, the presence of microcystins in drinking water.<sup>2</sup> Health risks arising from cyanobacterial blooms are also unequivocally stated in the new EU directive concerning the management of bathing water quality.<sup>3</sup>

Received 1 April 2008  
Accepted 23 April 2008

Correspondence to: Assist Prof. Bojan Sedmak, Ph.D., National Institute of Biology, Večna pot 111, 1000 Ljubljana, Slovenia, EU. Phone: +386 1 423 33 88; Fax: +386 1 241 29 80; E-mail: bojan.sedmak@nib.si

There are various reasons why the presence of different types of cyclic peptides in the bloom should be monitored. The harmful effects of cyanobacteria cannot be attributed just to hepatotoxins or neurotoxins. It was recently demonstrated that similarly to microcystins also anabaenopeptins and anabaenopeptilides inhibit protein phosphatase activity and that they may be found in tissues of various aquatic animals.<sup>4</sup> There is also the possibility of synergistic interactions between different toxic and "non-toxic" cyanobacterial metabolic products released in the water environment. Thus, crude cyanobacterial extracts exert stronger effects on vertebrates and invertebrates than exposure to the purified toxins.<sup>5,6</sup> In the area of human health risk assessment, the genotoxicity of microcystins is probably of major importance.<sup>7,8</sup>

Recent studies have provided evidence that the presence of different cyanobacterial cyclic peptides influence also the physiology of cyanobacteria themselves and may have a strong impact on their blooming capacity.<sup>9-12</sup> Last but not least the presence of cyanobacterial metabolites is in strong negative correlation with phytoplankton biodiversity.<sup>13,14</sup>

Detection of the separated peaks at a number of specific wavelengths, as described in this work, makes possible a simple and rapid qualitative and quantitative assessment of the presence and dominance of specific cyclic peptides. This method has broader application as a tool in ecotoxicological studies and monitoring of cyanobacterial blooms. At the same time the method when used for preparative purposes provides a fast and simple isolation method, especially for the more recent planktopeptins.<sup>15</sup>

Data from isolated cyanobacterial colonies and filaments reveal the enormous potential for synthesis of different types and groups of bioactive peptides. There is great variabil-

ity, not only in the microcystin group with over 60 known variants<sup>16</sup>, but also in the two major groups of "non-toxic" cyclic peptides. These are cyclic depsipeptides with the Ahp moiety, comprising at least 68 variants, and cyclic peptides possessing a ureido linkage such as anabaenopeptins with 29 variants. Representatives of both groups are regularly found in cyanobacterial bloom forming species.<sup>17</sup> In spite of the great metabolic potential and the variety of possible variants, only a few bioactive cyclic peptides dominate in individual natural blooms. This fact is not surprising since we know that representatives of individual groups although slightly diverse (microcystins) show basically the same effects on various phytoplanktons when present in the environment.<sup>11,12</sup> Similarly representatives of the two major groups of "non-toxic" cyclic peptides share a specific activity; the ability to trigger the lytic cycle in lysogen cyanobacterial cells.<sup>18</sup>

## Materials and methods

### Sampling site

Lake Bled: Latitude N (°) 46.362839, Longitude E (°) 14.098068, height 475m a.s.l. The lake is 2120 m long, 1080 m wide, 30 m deep and ca. 14.000 years old. Currently it contains  $31 \times 10^6$  m<sup>3</sup> water with a retention time of 3 years. The average water temperature is 12° C; in summer it reaches 24° C, and is covered with ice in winter. It is a dimictic oligotrophic - mesotrophic lake. The productivity is normally low and the inflows are rich and permanent. The nutrients in the phase of summer stratification diffuse from the lake bottom and support metalimnetic blooms. Almost every year *Planktothrix rubescens* (DC. ex Gomont) blooms appear in the lake and, under favourable meteorological and climatic conditions, migrate to the surface, frequently covering almost the entire lake.<sup>14</sup>

### Species determination

The species was identified according to Starmach<sup>19</sup> as *Oscillatoria rubescens* (DC. ex Gom.). Anagnostidis and Komarek<sup>20</sup> have introduced a new classification system of the order *Oscillatoriales* that takes into consideration up-to-date phenotypic as well as ultrastructural, biochemical, physiological and ecological characteristics. In this work *Oscillatoria rubescens* was redefined as *P. rubescens* comb. n. [basonym *Oscillatoria rubescens* DC. ex Gom. Ann. Sci. Nat. VII Bot., 16:204, 1892] (family: *Phormidiaceae*, order: *Oscillatoriales*).<sup>21</sup>

The bloom samples were analysed for plankton species composition and taxonomic determination under an inverted microscope (Nikon Eclipse TE300). Filaments and cells were measured with Lucia (System for Image Processing and Analysis LUCIA 4.6, Laboratory Imaging Ltd.). Cyanobacterial abundance was calculated by measuring the cumulative length of the filaments using the Bürker-Türk haemocytometer. The hypothetical 1 mm *P. rubescens* filament was in average composed of 336 cells. The cell concentration was determined by multiplying the total length in millimetres by the average cell number.

### Sampling procedure

The cyanobacterium *P. rubescens* was harvested with a 50 µm plankton net. The samples were kept cool in the dark until brought to the laboratory. They were concentrated in glass cylinders under natural light. In this way cell buoyancy was increased so that the cyanobacterial material that floated towards the surface was collected, while the remaining algal material, together with the zooplankton, sank to the bottom. The bloom was freeze-dried on a Christ Alpha 2-4 freeze dryer (Martin Christ, Germany).

### Analytical and preparative HPLC methods

For the extraction and isolation of cyclic peptides we optimized the Harada method.<sup>22,23</sup> Dried cyanobacteria (1000 mg) were extracted three times with 5% aqueous acetic acid (3 x 20 mL) for 30 min while stirring. The mixture was frozen to further disintegrate the filaments and to increase sedimentation. The extracts were centrifuged at 4000 rpm for 10 min. The combined supernatants were applied to preconditioned 500 mg reversed-phase disposable columns (LiChrolut RP-18, Merck). The columns containing the extract were washed with 20 mL of 10% methanol and the cyclic peptides eluted with 2 mL methanol (LiChrosolv, Merck), evaporated to dryness under nitrogen stream and the residues, eluted from the columns dissolved in the buffer for HPLC analysis.

Analytical HPLC method: Samples were analysed by HPLC, using isocratic elution with methanol:0.05 M phosphate buffer 58:42 (v/v) pH 3.0.<sup>13</sup> In order to obtain a better resolution of the peaks of interest, we modified the ratio of the mobile phase to methanol: 0.05 M phosphate buffer 50:50 (v/v) pH 3. The extracts were separated on an analytical Hibar Pre-Packed RT 125-4 LiCrospher 100 RP-18 (5 µm) column (Merck), flow rate 1 mL min<sup>-1</sup>, using HPLC/PDA (Waters) to visualise cyclic peptides.

Preparative HPLC method: Cyclic peptides were isolated from the combined supernatants under the same conditions as above using a preparative Spherisorb S 10 ODS2 column (Phase Separation Inc., UK) with a flow rate of 10 mL min<sup>-1</sup>.<sup>13</sup> The HPLC/PDA equipment consisted of a Waters 600 Controller, Waters 616 pump and Waters PDA Detector. Millennium<sup>(32)</sup> software (Ver. 3.0, Waters) was used to run the hardware and to process the data.

### Identification and visualisation of cyclic peptides with a photodiode array detector (PDA)

The column eluate was monitored at four different wavelengths ( $\lambda_{\text{max}}$ ) – 238, 225, 220 and 215 nm – in order to locate and distinguish microcystins from other bioactive cyclic peptides of interest. The wavelengths are characteristic of individual cyclic peptides; microcystins have a characteristic absorption at 238 nm, while representatives of the other two groups have absorption maxima at lower wavelengths. The depsipeptide planktopeptin BL1125 was detected at 225 nm and anabaenopeptins B and F at 220 nm and 215 nm respectively. Both types of non-toxic cyclic peptides have additional characteristic absorption maxima at 278-279 nm.<sup>15</sup> The presence of these absorption maxima confirmed the preliminary identification. From the individual peaks the amounts of the cyclic peptides were calculated by comparison of the integrated peak areas with the values from the calibration curves that were standardised by previously isolated cyclic peptides in pure form.

### Molecular mass determination by mass spectrometry (MS)

Molecular masses were determined with a Finnigan LCQ Classic ion trap mass spectrometer (Thermo Finnigan, San Jose, USA) with ESI ion source. Samples, dissolved in pure methanol, were injected directly at a rate of 5  $\mu\text{L min}^{-1}$ . Analysis conditions were: spray voltage 6 kV, sheath gas flow 60 (arbitrary units) and auxiliary gas flow 5 (arbitrary units); tube lens offset 55 V, capillary voltage 40 V and capillary temperature 220 °C. The isolated cyclic peptides were scanned from 150 to 2000 Daltons at positive polarity.

### Chlorophyll a determination

Chlorophyll *a* was determined by the method of Vollenweider.<sup>24</sup> Cells were harvested by concentrating samples on glass microfibre Whatman GF/C filters (Whatman Ltd, Maidstone, UK), followed by extraction with hot methanol.

### Enzyme assays

Porcine pancreatic elastase (Serva, Germany) activity was assayed spectrophotometrically<sup>25</sup>, using N-Succinyl-Ala-Ala-Ala-*p*-nitroanilide (Suc(Ala)<sub>3</sub>-NA, Sigma, Germany) as the substrate<sup>27</sup> in a total volume of 200  $\mu\text{L}$ . A sample (20  $\mu\text{L}$  of inhibitor) was added to the assay mixture (70  $\mu\text{L}$ ) containing 90 mM Tris-HCl pH 8.0, 10 mM CaCl<sub>2</sub> and 50 mEU of elastase (10  $\mu\text{L}$ ). After incubation for 30 minutes at room temperature (20 °C), 100  $\mu\text{L}$  of 2 mM substrate was added to the assay mixture at 25 °C. The reaction was monitored at 405 nm in microtiter plates, using a GENios microplate reader (Tecan, Austria). The data were analysed using Magellan software (Tecan, Austria).

Values of inhibition constants,  $K_i$ , were obtained for inhibition of the elastase catalysed hydrolysis by cyclic peptides. Three different substrate concentrations (0.5 mM, 0.75 mM and 1 mM) were used. The concentrations of inhibitors were: unknown (Unk.): 0.09 – 1.76  $\mu\text{M}$ ; AnP B: 0.65 – 64.6  $\mu\text{M}$ ; AnP F: 0.68–68.2  $\mu\text{M}$ ; PP BL1125: 0.01 – 5.96  $\mu\text{M}$ . Michaelis constants,  $K_M$ , were determined by fitting the Michaelis-Menten equation directly to the data using a Lineweaver-Burk plot<sup>27</sup>. An Easson-Stedman plot yields the apparent inhibition constant,  $K_i$  (*app*), from which  $K_i$  was calculated<sup>28</sup> according to

$$K_i = \frac{K_i(\text{app.})}{1 + \frac{(S^\circ)}{K_M}}$$

**Table 1.** Effectiveness of serial extraction of cyclic peptides from *Planktothrix rubescens* with 5% acetic acid

Extraction number	AnP B		AnP F		PP BL1125		[D-Asp <sup>3</sup> ]MC-RR	
	R.T. 2.9 min		R.T. 3.0 min		R.T. 3.3 min		R.T. 4.7 min	
	mg/ml*	Tot. yield**	mg/ml*	Tot. yield**	mg/ml*	Tot. yield**	mg/ml*	Tot. yield**
I.	1.9	41.2	1.56	43.5	1.0	33.1	9.0	46.4
II.	2.7	57.8	2.0	55.7	2.0	66.2	10.0	51.6
III.	< 0.1	1.0	< 0.1	0.8	< 0.1	0.7	0.4	2.0
Σ =	4.7		3.6		3.0		19.4	

Legend:

R.T. – retention time

AnP B – anabaenopeptin B, AnP F – anabaenopeptin F, PP BL – planktopeptin BL1125, [D-Asp<sup>3</sup>]MC-RR – [D-Asp<sup>3</sup>]microcystin RR

\* The quantities for a particular cyclic peptide were read from the related standard curve, based on the peak area.

\*\* Figures are the percentage of the total yield for cyclic peptides.

where ( $S^{\circ}$ ) is the substrate concentration. Assays were performed in triplicate.

### Cell viability assay (MTT)

The MTT test was used to assess viability, based on the capacity of viable cells to metabolise a tetrazolium colourless salt to the blue formazan in mitochondria.<sup>29</sup> Mammalian B 16 cells ( $5 \times 10^4$  cells ml<sup>-1</sup>) in the exponential growth phase were plated onto 96-microwell plates (200 µl) and chronically exposed to three final concentrations, 1 µM, 10 µM and 100 µM, of individual cyclic peptides – planktopeptin BL1125, anabaenopeptin B and anabaenopeptin F – for 24 hours. After 21 hours the cells were assayed using 3-(4,5-Dimethylthiazolyl-2)-2,5-diphenyltetrazolium salt (MTT, Sigma) and incubated for an additional three hours. The medium was removed and the formazan produced was dissolved 200 µl DMSO (Sigma). The optical density (OD) was read at 570 nm, relative to a reference wavelength of 690 nm, with a GENios microplate reader (Tecan, Austria). Cells were grown in a CO<sub>2</sub> incubator at 37°C in an atmosphere of 5% CO<sub>2</sub>, and maintained

during the experiment in DMEM medium supplemented with 10% FBS and 1% penicillin/streptomycin (all Sigma). All assays were performed in triplicate.

## Results

The *P. rubescens* samples were over 99% monospecific. The species could be determined unequivocally on the basis of the taxonomic characteristics and of the red pigmentation caused by the presence of the accessory pigment phycoerythrin.

### Extraction yields

The three fold extraction procedure with acetic acid proved to be appropriate. Different cyclic peptides were extracted in various amounts in the three steps. In the second step the majority of all four major cyclic peptide representatives were extracted in amounts exceeding 50% of the total yield and less than 2% remained available for the third extraction (Table 1). Each 250 ml of concentrated bloom, with chlorophyll *a* content of 52.4 µg mL<sup>-1</sup> and cyanobacteri-

**Table 2.** Overall yields of biologically active peptides from *Planktothrix rubescens* bloom using 5 % acetic acid

Cyclic peptide	Extraction yield
	(% of dry weight)* 5% CH <sub>3</sub> COOH
AnP B	0.35
AnP F	0.27
PP BL1125	0.23
[D-Asp <sup>3</sup> ]MC-RR	1.5
Σ =	2.35

Legend:

Abbreviations as in Table 1.

The percentages of cyclic peptides were read from the related standard curves, based on the peak area.

\* Figures are the percentage of the total extraction yields for individual cyclic peptide.

al concentration of  $2.8 \times 10^8$  cells ml<sup>-1</sup>, gave on average 1.340 mg of lyophilized starting material. Chlorophyll *a* accounted for 0.97% of the dry weight of *P. rubescens*, and cyclic peptides 2.35% (Table 2). The average value for the intracellular content of chlorophyll *a* was 0.18 pg Chl *a* cell<sup>-1</sup> and, for microcystin RR, which was the major cyclic peptide in the sample, 0.29 pg [D-Asp<sup>3</sup>]MC-RR cell<sup>-1</sup>. The average microcystin quota per unit cell volume was 2.6 fg (μm<sup>3</sup>)<sup>-1</sup>.

### Isolation efficiency

Separation on the analytical column, using methanol:phosphate buffer 58:42, resulted in rapid elution of the analytes (Figure 1). However the resolution was better using

**Table 3.** The inhibition constants ( $K_i$ ) for four cyclic peptide inhibitors isolated from *Planktothrix rubescens* for porcine pancreatic elastase, using Suc(Ala)<sub>3</sub>-NA as substrate are presented. The abbreviations are the same as in Fig. 2. SE represents standard error.

Inhibitor	Elastase $K_i$ (nM) ± SE
Unknown	55.1 ± 1.4
AnP B	1768.0 ± 211.0
AnP F	1400.0 ± 130.0
PP BL 1125	5.5 ± 0.6

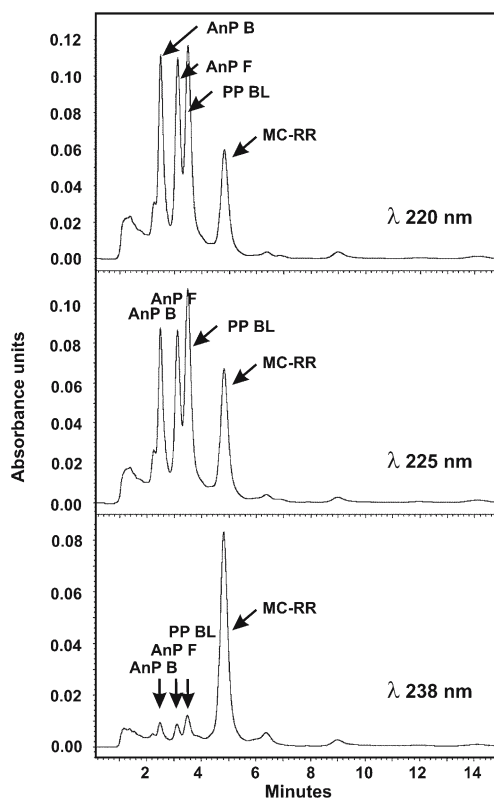


**Figure 1.** HPLC chromatogram of *Planktothrix rubescens* extract run on an analytical column. The diagrams show the same elution pattern monitored at three different wavelengths. MC-RR is clearly visible at the characteristic  $\lambda_{max}$  of 238 nm, while the other three cyclic peptides are seen only as minor peaks (the lowest panel). PP BL, AnP B and AnP F are better detected at lower wavelengths (upper two panels). Elution was with methanol: 0.05 M phosphate buffer 52:48 (v/v) pH 3. AnP B = anabaenopeptin B; AnP F = anabaenopeptin F; PP BL = planktopeptin BL1125; MC-RR = [D-Asp<sup>3</sup>]microcystin RR

a 50:50 ratio of the same mobile phase (Figure 2). Purification on the preparative column gave a larger number of peaks, indicating the presence of five microcystins and one additional protease inhibitor denoted as unknown (Figure 3). All major peaks were clearly separated and gave relatively pure substances as established with MS (Figure 4).

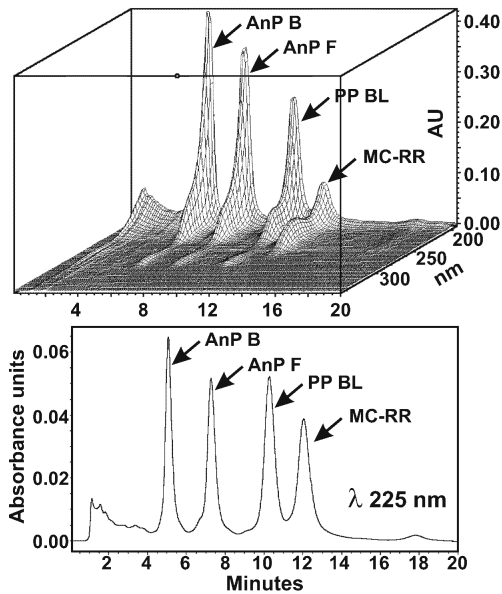


**Figure 2.** Isocratic elution with methanol: 0.05 M phosphate buffer 50:50 (v/v) pH 3 using the analytical column. The spectra of the four major cyclic peptides demonstrate the effectiveness of separation (upper panel). The same elution monitored at  $\lambda$  225 nm (lower panel).

Legend:

- R.T. = retention time
- AnP B = anabaenopeptin B
- AnP F = anabaenopeptin F
- MC = undetermined microcystin
- PP BL = planktopeptin BL1125
- MC-RR = [D-Asp<sup>3</sup>]microcystin RR
- Unk. = undetermined cyclic peptide

### Elastase inhibition

All four purified non-toxic cyclic peptides inhibited porcine pancreatic elastase. The unknown inhibitor and the depsipeptide PP BL1125 were the most effective inhibitors, with  $K_i = 5.5$  nM for PP BL1125 (Table 3).

### MTT cell proliferation assay

None of the three cyclic peptides tested showed cytotoxic effects even at the highest 100  $\mu$ M concentration. No effects were observed on the adhesive characteristics of

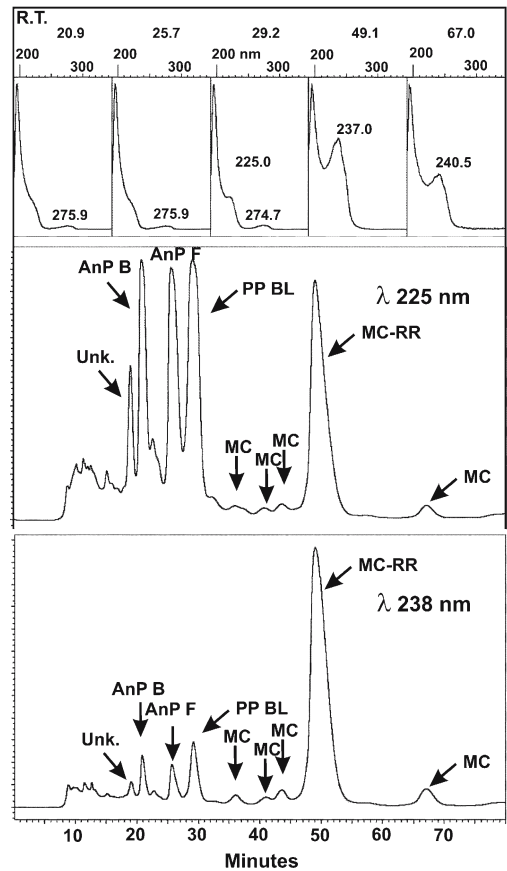


**Figure 3.** HPLC chromatogram of the *Planktothrix rubescens* extract monitored at 238 nm and 225 nm. The elution pattern was obtained from a preparative column using isocratic elution with methanol: 0.05 M phosphate buffer 50:50 (v/v) pH 3. The upper portion of the Figure shows the spectra of the three major non-toxic cyclic peptides and two microcystins with corresponding retention times. The lower two panels show the same elution chromatogram monitored at two wavelengths;  $\lambda$  225 nm for planktopeptin and 238 nm for microcystins. Apply legend as in Fig. 2.

the B16 cells, which remained attached during the course of the experiment.

## Discussion

The method makes possible a rapid separation and assessment in one HPLC step

**Table 4.** The impact of increasing concentrations of anabaenopeptin B anabaenopeptin F and planktopeptin BL1125, (1, 10 and 100  $\mu$ M) and exposure time (24 hours) on B16 cells as assessed by the MTT assay. The optical density of formazan production was read at 570 nm, relative to a reference of 690 nm. Each value represents triplicate data  $\pm$  S.E.

Inhibitor	CONCENTRATION ( M)			
	Control	1	10	100
	Optical density $\pm$ S.E.			
AnP B	1.131 $\pm$ 0.056	1.150 $\pm$ 0.163	1.108 $\pm$ 0.049	0.974 $\pm$ 0.134
AnP F	1.131 $\pm$ 0.056	1.123 $\pm$ 0.072	1.144 $\pm$ 0.111	1.198 $\pm$ 0.098
PP BL1125	1.003 $\pm$ 0.076	1.118 $\pm$ 0.124	1.056 $\pm$ 0.057	1.148 $\pm$ 0.036

of three groups of cyanobacterial cyclic peptides; depsipeptides and cyclic peptides with an ureido linkage and major microcystins. We focused on these three groups because they are related in structure and type of synthesis and are produced in large amounts that exceed even the production of chlorophyll *a*, which is the vital molecule in photoautotrophs (Table 2). The method, when applied for analytical purposes, gave good resolution of the cyclic peptides in symmetrical peaks (Figure 2).

#### *Extraction of cyclic peptides*

Five percent acetic acid aqueous extraction, in combination with solid phase extraction, was used for microcystin isolation, as introduced by Harada and co-workers.<sup>22,23</sup> It is effective for extracting almost all the peptides produced by cyanobacteria<sup>30</sup>, and does not extract many of the pigments that often make purification difficult; it enhances pellet formation and gives reasonable recovery.<sup>32</sup> The extraction procedure has proved to be selective for the cyclic peptides, since the major peaks corresponded to the three groups of cyanobacterial non-ribosomal cyclic products of interest (Figure 1 and Table 2).

#### *HPLC chromatography*

Use of a PDA detector at a number of wavelengths characteristic of the different groups of cyclic peptides enabled the latter

to be more readily identified and quantitatively estimated. Separation using the preparative column was highly effective and no further purification of cyclic peptides was needed (Figures 3, 4).

#### *Identification of cyclic peptides*

The identity of individual cyclic peptide was confirmed with the molecular weight information obtained from mass spectrometry (Figure 4). The "non-toxic" peptides were additionally identified by biological assay using elastase inhibition (Table 3). PP BL1125 exhibited the lowest inhibition constant, and the putative absence of cytotoxicity to mammalian cell lines suggested that this cyclic peptide is a potentially useful tool for studying the role of elastase in pathophysiological processes, such as inflammation and cancer. Planktopeptin and the anabaenopeptins were confirmed to be non-cytolytic, using the MTT cell proliferation assay (Table 4).

#### *Ecological implications of cyclic peptide production*

Cyanobacterial blooms are almost always mixtures of different cyanobacterial species and other phytoplankton organisms. Algae are progressively excluded from eutrophic water, and dominated by cyanobacteria.<sup>14</sup> Surface blooms and scums exhibit the lowest diversity which correlates higher total microcystin concentrations.<sup>13</sup>

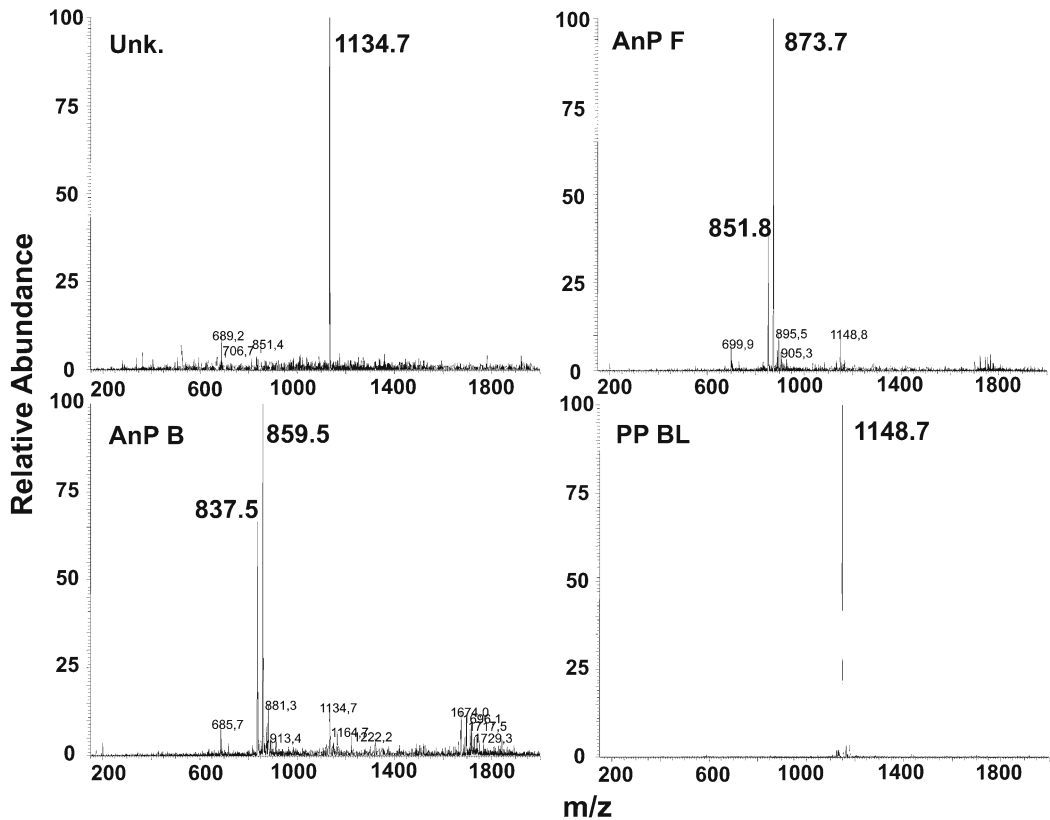


**Figure 4.** The MS spectra of four different cyclic peptides isolated from *Planktothrix rubescens*; unknown (Unk.), An F (upper figs.), AnP B and PP BL1125 (lower figs.). Note that, on MS spectra, the Unk. value 1134.7 refers to the ion  $[M+H]^+$ , AnP B value 859.5 refers to the ion  $[M+Na]^+$ , AnP F value 873.7 refers to the ion  $[M+Na]^+$  and PP BL1125 value 1148.7 refers to the ion  $[M+Na]^+$ . Abbreviations as in Fig. 2.

However, even in monospecific blooms, the production of bioactive cyclic peptides is highly variable. Bloom forming species belonging to the coccoid genera, such as *Microcystis*, and to filamentous genera, such as *Planktothrix*, include microcystin-producing and non-microcystin-producing strains.<sup>32,33</sup> Additionally, those genotypes that contain *mcy* genes can, in the case of the toxic cyanobacterium *Microcystis* spp.<sup>34</sup> and of the toxic cyanobacterium *Planktothrix* spp.<sup>36</sup>, be either active or inactive. The determination of the actual cyclic peptide presence is therefore the only reliable measure for their production.

In general, only particular cyanobacterial species prevail under specific environmental conditions. For example, the filamentous cyanobacterium *Planktothrix agardhii* is primarily distributed in eutrophic polymictic shallow lakes, frequently blooming during late summer<sup>36</sup>, whereas *P. rubescens* occurs in oligotrophic to mesotrophic deep dimictic lakes, blooming throughout the year, and often stratifies in the metalimnic layer.<sup>37</sup> Although the two species occupy different types of water body their natural blooms show very similar and stable cyclopeptide production. The main microcystin is almost always MC-RR, with its

de-methylated variant, together with ana-baenopeptins B and F and micropeptin representatives.<sup>15,38,39,40,41,42</sup> The microcystin composition in field populations of a single species changes little over time, as long as dominance of the particular species persists.<sup>40</sup> However there is also evidence that the predominating anabolism of defined bioactive cyclic peptides is not linked exclusively to cyanobacterial species and genera, but that their synthesis can be affected by geographical trends.<sup>42</sup>

The production of microcystins in *P. rubescens* blooms in Slovenia is high, which correlates well with the most recent data on toxin content from other locations.<sup>44</sup> The co-occurring non-toxic peptides, as well as the microcystin variants, were similar regardless of geographical provenance<sup>e.g.</sup><sup>42</sup> Thus, in the case of *Planktothrix rubescens*, the anabolism of cyclic peptides is linked primarily to the species and depends less on ecological factors.

Planktopeptins are new micropeptin-type serine protease inhibitors that are the most abundant of the "non-toxic" cyclic depsipeptides produced in *P. rubescens* blooms in Slovenia. Planktopeptin BL1125 is also the most potent Ahp-containing chymotrypsin and elastase inhibitor discovered so far<sup>15</sup>, with an inhibition constant in the nanomolar range.

It seems that all cyanobacterial cyclic peptides possess strong biological activities ranging between lethal effects on mammals<sup>45</sup> to the influence on morphology, physiology on algae and cyanobacteria<sup>11</sup> and gene expression in cyanobacteria themselves.<sup>12</sup> Evidently we have to reconsider the term non toxic cyclic peptides, since beside their strong biological activity as protease inhibitors they may be the main cause of cyanobacterial bloom collapse. Recently it was demonstrated that representatives of both groups of "non-toxic" cyclic peptides, ana-baenopeptins and planktopeptins, are

able to trigger the lytic cycle of temperate cyanophages inducing rapid lysis of cyanobacterial cells. The monitoring of these metabolic and/or ultrastructural disturbers is important, since they can be a valuable element for the prediction of cyanobacterial bloom lysis and the consequent release of toxic genotoxic and tumour promoting substances.<sup>19,46</sup>

## Acknowledgements

The work was supported by research project no. J1-7376, research program N° P1-0245ARRS (Slovenian Research Agency) and Ministry of Defence, Protection and Rescue 214-00-167/2003-30. We also thank Professor Roger Pain for critical reading of the manuscript.

## References

1. WHO. *Guidelines for Safe Recreational Water Environments*, Vol.1: Coastal and Fresh Waters, Geneva: World Health Organization; 2003.
2. WHO. *Guidelines for Drinking-water Quality*, 1<sup>st</sup> addendum to 3<sup>rd</sup> edition, Recommendations, Geneva: World Health Organization; 2006.
3. *Directive 2006/7/EC of the European Parliament and of the Council* of 15 February 2006 concerning the management of bathing water quality and repealing Directive 76/160/EEC. *Official J EU*, L 64: 37-51.
4. Gkelis S, Lanaras T, Sivonen K. The presence of microcystins and other cyanobacterial bioactive peptides in aquatic fauna collected from Greek freshwaters. *Aquatic Toxicol* 2006; **78**: 2-41.
5. Šuput D, Milutinovič A, Serša I, Sedmak B. Chronic exposure to cyanobacterial lyophilizate reveals stronger effects than exposure to pure microcystins - a MRI study. *Radiol Oncol* 2002; **36**: 165-7.
6. Keil C, Forchert A, Fastner J, Szewzyk U, Rotard W, Chorus I, Krätke R. Toxicity and microcystin content of extracts from a *Planktothrix* bloom and two laboratory strains. *Water Res* 2002; **36**: 2133-9.

7. Žegura B, Sedmak B, Filipič M. Microcystin-LR induces oxidative DNA damage in human hepatoma cell line HepG2. *Toxicon* 2003; **41**: 41-8.
8. Žegura B, Lah TT, Filipič M. The role of reactive oxygen species in microcystin-LR induced DNA damage. *Toxicology* 2004; **200**: 59-68.
9. Sukenik A, Eshkol R, Livne A, Hadas O, Rom M, Tchernov D, et al. Inhibition of growth and photosynthesis of the dinoflagellate *Peridinium gatunense* by *Microcystis* sp. (cyanobacteria): a novel allelopathic mechanism. *Limnol Oceanogr* 2002; **47**: 1656-63.
10. Vardi A, Schatz D, Beeri K, Motro U, Sukenik A, Levine A, Kaplan A. Dinoflagellate-cyanobacterium communication may determine the composition of phytoplankton assemblage in a mesotrophic lake. *Curr Biol* 2002; **12**: 1767-72.
11. Sedmak B, Eleršek T. Microcystins induce morphological and physiological changes in selected representative phytoplanktons. *Microbial Ecol* 2006; **51**: 508-15.
12. Schatz D, Keren Y, Vardi A, Sukenik A, Carmeli S, Börner T, et al. Towards clarification of the biological role of microcystins, a family of cyanobacterial toxins. *Environm Microbiol* 2007; **9**: 965-70.
13. Sedmak B, Kosi G. The role of microcystins in heavy cyanobacterial bloom formation. *J Plankton Res* 1998; **20**: 691-708; 1998; **20**: 1421.
14. Sedmak B, Kosi G. Harmful cyanobacterial blooms in Slovenia – Bloom types and microcystin producers. *Acta Biol Slovenica* 2002; **45**: 17-30.
15. Grach-Pogrebinsky O, Sedmak B, Carmeli S. Protease inhibitors from a Slovenian Lake Bled toxic waterbloom of the cyanobacterium *Planktothrix rubescens*. *Tetrahedron* 2003; **59**: 8329-36.
16. Sivonen K, Jones G. Cyanobacterial toxins. In Chorus I Bartram J, editors. *Toxic cyanobacteria in water*, Geneva: World Health Organization, E & FN Spon, 1999: 41-410.
17. Welker M, Brunke M, Preussel K, Lippert I, von Döhren H. Diversity and distribution of *Microcystis* (Cyanobacteria) oligopeptide chemotypes from natural communities studied by single-colony mass spectrometry. *Microbiol* 2004; **150**: 1785-96.
18. Sedmak B, Carmeli S, Eleršek T. »Non-toxic« cyclic peptides induce lysis of cyanobacteria - an effective cell population density control mechanism in cyanobacterial blooms. *Microb Ecol* 2007; DOI 10.1007/s00248-007-9336-9. *Radiol Oncol* 2008; **42**(2): 102-13.
19. Starmach K. *Cyanophyta – sinice, Glaucophyta – glaucofiti*. Flora słodkow. Polski 2. Warszawa: P.W.N.; 1966: 807 pp.
20. Anagnostidis K, Komarek J. Modern approach to the classification system of cyanophytes. 3 – *Oscillatoriales*. *Arch Hydrobiol* 1988; Suppl **80**: 1-4.
21. Gomont MM. Monographie des Oscillariées (Nostocacées, homocystées). *Ann Sci Nat Bot Ser* 7 1892; **15**: 263-368; **16**: 91-264.
22. Harada K-I, Matsuura K, Suzuki M, Oka H, Watanabe MF, Oishi S, et al. Analysis and purification of toxic peptides from cyanobacteria by reversed-phase high-performance chromatography. *J Chromatogr A* 1988; **448**: 275-83.
23. Harada K-I, Suzuki M, Dahlem AM, Beasley VR, Carmichael WW, Rinehart KL. Improved method for purification of toxic peptides produced by cyanobacteria. *Toxicon* 1988; **26**: 433-9.
24. Vollenweider RA. *Primary Production in Aquatic Environments*. Int Biol Prog Handbook 12, London: Blackwell Science 1974
25. Erlendsson LS, Fillippusson H. Purification and characterisation of ovine pancreatic elastase. *Comp Biochem Physiol Part B* 1998; **120**: 549-57.
26. Bieth J, Spiess B, Wermuth CG. The synthesis and analytical use of a highly sensitive and convenient substrate of elastase. *Biochem Med* 1974; **11**: 350-7.
27. Dixon M, Webb EC, Thorne CJR, Tipton KF. *Enzymes*, 3<sup>th</sup> ed., London: Longman; 1979.
28. Bieth JG. Pathophysiological interpretation of kinetic constants of protease inhibitors. *Bull Europ Physiopath Resp* 1980; **16**: 183-97.
29. Holst-Hansen C, Brünner N. MTT – cell proliferation assay. In: Celis JE, editor. *Cell biology: a laboratory handbook*, 2<sup>nd</sup> ed. San Diego: Academic Press; 1998; 16-18.
30. Fujii K, Sivonen K, Nakano T, Harada K-I. Structural elucidation of cyanobacterial peptides encoded by peptide synthetase gene in *Anabaena* species. *Tetrahedron* 2002; **58**: 6863-71.
31. Lawton LA, Edwards C. Purification of microcystins. *J Chromatogr A* 2001; **912**: 191-209.

32. Via-Ordorika L, Fastner J, Kurmayer R, Hisbergues M, Dittmann E, Komarek J, et al. Distribution of microcystin-producing and non-microcystin-producing *Microcystis* sp. in European freshwater bodies: Detection of microcystins and microcystin genes in individual colonies. *System Appl Microbiol* 2004; **27**: 592-602.
33. Mbedi S, Welker M, Fastner J, Wiedner C. Variability of the microcystin synthetase gene cluster in the genus *Planktothrix* (Oscillatoriales, Cyanobacteria). *FEMS Microbiol Lett* 2005; **245**: 299-306.
34. Kurmayer R, Dittmann E, Fastner J, Chorus I. Diversity of microcystin genes within a population of the toxic cyanobacterium *Microcystis* spp. In Lake Wannsee (Berkin, Germany). *Microbial Ecol* 2002; **43**: 107-118.
35. Kurmayer R, Christiansen G, Fastner J, Börner T. Abundance of active and inactive microcystin genotypes in populations of the toxic cyanobacterium *Planktothrix* spp. *Environ Microbiol* 2004; **6**: 831-41.
36. Scheffer M, Rinaldi S, Gagnani A, Mur LR, Van Nes EH. On the dominance of filamentous cyanobacteria in shallow, turbid lakes. *Ecology* 1997; **78**: 272-82.
37. Feuillade J. Studies on lake Nantua: The cyanobacterium (blue-green alga) *Oscillatoria rubescens* DC. *Arch Hydrobiol Beih Ergebn Limnol* 1994; **41**: 77-93.
38. Lindholm T, Meriluoto JAO. Recurrent depth maxima of the hepatotoxic cyanobacterium *Oscillatoria agardhii*. *Can J Fish Aquat Sci* 1991; **48**: 1629-34.
39. Namikoshi M, Rinehart KL. Bioactive compounds produced by cyanobacteria. *J Ind Microbiol* 1996; **17**: 373-84.
40. Fastner J, Erhard M, Carmichael WW, Sun F, Rinehart KL, Ronicke H, et al. Characterization and diversity of microcystins in natural blooms and strains of the genera *Microcystis* and *Planktothrix* from German freshwaters. *Arch Hydrobiol* 1999; **145**: 147-63.
41. Grach-Pogrebinsky O, Sedmak B, Carmeli S. Seco[D-Asp<sup>3</sup>]microcystin-RR and [D-Asp<sup>3</sup>, D-Glu(OMe)<sup>6</sup>]microcystin-RR, two new microcystins from a toxic water bloom of the cyanobacterium *Planktothrix rubescens*. *J Nat Prod* 2004; **67**: 337-42.
42. Barco M, Flores C, Rivera J, Caixach J. Determination of microcystin variants and related peptides present in a water bloom of *Planktothrix* (*Oscillatoria*) *rubescens* in a Spanish drinking water reservoir by LC/ESI-MS. *Toxicon* 2004; **44**: 881-6.
43. Gkelis S, Harjunpaa V, Lanaras T, Sivonen K. Diversity of hepatotoxic microcystins and bioactive anabaenopeptins in cyanobacterial blooms from Greek freshwaters. *Env Toxicol* 2005; **20**: 249-56.
44. Akcaalan R, Young FM, Metcalf JS, Morrison LF, Albay M, Codd GA. Microcystin analysis in single filaments of *Planktothrix* spp. in laboratory cultures and environmental blooms. *Water Res* 2006; **40**: 1583-90.
45. Carmichael WW. The toxins of cyanobacteria. *Sci Am* 1994; **270**: 64-72.
46. Filipič M, Žegura B, Sedmak B, Horvat-Žnidaršič I, Milutinović A, Šuput D. Subchronic exposure of rats to sublethal dose of microcystin-YR induces DNA damage in multiple organs. *Radiol Oncol* 2007; **41**: 15-22.



## Ugotavljanje povezanosti Bakerjeve ciste in pridruženega osteoartritisa medialnega dela kolena z magnetno resonanco (MR)

Vasilevska V, Szeimies U, Staebler A

**Izhodišča.** Namen raziskave je bil oceniti pomembnost povezave med povečanjem Bakerjeve ciste in osteoartritisom medialnega dela kolena.

**Bolniki in metode.** V obdobju dveh let smo z magnetno resonanco (MR) ovrednotili 66 bolnikov z znaki Bakerjeve ciste in osteoartritisom medialnega dela kolena (srednja starost 56 let, od 34-84 let, 23 moških in 43 žensk).

Ena skupina bolnikov je pokazala MR znake velike Bakerjeve ciste in druga znake majhne Bakerjeve ciste. Osteoarthritis medialnega dela kolena smo ocenjevali po naslednjih kriterijih: debelina hrustanca, degeneracija meniskusa, edem kostnega mozga, izliv. Medialni del sklepa pa je bil normalen.

**Rezultati.** V skupini z veliko Bakerjevo cisto smo pri 26 od 31 primerih (84%) ugotovili izgubo hrustanca. 18 od njih (69%) je imelo degeneracijo meniskusa 3. stopnje; 5 od 31 primerov (16%) pa degeneracijo medialne stopnje.

V drugi skupini bolnikov z majhno Bakerjevo cisto smo pri 17 od 35 primerih (48%) ugotovili izgubo hrustanca. 14 od njih (82%) je imelo degeneracijo meniskusa 3. stopnje. Pri 18 od 35 bolnikov (52%) smo ugotovili samo degeneracijo meniskusa brez izgube hrustanca; 67% jih je imelo degeneracijo 1. stopnje. Ugotovili smo statistično pomembno razliko med stopnjo povečanosti Bakerjeve ciste in stopnjo degeneracije medialnega meniskusa.

**Zaključki.** Velikost Bakerjeve ciste je močno povezana z degenerativnimi spremembami hrustanca in meniskusa medialnega dela kolenskega sklepa.

## Ovčja vratna vena kot model v intervencijski radiologiji

Lu W, Park WK, Uchida B, Timmermans HA, Pavcnik D, Keller FS, Rösch J

**Izhodišča.** Natančno poznavanje anatomije in fiziologije ovčje vratne vene omogoča uporabo ovce kot modela pri raziskovanju in proučevanju metod intervencijske radiologije. Zato smo v raziskavi želeli oceniti velikost ovčje vratne vene (VV) in anatomijo njenih zaklopk.

**Material in metode.** Pri 25 ovcah smo napravili ascendentno in descendentno venografijo VV.

**Rezultati.** V povprečju je največji premer VV znašal 13,34+/-1,18 mm. V vsaki veni smo našli povprečno 4,36+/-0,98 zaklopke. Vse zaklopke so bile zdrave in v 96,3% dvolistne.

**Zaključki.** Ovčja VV in človeška stegenska vena sta primerljivi tako po velikosti, številu in tipu zaklopk, kot po načinu delovanja zaklopk v pogojih zvišanega centralnega in hidrostatskega tlaka. Zato je ovčja VV dober model za oceno poslabšanja delovanja zaklopk na VV, zlasti pri perkutanih presaditvah zaklopk in pri ocenjevanju delovanja umetnih zaklopk.

## Epidermoid lateralnega ventrikla

Franko A, Holjar-Erlić I, Miletić D

**Izhodišča.** Epidermoidi, ki nastanejo v lateralnem ventriklu, so zelo redka bolezen. To so počasi rastoči tumorji, ki običajno povzročajo neznačilne znake poslabšanja miselnih funkcij.

**Prikaz primera.** Avtorji opišejo primer 49-letne bolnice z epidermoidom, ki je ležal v frontalnem delu lateralnega ventrikla. Pred operacijo in dokončno histološko potrditvijo bolezni so naredili preiskavo z magnetno resonanco.

**Zaključki.** Čeprav epidermoidi redko ležijo supraselarno in intraventrikularno, jih moramo upoštevati pri diferencialni diagnozi, vključno z meningeomi, ependimomi, subependimomi in papilomi horoidnega pleteža.

## Katepsini cisteinske skupine in stefini pri raku glave in vratu: pregled kliničnih raziskav

Strojan P.

**Izhodišča.** Rak glave in vratu predstavlja raznoliko skupino bolezni. V širokem spektru novejših biokemičnih in histoloških označevalcev ni bil do sedaj prepoznan še noben dejavnik kot dovolj zanesljiv napovedovalec poteka te bolezni in njenega odgovora na zdravljenje, da bi ga lahko uporabili pri vsakodnevem kliničnem delu. Med dejavniki, ki prispevajo k rasti tumorjev in zasevanju, so bile preiskovane tudi različne skupine proteaz, vpletenih v proteolitično razgradnjo sestavin zunajceličnega matriksa. Med njimi so tudi papainu podobne lizosomske cisteinske proteaze (npr. katepsina B in L) in njihovi fiziološki inhibitorji cistatini (npr. stefina A in B, cistatin C). Namen prispevka je podati pregled objavljenih raziskav, ki se nanašajo na klinično uporabnost katepsinov cisteinske skupine in njihovih endogenih inhibitorjev stefinov pri ploščatoceličnem karcinomu glave in vratu, ter predstaviti novejša rezultate raziskav s tega področja, izvedene na Onkološkem inštitutu Ljubljana in ORL kliniki Univerzitetnega kliničnega centra Ljubljana, Slovenija.

**Zaključki.** Kot kažejo naše izkušnje, ima imunohistokemično določanje katepsinov cisteinske skupine in stefinov omejeno napovedno vrednost. Nasprotno pa bi morali rezultate raziskav napovednega pomena stefina A v vzorcih citosola tkiva tumorjev obravnavati kot dosežke, ki omogočajo porajanje novih hipotez in zato zaslužijo nadaljnje vrednotenje v kontekstu prospektivne kontrolirane multicentrične raziskave.

## Ovrednotenje utišanja genov z molekulami shRNA s pomočjo elektroporacije v LPB fibrosarkomskih celicah

Mesojednik S, Kamenšek U, Čemazar M

**Izhodišča.** Utišanje onkogenov in ostalih genov, ki so vpleteni v razvoj in napredovanje malignih tumorjev, je obetaven način zdravljenja raka. Učinkovito in specifično utišanje genov lahko dosežemo z RNAi tehnologijo, z uporabo t.i. kratkih interferenčnih RNA (siRNA-short interfering RNA) oz. kratkih lasničnih RNA (shRNA-short hairpin RNA) molekul. Glavno oviro te tehnologije predstavlja nezadosten vnos interferenčnih molekul v tarčne celice. Namen naše raziskave je bil ovrednotiti učinkovitost elektroporacije kot metode za *in vitro* vnos plazmidne DNA, ki kodira shRNA, v mišje fibrosarkomske LPB celice.

**Zaključki.** Rezultati naše raziskave so pokazali, da je elektroporacija učinkovita metoda za vnos plazmidne DNA, ki kodira shRNA, v mišje fibrosarkomske LPB celice. Elektrotransfekcija zeleno fluorescirajočih LPB fibrosarkomskih celic (LPB<sub>GFP</sub>) s plazmidno DNA, ki kodira shRNA, specifično za GFP, je zmanjšala izražanje GFP gena. To smo pokazali na nivoju proteinov, kot tudi z merjenjem intenzitete GFP fluorescence v celicah. Zmanjšano izražanje GFP gena smo zaznali od drugega do petega dne po elektrotransfekciji celic. Elektroporacija je primerna metoda tudi zato, ker je enostavno izvedljiva in sama po sebi ne povzroča drastičnih celičnih poškodb, kar je pomembno za nadaljnje *in vivo* študije.

## Optimizacija položaja elektrod in amplitude električnih pulzov v elektrokemoterapija

Županič A, Čorović S, Miklavčič D

**Izhodišča.** Za uspešno elektrokemoterapijo je pomembno, da je poleg kemoterapevtika v tumorju in ob dovajanju električnih pulzov, ves tumor izpostavljen dovolj visokemu električnemu polju. Električno polje okoli tumorja pa mora biti čim nižje, da ne poškodujemo zdravega tkiva. Oboje je mogoče doseči s primerno postavitvijo elektrod in primerno amplitudo dovedenih električnih pulzov.

**Metode.** Za optimizacijo položaja elektrod in amplitude električnih pulzov smo uporabili 3D numerični model tumorja v tkivu in genetski algoritem. Uporabili smo tri različne tumorske geometrije različnih oblik in velikosti ter model realističnega možganskega tumorja, ki smo ga izdelali iz medicinskih slik.

**Rezultati.** V vseh tumorskih modelih so paralelna polja igelnih elektrod pokazala boljše rezultate kot heksagonalna polja igelnih elektrod, saj smo z njihovo uporabo porabili manj električne energije in povzročili manj poškodb zdravega tkiva. Ne glede na geometrijo tumorskega modela in na konfiguracijo igelnih elektrod, je bila optimalna globina vboda igelnih elektrod v tkivo vedno globlja kot najgloblji del tumorja.

**Zaključki.** Naša optimizacijska metoda je v vseh obravnavanih primerih pokazala optimalen rezultat. Ob dodatnem izboljšanju bi lahko postala uporabno klinično orodje v načrtovanju zdravljenja z elektrokemoterapijo.

## **Ekotoksikološko pomembni ciklični peptidi iz cianobakterijskega cveta (*Planktothrix rubescens*) – grožnja človeškemu in okoljskemu zdravju**

**Sedmak B, Eleršek T, Grach-Pogrebinsky O, Carmeli S, Sever N, Lah TT**

**Predpostavke.** Celovito poznavanje tvorbe glavnih cianobakterijskih cikličnih peptidov v vodnem telesu je osnova za oceno tveganja in za napoved bodočega razvoja cianobakterijskega cveta. Predstavljamo postopek, ki nam omogoča celovit pregled nad prisotnostjo toksičnih in ne-hepatotoksičnih vodotopnih cikličnih peptidov. To je pomembno za ovrednotenje ekoloških razmer in napovedovanje pojavljanja nevarnih tumorskih promotorjev in drugače strupenih snovi v vodnem okolju.

**Metode.** Ciklične peptide smo določili na podlagi njihovih retenzijskih časov, značilnih spektrov, molekularnih mas in bioloških aktivnosti. Ne-hepatotoksične ciklične peptide označuje inhibicija svinjske pankreasne elastaze, njihovo citotoksičnost pa smo preizkusili na celični liniji B16 z MTT testom.

**Zaključki.** Predstavljena metoda omogoča hitro in sočasno ugotavljanje količine ter vrste biološko aktivnih cikličnih peptidov. Tvorba večjih količin ne-hepatotoksičnih cikličnih peptidov omogoča nenadno sprostitvev različnih toksičnih in drugače biološko aktivnih snovi, ki povzročajo sistemsko genotoksičnost pri sesalcih.

## Notices

*Notices submitted for publication should contain a mailing address, phone and/or fax number and/or e-mail of a **Contact** person or department.*

---

### Lung cancer

June 12-14, 2008

The "11<sup>th</sup> Central European Lung Cancer Conference" will be offered in Ljubljana, Slovenia.

**Contact** Conference secretariat, Ms. Ksenia Potocnik, Department of Thoracic Surgery, Medical Centre Ljubljana, Slovenia; or call +386 1 522 2485; or fax +386 1 522 3968; or e-mail ksenia.potocnik@kclj.si; or see <http://www.ce-lung2008.org/>

---

### Cancer research

July 5-8, 2008

The "20<sup>th</sup> Meeting of the European Association for Cancer Research (EACR 20)" will be offered in Lyon, France.

**See** <http://www.ecco-org.eu>

---

### Lung cancer

July 9-12, 2008

The "International Lung Cancer Conference Liverpool 2008" will be offered in Liverpool, UK.

**E-mail:** [j.k.field@liv.ac.uk](mailto:j.k.field@liv.ac.uk); or see <http://www.ILCCL2008.com>

---

### Oncology

August 27-31, 2008

The UICC "2008 World Cancer Congress" will be offered in Geneva, Switzerland.

**See** <http://www.ecco-org.eu> or <http://www.worldcancercongress.org/uicc-congress08.html>

---

### Surgical oncology

September 10-13, 2008

The 14<sup>th</sup> Congress of the European Society of Surgical Oncology (ESSO 2008) will be offered in The Hague, The Netherlands.

**See** <http://www.ecco-org.eu>

---

### Neurooncology

September 12-14, 2008

The "8<sup>th</sup> Congress of the European Association of Neurooncology EANO 2008" will be offered in Barcelona, Spain.

**E-mail** [eano2008@medacad.org](mailto:eano2008@medacad.org) see <http://www.medacad.org/eano2008/>

---

### Medical oncology

September 12-16, 2008

The "33<sup>rd</sup> ESMO Congress" will be offered in Stockholm, Sweden.

**See** <http://www.esmo.org>

---

### Therapeutic radiology and oncology

September 14-18, 2008

The "European Society for Therapeutic Radiology and Oncology Meeting ESTRO 27" will take place in Göteborg, Sweden.

**Contact** ESTRO 27, <http://www.estro27.org>

---

**Therapeutic radiology and oncology**

*September 21-25, 2008*

The "50th American Society for Therapeutic Radiology and Oncology Annual Meeting ASTRO" will take place in Boston, USA.

**Contact** ASTRO, 8280 Willow Oaks Corporate Dr., Suite 500, Fairfax, VA 22031; or call +1 703 502-1550; or see <http://www.astro.org>

---

**Thoracic oncology**

*October 1-5, 2008*

The "International Thoracic Oncology Congress" will be offered in Dresden, Germany.

**E-mail:** [prof.manegold@t-online.de](mailto:prof.manegold@t-online.de)

---

**Paediatric oncology**

*October 2-6, 2008*

The "40th Congress of the International Society of Paediatric Oncology (SIOP)" will be offered in Berlin, Germany.

**See** <http://www.ecco-org.eu>

---

**Oncology**

*October 9-10, 2008*

The "3rd Latin American Cancer Conference" will take place in Vina del Mar, Chile.

**E mail** [nisehy@uol.com.br](mailto:nisehy@uol.com.br) or [rodrigo.arriagada@ki.se](mailto:rodrigo.arriagada@ki.se)

---

**Cancer therapy**

*October 21-24, 2008*

The 20th EORTC-NCI-AACR Symposium on "Molecular Targets and Cancer Therapeutics" will be offered in Geneva, Switzerland.

**Contact** EORTC-NCI-AACR 2008 Secretariat; C/o ECCO-European CanCer Organisation; Avenue E. Mounier, 83; B - 1200 Brussels Belgium; or phone +32 2 775 02 47; or fax +32 2 775 02 00; or e-mail: [barbara.vanbelle@ecco-org.eu](mailto:barbara.vanbelle@ecco-org.eu)

---

**Gastrointestinal neoplasia**

*November 3-4, 2008*

The ESO course "the Role of Endoscopy in the Management of Gastrointestinal Neoplasia" will be offered in Stresa, Italy.

**Contact** <http://www.ecco-org.eu>

*Radiol Oncol 2008; 42(2): VII-IX.*

---

**Oncology**

*November 13-15, 2008*

The Chicago/IASLC/ASCO/ASTRO symposiums "Malignancies of the Chest and Head and Neck" will be offered in Chicago.

**E-mail:** [evokes@medicine.bsd.uchicago.edu](mailto:evokes@medicine.bsd.uchicago.edu)

---

**Lung cancer**

*December 5-7, 2008*

The "3rd Asia Pacific Lung Cancer Congress" will be offered in Hyderabad; India.

**Contact** by e-mail Dr AA. Ranade [draaranade@yahoo.com](mailto:draaranade@yahoo.com); or see <http://www.aplcc.cpm>

---

**Head and neck oncology**

*February 26-28, 2009*

The "2nd International Conference on Innovative Approaches in Head and Neck Oncology" will take place in Barcelona, Spain.

See <http://www.estro.be>

---

**Targeted therapies**

*April 1-5, 2009*

The "4th IASLC/ASCO/ESMO International Meeting on Targeted Therapies on Lung Cancer" will be offered in Saint Paul de Vence, France.

**E-mail:** [pia.hirsch@uchsc.edu](mailto:pia.hirsch@uchsc.edu)

---

**Clinical oncology**

*May 29 – June 2, 2009*

The American Society of Clinical Oncology Conference (ASCO 2009) will be offered in Orlando, USA.

E mail [enews@asco.org](mailto:enews@asco.org); or see <http://www/asco.org>

---

**Lung cancer**

*July 31 - August 4, 2009*

The "13<sup>th</sup> World Conference on Lung Cancer" will be offered in San Francisco, USA.

**Contact** Conference Secretariat; e-mail [WCLC2007@ncc.re.kr](mailto:WCLC2007@ncc.re.kr); or see <http://www.iaslc.org/lumages/12worldconfannounce.pdf>

---

**Oncology**

September 4-8, 2009

The "34<sup>th</sup> ESMO Congress" will take place in Vienna, Austria.

**Contact** ESMO Head Office, Congress Department, Via La Santa 7, CH-6962 Viganello-Lugano, Switzerland; or +41 (0)91 973 19 19; or fax +41 (0)91 973 19 18; or e-mail [congress@esmo.org](mailto:congress@esmo.org); or see <http://www.esmo.org>

---

**Oncology**

September 20-24, 2009

The "15<sup>th</sup> ECCO and 34<sup>th</sup> ESMO Multidisciplinary Congress" will be offered in Berlin, Germany.

**See** <http://www.ecco-org.eu>

---

**Therapeutic radiology and oncology**

November 1-5, 2009

The "American Society for Therapeutic Radiology and Oncology Annual Meeting ASTRO" will take place in Chicago, USA.

**Contact** ASTRO, 8280 Willow Oaks Corporate Dr., Suite 500, Fairfax, VA 22031; or call +1 703 502-1550; or see <http://www.astro.org>

---

**Oncology**

October 8-12, 2010

The "35<sup>th</sup> ESMO Congress" will take place in Milan, Italy.

**Contact** ESMO Head Office, Congress Department, Via La Santa 7, CH-6962 Viganello-Lugano, Switzerland; or +41 (0)91 973 19 19; or fax +41 (0)91 973 19 18; or e-mail [congress@esmo.org](mailto:congress@esmo.org); or see <http://www.esmo.org>

---

**Oncology**

September 23-27, 2011

The "16<sup>th</sup> ECCO and 36<sup>th</sup> ESMO Multidisciplinary Congress" will be offered in Stockholm, Sweden.

**See** <http://www.ecco-org.eu>

---

**Oncology**

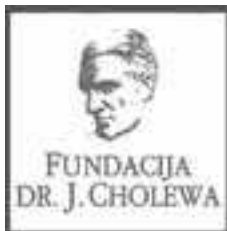
September 27 – October 1, 2013

The "17<sup>th</sup> ECCO and 38<sup>th</sup> ESMO Multidisciplinary Congress" will be offered in Amsterdam, The Netherlands.

**See** <http://www.ecco-org.eu>

*As a service to our readers, notices of meetings or courses will be inserted free of charge.*

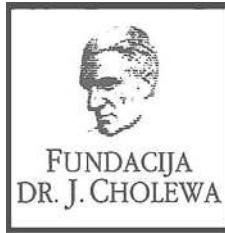
*Please send information to the Editorial office, Radiology and Oncology, Zaloška 2, SI-1000 Ljubljana, Slovenia.*



FUNDACIJA "DOCENT DR. J. CHOLEWA"  
JE NEPROFITNO, NEINSTITUCIONALNO IN NESTRANKARSKO  
ZDRUŽENJE POSAMEZNIKOV, USTANOV IN ORGANIZACIJ, KI ŽELIJO  
MATERIALNO SPODBUJATI IN POGLABLJATI RAZISKOVALNO  
DEJAVNOST V ONKOLOGIJI.

DUNAJSKA 106  
1000 LJUBLJANA

ŽR: 02033-0017879431



## **Activity of "dr. J. Cholewa" Foundation for Cancer Research and Education - a report for the second quarter of 2008**

The "Docent Dr. L Cholewa Foundation for Cancer Research and Education" continues to focus its activities and attention to cancer research and education in Slovenia. The Foundation also supports all the activities concerned with transmitting the latest diagnostic and therapy methods to the everyday research and clinical life and environment in Slovenia. With this in mind, it continues to assess carefully all the requests and proposals for research grants and scholarships submitted by Slovenian experts in oncology and other associated scientific activities.

The "Docent Dr. L Cholewa Foundation for Cancer Research and Education" continues to support the regular publication of "Radiology and Oncology" international medical scientific journal, that is edited, published and printed in Ljubljana, Slovenia. The support for "Radiology and Oncology" emphasizes the need for the spread of information and knowledge about advances in cancer among professionals and to many interested individuals in public in Slovenia and elsewhere. "Radiology and Oncology" is an open access journal, available on its own website, thus allowing its users and readers to access it freely.

As elsewhere, high quality research demands a lot of dedication and ample financial support, and many excellent ideas must not be prevented to succeed for the simple lack of it. In many developed countries with extensive research capabilities, especially in medicine and oncology, the researchers can often count on financial assistance in the form of grants and stipends provided by an ever growing number of funds and foundations. There are numerous opportunities for the "Docent Dr. L Cholewa Foundation for Cancer Research and Education" to offer similar assistance to researchers in oncology in Slovenia. With recent developments regarding the prevention and early detection of cancer in Slovenia, it could play an important role in supporting the collaboration and constant exchange of views among the experts in various scientific disciplines associated with aforementioned goals.

The Foundation considers the support of the publication of the results from cancer research in Slovenia and from Slovenian authors in international scientific journals and other means of communication worldwide as one of its main activities.

Tomaž Benulič, MD  
Borut Štabuc, MD, PhD  
Andrej Plesničar, MD

# SIEMENS

SiemensMedical.com/oncology



Oncology Care Systems • 4000 Nimitz Avenue, Concord, CA 94520 • (925) 246-8000  
© 2002 Siemens Medical Solutions USA, Inc.

## SEEK-FIND-ACT-FOLLOW - the Continuum of Oncology Care™

Siemens oncology portfolio comprises comprehensive workflow solutions integrating the full spectrum of care from screening/early detection and diagnosis through therapy and follow-up. All from one provider — with over 100 years history of innovation in medical technology.

Siemens proven clinical methods can help you to achieve more successful outcomes. How? Through industry-leading technology, increased productivity measures for

maximized utilization potential, and patient-friendly design and features.

Every day in the United States alone, 29,000 cancer patients receive radiation therapy delivered by Siemens linear accelerators. As clinical protocols transition to include IMRT and IGRT, Siemens seamlessly integrates the diagnostic and treatment modalities. That's what we call **Best Practice Oncology Care**.



Siemens medical  
Solutions that help

An X-ray image of a human knee joint, showing the femur, tibia, and patella. The image is presented as a dark rectangular frame with a white border, mimicking a physical X-ray print. In the top right corner of the frame, there is a small white label with some illegible text and a white arrow pointing to the right. The main text is overlaid on the lower part of the X-ray.

# Vse za rentgen

dobite pri nas!

- rentgenski filmi in kemikalije
- rentgenska kontrastna sredstva
- rentgenska zaščitna sredstva
- aparati za rentgen, aparati za ultrazvočno diagnostiko in vsa ostala oprema za rentgen

Sanolabor, d.d., Leskoškova 4, 1000 Ljubljana  
tel: 01 585 42 11, fax: 01 524 90 30  
[www.sanolabor.si](http://www.sanolabor.si)

 **Sanolabor**

# LABORMED

ZASTOPA PODJETJA:



## MENTOR

Prsni vsadki napolnjeni s silikonskim gelom, ekspanderji in drugi pripomočki pri rekonstrukciji dojke



### Köttermann (Nemčija):

laboratorijsko pohištvo, varnostne omare za kisline, luge, topila, pline in strupe, ventilacijska tehnika in digestorji



### Angelantoni scientifica (Italija):

hladilna tehnika in aparati za laboratorije, transfuzije, patologijo in sodno medicino

## CORNING

### Corning (Amerika):

specialna laboratorijska plastika za aplikacijo v imunologiji, mikrobiologiji, virologiji, ipd., mehanske eno- in večkanalne pipete in nastavki



MICRONIC

### Micronic (Nizozemska):

sistemi za shranjevanje vzorcev, pipete, nastavki za pipete



There's No Reason to Operate with Anyone Else

### Implantech (Amerika):

obrazni in glutealni vsadki



### Biomerica (Amerika):

hitri testi za diagnostiko, EIA /RIA testi



### Ehret (Nemčija):

Laminar flow tehnika, inkubatorji, sušilniki, suhi sterilizatorji in oprema za laboratorijsko vzrejo živali - kletke



### Dako (Danska):

testi za aplikacijo v imunohistokemiji, patologiji, mikrobiologiji, virologiji, mono- in poliklonalna protitelesa



### Sakura finetek (Evropa):

aparati za pripravo histoloških preparatov: mikro-inkriotomi, zalivalci, tkivni procesorji, barvalci, pokrivalci



### Integra Biosciens (Švica):

laboratorijska oprema za mikrobiologijo, biologijo celic, molekularno biologijo in biotehnologijo



### SpectrumDesigns MEDICAL (Amerika):

moški pektoralni vsadki



### Byron (Amerika):

liposuktorji in kanile za liposukcijo

LABORMED d.o.o.

Bežigranski dvor  
Peričeva 29, Ljubljana  
Tel.: (0)1 436 49 01  
Fax: (0)1 436 49 05

info@labormed.si

www.labormed.si

## ERBITUX – izbira za izboljšano učinkovitost

- Kolorektalni rak: učinkovitost dokazana v kombinaciji z irinotekanom
- Lokalno napredovali rak glave in vratu: signifikantno podaljšanje preživetja v kombinaciji z radioterapijo

Merck Serono Onkologija / biološko zdravljenje za boljšo kakovost življenja

### Erbitux 5 mg/ml raztopina za infundiranje (skrajšana navodila za uporabo)

Cetuksimab je monoklonsko IgG<sub>1</sub> protitelo, usmerjeno proti receptorju za epidermalni rastni faktor (EGFR). **Terapevtske indikacije:** Zdravilo Erbitux je v kombinirani terapiji z irinotekanom indicirano za zdravljenje bolnikov z metastatskim rakom debelega črevesa in danke in sicer po neuspešni citotoksični terapiji, ki je vključevala tudi irinotekan. Zdravilo Erbitux je v kombinaciji z radioterapijo indicirano za zdravljenje bolnikov z lokalno napredovalim rakom skvamoznih celic glave in vratu. Odmerjanje in način uporabe: Zdravilo Erbitux pri vseh indikacijah infundirajte enkrat na teden. Začetni odmerek je 400 mg cetuksimaba na m<sup>2</sup> telesne površine. Vsi naslednji tedenski odmerki so vsak po 250 mg/m<sup>2</sup>. **Kontraindikacije:** Zdravilo Erbitux je kontraindicirano pri bolnikih z znano hudo preobčutljivostno reakcijo (3. ali 4. stopnje) na cetuksimab. **Posebna opozorila in previdnostni ukrepi:** Če pri bolniku nastopi blaga ali zmerna reakcija, povezana z infundiranjem, lahko zmanjšate hitrost infundiranja. Priporočljivo je, da ostane hitrost infundiranja na nižji vrednosti tudi pri vseh naslednjih infuzijah. Če se pri bolniku pojavi huda kožna reakcija (≥ 3. stopnje po kriterijih *US National Cancer Institute, Common Toxicity Criteria*; NCI-CTC), morate prekiniti terapijo s cetuksimabom. Z zdravljenjem smete nadaljevati le, če se je reakcija pomirila do 2. stopnje. Priporoča se določanje koncentracije elektrolitov v serumu pred zdravljenjem in periodično med zdravljenjem s cetuksimabom. Po potrebi se priporoča nadomeščanje elektrolitov. Posebna previdnost je potrebna pri oslabljenih bolnikih in pri tistih z obstoječo srčno-pljučno boleznijo. Neželeni učinki: Zelo pogosti (≥ 1/10): dispneja, blago do zmerno povečanje jetrnih encimov, kožne reakcije, blage ali zmerne reakcije povezane z infundiranjem, blag do zmeren mukozitis. Pogosti (≥ 1/100, < 1/10): konjunktivitis, hude reakcije povezane z infundiranjem. Pogostost ni znana: Opazili so progresivno zniževanje nivoja magnezija v serumu, ki pri nekaterih bolnikih povzroča hudo hipomagnezijo. Glede na resnost so opazili tudi druge elektrolitske motnje, večinoma hipokalcemijo ali hipokaliemijo. **Posebna navodila za shranjevanje:** Shranjujte v hladilniku (2 °C - 8 °C). Ne zamrzujte. **Vrsta ovojnine in vsebina:** 1 viala po 20 ml ali 100 ml. Imetnik dovoljenja za promet: Merck KGaA, 64271 Darmstadt, Nemčija. Podrobne informacije o zdravilu so objavljene na spletni strani Evropske agencije za zdravila (EMA) <http://www.emea.europa.eu>.

**Dodatne informacije so vam na voljo pri:** Merck, d.o.o., Dunajska cesta 119, 1000 Ljubljana, tel.: 01 560 3810, faks: 01 560 3831, el. pošta: [info@merck.si](mailto:info@merck.si)



# Epufen<sup>TM</sup>

fentanil

Nežen  
dotik skrije  
bolečino

**NOVO**  
MATRIX oblika

#### SKRAJŠAN POVZETEK GLAVNIH ZNAČILNOSTI ZDRAVILA

**Epufen 12,5, 25, 50 in 100 mikrogramov/uro transdermalni obliži** **SESTAVA:** 1 transdermalni obliž vsebuje 2,89 mg, 5,78 mg 11,56 mg ali 23,12 mg fentanila. **TERAPEVTSKE INDIKACIJE:** Huda kronična bolečina, ki se lahko ustrezno zdravi le z opioidnimi analgetiki. **ODMERJANJE IN NAČIN UPORABE:** Odmerjanje je treba individualno prilagoditi ter ga po vsaki uporabi redno oceniti. Izbira začetnega odmerka: velikost odmerka fentanila je odvisna od predhodne uporabe opioidov, kjer se upošteva možnost pojava tolerance, sočasnega zdravljenja, bolnikovega splošnega zdravstvenega stanja in stopnje resnosti obolenja. Pri bolnikih, ki pred tem niso dobivali močnih opioidov, začetni odmerek ne sme preseči 12,5-25 mikrogramov na uro. Zamenjava opioidnega zdravljenja: pri zamenjavi peroralnih ali parenteralnih opioidov s fentanilom je treba začetni odmerek izračunati na osnovi količine analgetika, ki je bila potrebna v zadnjih 24 urah, jo pretvoriti v odgovarjajoči odmerek morfina s pomočjo razpredelnice in nato preračunati ustrezen odmerek fentanila, spet s pomočjo razpredelnice (glejte SmPC). Prvih 12 ur po prehodu na transdermalni obliž Epufen bolnik še vedno dobiva predhodni analgetik v enakem odmerku kot prej; v naslednjih 12 urah se ta analgetik daje po potrebi. Titracija odmerka in vzdrževalno zdravljenje: obliž je treba zamerjati vsakih 72 ur. Odmerek je treba titrirati individualno, dokler ni dosežen analgetični učinek. Odmerek 12,5 mikrogramov/uro je primeren za titriranje odmerka v manjšem odmernem območju. Če analgezija na koncu začetnega obdobja nošenja obliža ni zadostna, se lahko odmerek po 3 dneh zveča. Možno je, da bodo bolniki potrebovali občasne dodatne odmerke kratko delujočih analgetikov (npr. morfina) za prekinitev bolečine. Sprememba ali prekinitev zdravljenja: vsaka zamenjava z drugim opioidom mora potekati postopoma, z majhnim začetnim odmerkom in počasnim zvečevanjem. Splošno veljavno pravilo je postopna ustavitve opioidne analgezije, da bi preprečili odtegnitvene simptome: kot so navzeja, bruhanje, diareja, anksioznost in mišični tremor. Uporaba pri starejših bolnikih: starejše in oslabiljene bolnike je treba skrbno opazovati zaradi simptomov prevelikega odmerjanja ter odmerek po potrebi zmanjšati. Uporaba pri otrocih: transdermalni obliži Epufen se lahko uporabljajo le pri pediatričnih bolnikih (starih od 2 do 16 let), ki tolerirajo opioide in peroralno že dobivajo opioide v odmerku, enakovrednemu najmanj 30 mg morfina na dan. Bolnik mora prvih 12 ur po prehodu na Epufen še vedno dobivati predhodni analgetik v enakem odmerku kot prej. V naslednjih 12 urah je treba ta analgetik dajati odvisno od kliničnih potreb. Titracija odmerka in vzdrževalno zdravljenje: če je analgetični učinek Epufena prešibak, je treba bolniku dodati morfin ali drugi opioid s kratkim delovanjem. Odvisno od dodatnih potreb po analgeziji in jakosti bolečine pri otroku se lahko uporabi več obližev. Odmerek je treba prilagajati korakoma, po 12,5 mikrogramov/uro. Uporaba pri bolnikih z jetno ali ledvično okvaro: Zaradi možnosti pojava simptomov prevelikega odmerjanja je treba te bolnike skrbno spremljati in odmerek ustrezno zmanjšati. Uporaba pri bolnikih s povečano telesno temperaturo: Pri teh bolnikih bo morda treba prilagoditi odmerek. **Način uporabe:** transdermalni obliž Epufen je treba takoj po odprtju vrečke nalepti na nerazdraženo, neobsevano kožo, na ravno površino prsnega koša, zgornjega dela hrbta ali nadlakti. Po odstranitvi zaščitne plasti je treba obliž trdno pritrditi na izbrano mesto in z dlanjlo pritisniti približno 30 sekund, da se obliž popolnoma nalepi, še zlasti na robovih. Uporaba pri otrocih: pri mlajših otrocih je obliž priporočljivo nalepti na zgornji del hrbta, ker je manjša verjetnost, da bi otrok odstrani obliž. Transdermalna obliža se ne sme deliti, ker podatki o tem ni na voljo. **KONTRAINDIKACIJE:** Preobčutljivost za zdravilno učinkovino, hidrogenerano kolonofono, sojo, araršide ali katerokoli pomožno snov. Akutna ali pooperativna bolečina, ko v kratkem časovnem obdobju ni možno titriranje odmerka in obstaja verjetnost za življenjsko ogrožajočo respiratorno depresijo. Huda okvara osrednjega živčnega sistema. Sočasna uporaba MAO ali v obdobju 14 dni po prekinitvi jemanja zaviralcev MAO. **POSEBNA OPOZORILA IN PREVIDNOSTNI UKREPI:** Zaradi razpolovne dobe fentanila je treba bolnika v primeru pojava neželenega učinka opazovati še 24 ur po odstranitvi obliža. Pri nekaterih bolnikih, ki uporabljajo transdermalni obliž Epufen, se lahko pojavi respiratorna depresija. Epufen je treba previdno dajati: bolnikom s kronično pljučno boleznijo, zvišanim intrakranialnim tlakom, možganskim tumorjem, boleznimi srca, jeter in ledvic, tistim z zvišano telesno temperaturo, pri starejših bolnikih in otrocih, bolnikih z miastenijo gravis. Odvisnost od zdravila: kot posledica ponavljajoče se uporabe se lahko razvija toleranca na učinkovino ter psihična in/ali fizična odvisnost od nje. Ostali: lahko se pojavijo neepileptične (mio)klonične reakcije. **MEDSEBOJNO DELOVANJE Z DRUGIMI ZDRAVILI IN DRUGE OBLIKE INTERAKCIJ:** Derivati barbiturne kisline, opiodi, anksiolitiki in pomirjevala, hipnotiki, splošni anestetiki, fenotiazini, mišični relaksanti, sedativni antihistaminiki in alkoholne pijače, zaviralci MAO, itrakonazol, ritonavir, ketokonazol, nekateri makrolidni antibiotiki, pentazon, buprenorfin. **VPLIV NA SPOSOBNOST VOŽNJE IN UPRAVLJANJA S STROJI:** Zdravilo ima močan vpliv na sposobnost vožnje in upravljanja s stroji. **NEŽELENI UČINKI:** Najbolj resen neželen učinek fentanila je respiratorna depresija. Zelo pogosti ( $\geq 1/10$ ): dremavost, glavobol, navzeja, bruhanje, zaprtje, znojenje, srbenje, somnolenca. Pogosti ( $\geq 1/100$  do  $< 1/10$ ): kserostomija, dispepsija, reakcije na koži na mestu aplikacije, sedacija, zmedenost, depresija, tesnoba, živčna napetost, halucinacije, zmanjšan apetit. Občasni ( $\geq 1/1000$  do  $< 1/100$ ): tahikardija, bradikardija, tremor, parastezija, motnje govora, dispneja, hipoventilacija, diareja, zastajanje urina, izpuščaji, rdečina, hipertenzija, hipotenzija, evforija, amnezija, nespečnost, vznemirljivost. Nekateri od naštetih neželenih učinkov so lahko posledica osnovne bolezni ali drugih zdravljenj. Drugi neželeni učinki: odpornost, fizična in psihična odvisnost se lahko razvijeta med dolgotrajno uporabo fentanila. Pri nekaterih bolnikih se lahko pojavijo odtegnitveni simptomi, ko zamenjajo prejšnje opioidne analgetike s transdermalnim obližem s fentanilom ali po nenadni prekinitvi zdravljenja. **NAČIN IZDAJE:** Samo na zdravniški recept. **OPREMA:** Škatle s 5 transdermalnimi obliži. **IMETNIK DOVOLJENJA ZA PROMET:** Lek farmacevtska družba, d.d., Verovškova 57, Ljubljana, Slovenija **INFORMACIJA PRIPRAVLJENA:** november 2007



član skupine Sandoz

[www.lek.si/vademekum](http://www.lek.si/vademekum)

vedno svež vir informacij





## Posodobili smo slovar

### Sestava zdravila: glavnih značilnosti zdravila Arimidex® 1 mg filmsko obložene tablete

**Sestava zdravila:** Ena tableta vsebuje 1 mg anastrozola.

**Indikacije:** Adjuvantno zdravljenje žensk po menopavzi, ki imajo zgodnji invazivni rak dojke s pozitivnimi estrogenskimi receptorji. Adjuvantno zdravljenje zgodnjega raka dojke s pozitivnimi estrogenskimi receptorji pri ženskah po menopavzi, ki so se dve do tri leta adjuvantno zdravile s tamoksifenom. Zdravljenje napredovalega raka dojke pri ženskah po menopavzi. Učinkovitost pri bolnicah z negativnimi estrogenskimi receptorji ni bila dokazana razen pri tistih, ki so imele predhodno pozitiven klinični odgovor na tamoksifen.

**Odmerjanje in način uporabe:** Odrasle (tudi starejše) bolnice: 1 tableta po 1 mg peroralno, enkrat na dan. Odmerka zdravila ni treba prilagajati pri bolnicah z blago ali zmerno ledvično odpovedjo ali blagim jetrnim odpovedovanjem. Pri zgodnjem raku je priporočljivo trajanje zdravljenja 5 let.

**Glavni neželeni učinki:** Zelo pogosti (≥ 10 %): navali vročine, običajno blagi do zmerni. Pogosti (≥ 1 % in < 10 %): astenija, bolečine/okorelost v sklepih, suhost vagine, razredčenje las, izpuščaji, slabost, diareja, glavobol (vsi običajno blagi do zmerni)

**Posebna opozorila in previdnostni ukrepi:** Uporabe Arimidexa ne priporočamo pri otrocih, ker njegova varnost in učinkovitost pri njih še nista raziskani. Menopavzo je potrebno biokemično določiti pri vseh bolnicah, kjer obstaja dvom o hormonskem statusu. Ni podatkov o varni uporabi Arimidexa pri bolnicah z zmerno ali hudo jetrno okvaro ali hujšo ledvično odpovedjo (očistek kreatinina manj kakor 20 ml/min (oziroma 0,33 ml/s)). Pri ženskah z osteoporozo ali pri ženskah s povečanim tveganjem za razvoj osteoporoze je treba določiti njihovo mineralno gostoto kosti z denzitometrijo, na primer s slikanjem DEXA na začetku zdravljenja, pozneje pa v rednih intervalih. Po potrebi je treba začeti z zdravljenjem ali preprečevanjem osteoporoze in to skrbno nadzorovati. Ni podatkov o uporabi anastrozola z analogi LHRRH. Arimidex znižuje nivo estrogena v obtoku, zato lahko povzroči zmanjšanje mineralne kostne gostote. Trenutno ni na voljo ustreznih podatkov o učinku bifosfonatov na izgubo mineralne kostne gostote, povzročene z anastrozolem, ali njihovi koristi, če se uporabijo preventivno. Zdravilo vsebuje laktozo.

**Kontraindikacije:** Arimidex je kontraindiciran pri: ženskah pred menopavzo, nosečnicah in doječih materah, bolnicah s hujšo ledvično odpovedjo (očistek kreatinina manj kot 20 ml/min (oziroma 0,33 ml/s)), bolnicah z zmernim do hudim jetrnim obolenjem, bolnicah, ki imajo znano preobčutljivost za anastrozol ali za katerokoli pomožno snov. Zdravila, ki vsebujejo estrogen, ne smete dajati sočasno z Arimidexom, ker bi se njegovo farmakološko delovanje izničilo. Sočasno zdravljenje s tamoksifenom.

**Medislojno delovanje z drugimi zdravili in druge oblike interakcij:** Klinične raziskave o interakcijah z antipirinom in cimetidinom kažejo, da pri sočasni uporabi Arimidexa in drugih zdravil klinično pomembne interakcije, posredovane s citokromom P450, niso verjetne. Pregled baze podatkov o varnosti v kliničnih preskušanjih pri bolnicah, ki so se zdravile z Arimidexom in sočasno jemale druga pogosto predpisana zdravila, ni pokazal klinično pomembnih interakcij.

**Imetnik dovoljenja za promet:** AstraZeneca UK Limited, 15 Stanhope Gate, London, W1K 1LN, Velika Britanija

Režim predpisovanja zdravila: Rp/Spec  
Datum priprave informacije: april 2007

Pred predpisovanjem, prosimo, preberite celoten povzetek glavnih značilnosti zdravila.

Dodatne informacije in literatura so na voljo pri:  
AstraZeneca UK Limited  
Podružnica v Sloveniji  
Veroškova ulica 55  
1000 Ljubljana

in na spletnih straneh:  
www.arimidex.net  
www.bco.org  
www.breastcancersource.com

### adjuvant [ae'dʒʊv\*nt]

1. adjective pomagljiv, koristen; ~ treatment with **Arimidex**; Adjuvantno zdravljenje žensk po menopavzi, ki imajo zgodnji invazivni rak dojke s pozitivnimi estrogenskimi receptorji.

### advanced [\*dva:nst]

1. adjective napreden; zvišan (cene); to be ~ napredovati; ~ in years visoke starosti; treatment of ~ breast cancer with **Arimidex**; Zdravljenje napredovalega raka dojke pri ženskah po menopavzi. Učinkovitost pri bolnicah z negativnimi estrogenskimi receptorji ni bila dokazana razen pri tistih, ki so imele predhodno pozitiven klinični odgovor na tamoksifen.

### switch [swič]

1. transitive verb udariti, bičati s šibo (z repom); šibati z, hitro mahati z; naglo pograbit; railway ranžirati, zapeljati (usmeriti) (vlak) na drug tir; electrical vključiti, vkllopiti; spremeniti (pogovor), obrniti drugam (tok misli); to ~ back to figuratively (v mislih) vrniti se na; ~ to **Arimidex**; Adjuvantno zdravljenje zgodnjega raka dojke s pozitivnimi estrogenskimi receptorji pri ženskah po menopavzi, ki so se dve do tri leta adjuvantno zdravile s tamoksifenom.

## Temodal 20 mg, 100 mg, 140mg, 180 mg, 250 mg.

**Sestava zdravila:** Vsaka kapsula zdravila Temodal vsebuje 20 mg, 100 mg, 140 mg, 180 mg ali 250 mg temozolomida.

Terapevtske indikacije Temodal kapsule so indicirane za zdravljenje bolnikov z:

- za zdravljenje novo diagnosticiranega glioblastoma multiforme, sočasno z radioterapijo in kasneje kot monoterapija

- malignim gliomom, na primer multiformnim glioblastomom ali anaplastičnim astrocitomom, ki se po standardnem zdravljenju ponovi ali napreduje.

**Odmerjanje in način uporabe** Temodal smejo predpisati le zdravniki, ki imajo izkušnje z zdravljenjem možganskih tumorjev. **Odrasli bolniki z**

**novo diagnosticiranim glioblastomom multiforme** Temodal se uporablja v kombinaciji z žariščno radioterapijo (faza sočasne terapije), temu pa sledi do 6 ciklov monoterapije z temozolomidom. **Faza sočasne terapije** Zdravilo Temodal naj bolnik jemlje peroralno v odmerku 75 mg/m<sup>2</sup> na dan

42 dni, sočasno z žariščno radioterapijo (60 Gy, danih v 30 delnih odmerkih). Odmerka ne boste zmanjševali, vendar se boste vsak teden odločili o

morebitni odložitvi jemanja temozolomida ali njegovi ukinitvi na podlagi kriterijev hematološke in nehematološke toksičnosti. Zdravilo Temodal lahko

bolnik jemlje ves čas 42-dnevnega obdobja sočasne terapije do 49 dni, če so izpolnjeni vsi od naslednjih pogojev: absolutno število nevtrofilcev

≥ 1,5 x 10<sup>9</sup>/l, število trombocitov ≥ 100 x 10<sup>9</sup>/l, skupni kriteriji toksičnosti (SKT) za nehematološko toksičnost ≤ 1. stopnje (z izjemo alopecije,

slabosti in bruhanja). Med zdravljenjem morate pri bolniku enkrat na teden pregledati celotno krvno sliko. **Faza monoterapije** Štiri tedne po

zaključku faze sočasnega zdravljenja z zdravilom Temodal in radioterapijo naj bolnik jemlje zdravilo Temodal do 6 ciklov monoterapije. V 1. ciklu

(monoterapija) je odmerek zdravila 150 mg/m<sup>2</sup> enkrat na dan 5 dni, temu pa naj sledi 23 dni brez terapije. Na začetku 2. cikla odmerek povečajte

na 200 mg/m<sup>2</sup>, če je SKT za nehematološko toksičnost za 1. cikel stopnje ≤ 2 (z izjemo alopecije, slabosti in bruhanja), absolutno število nevtrofilcev

(AŠN) ≥ 1,5 x 10<sup>9</sup>/l in število trombocitov ≥ 100 x 10<sup>9</sup>/l. Če odmerka niste povečali v 2. ciklusu, ga v naslednjih ciklusih ne smete povečevati. Ko

pa odmerek enkrat povečate, naj ostane na ravni 200 mg/m<sup>2</sup> na dan v prvih 5 dneh vsakega naslednjega ciklusa, razen če nastopi toksičnost. Med

zdravljenjem morate pregledati celotno krvno sliko na 22. dan (21 dni po prvem odmerku zdravila Temodal). **Ponavljajoči se ali napredujoči**

**maligni gliom Odrasli bolniki** Posamezen cikel zdravljenja traja 28 dni. Bolniki, ki še niso bili zdravljeni s kemoterapijo, naj jemljejo Temodal

peroralno v odmerku 200 mg/m<sup>2</sup> enkrat na dan prvih 5 dni, temu pa naj sledi 23-dnevni premor (skupaj 28 dni). Pri bolnikih, ki so že bili zdravljeni

s kemoterapijo, je začetni odmerek 150 mg/m<sup>2</sup> enkrat na dan, v drugem ciklusu pa se poveča na 200 mg/m<sup>2</sup> enkrat na dan 5 dni, če ni bilo

hematoloških toksičnih učinkov (glejte poglavje 4.4). **Pediatrični bolniki** Pri bolnikih starih 3 leta ali starejših, posamezen cikel zdravljenja traja 28

dni. Temodal naj jemljejo peroralno v odmerku 200 mg/m<sup>2</sup> enkrat na dan prvih 5 dni, potem pa naj sledi 23-dnevni premor (skupaj 28 dni). Otroci,

ki so že bili zdravljeni s kemoterapijo, naj prejmejo začetni odmerek 150 mg/m<sup>2</sup> enkrat na dan 5 dni, s povečanjem na 200 mg/m<sup>2</sup> enkrat na dan

5 dni v naslednjem ciklusu, če ni bilo hematoloških toksičnih učinkov (glejte poglavje 4.4). **Bolniki z motnjami v delovanju jeter ali ledvic** Pri

bolnikih z blagimi ali zmernimi motnjami v delovanju jeter je farmakokinetika temozolomida podobna kot pri tistih z normalnim delovanjem jeter.

Podatki o uporabi zdravila Temodal pri bolnikih s hudimi motnjami v delovanju jeter (razred III po Child-u) ali motnjami v delovanju ledvic niso na

voljo. Na podlagi farmakokinetičnih lastnosti temozolomida obstaja majhna verjetnost, da bo pri bolnikih s hudimi motnjami v delovanju jeter ali

ledvic potrebno zmanjšanje odmerka zdravila. Kljub temu je potrebna previdnost pri uporabi zdravila Temodal pri teh bolnikih. **Starejši bolniki:**

Analiza farmakokinetike je pokazala, da starost ne vpliva na očistek temozolomida. Kljub temu je potrebna posebna previdnost pri uporabi zdravila

Temodal pri starejših bolnikih. **Način uporabe** Temodal mora bolnik jemati na tešče. Temodal kapsule mora bolnik pogoltniti cele s kozarcem vode

in jih ne sme odpirati ali žvečiti. Predpisani odmerek mora vzeti v obliki najmanjšega možnega števila kapsul. Pred jemanjem zdravila Temodal ali

po njem lahko bolnik vzame antiemetik. Če po zaužitju odmerka bruha, ne sme še isti dan vzeti drugega odmerka. **Kontraindikacije** Temodal je

kontraindiciran pri bolnikih, ki imajo v anamnezi preobčutljivostne reakcije na sestavine zdravila ali na dakarbazin (DTIC). Temodal je kontraindiciran

tudi pri bolnikih s hudo mielosupresijo. Temodal je kontraindiciran pri ženskah, ki so noseče ali dojijo. **Posebna opozorila in previdnostni ukrepi**

Pilotno preskušanje podaljšane 42-dnevne sheme zdravljenja je pokazalo, da imajo bolniki, ki so sočasno prejeli zdravilo Temodal in radioterapijo,

še posebej veliko tveganje za nastanek pljučnice zaradi okužbe s *Pneumocystis carinii* (PCP). Profilaksa proti tovrstni pljučnici je torej potrebna

pri vseh bolnikih, ki sočasno prejemajo zdravilo Temodal in radioterapijo v okviru 42-dnevne sheme zdravljenja (do največ 49 dni), ne glede na število

limfocitov. Če nastopi limfopenija, mora bolnik nadaljevati s profilakso, dokler se limfopenija ne povrne na stopnjo ≤ 1. Antiemetična terapija: Z

jemanjem zdravila Temodal sta zelo pogosto povezana slabost in bruhanje. **Laboratorijske vrednosti:** Pred jemanjem zdravila morata biti izpolnjeni

naslednja pogoja za laboratorijske izvide: ANC mora biti ≥ 1,5 x 10<sup>9</sup>/l in število trombocitov ≥ 100 x 10<sup>9</sup>/l. Na 22. dan (21 dni po prvem

odmerku) ali v roku 48 ur od navedenega dne, morate pregledati celotno krvno sliko in jo nato spremljati vsak teden, dokler ni ANC nad 1,5 x 10<sup>9</sup>/l

in število trombocitov nad 100 x 10<sup>9</sup>/l. Če med katerikoli ciklusom ANC pade na < 1,0 x 10<sup>9</sup>/l ali število trombocitov na < 50 x 10<sup>9</sup>/l, morate

odmerek zdravila v naslednjem ciklusu zmanjšati za eno odmerno stopnjo. Odmerne stopnje so 100 mg/m<sup>2</sup>, 150 mg/m<sup>2</sup> in 200 mg/m<sup>2</sup>. Najmanjši

prilagojeni odmerek je 100 mg/m<sup>2</sup>. **Moški bolniki** Temozolomid lahko deluje genotoksično, zato morate moški, ki se zdravijo z temozolomidom

svetovati, da naj ne zaplodijo otroka še šest mesecev po zdravljenju. **Interakcije** Sočasna uporaba zdravila Temodal in ranitidina ni povzročila

spremembe obsega absorpcije temozolomida ali monometiltriazenoimidazol karboksamida (MTIC). Jemanje zdravila Temodal s hrano je povzročilo

33 % zmanjšanje C<sub>max</sub> in 9 % zmanjšanje površino pod krivuljo (AUC). Ker ne moremo izključiti možnosti, da bi bila sprememba C<sub>max</sub> lahko klinično

pomembna, naj bolniki jemljejo zdravilo Temodal brez hrane. Analiza populacijske farmakokinetike in preskušanjih druge faze je pokazala, da sočasna

uporaba deksametazona, proklorperazina, fenitoina, karbamazepina, ondansetrona, antagonistov receptorjev H<sub>2</sub> ali fenobarbitala ne spremeni

očistka temozolomida. Sočasno jemanje z valprojsko kislino je bilo povezano z majhnim, a statistično značilnim zmanjšanjem očistka temozolomida.

Uporaba zdravila Temodal v kombinaciji z drugimi mielosupresivnimi učinkovinami la hko poveča verjetnost mielosupresije. **Nosečnost** Študij na

nosečih ženskah ni bilo. Predklinične študije na podganah in kuncih z odmerkom 150 mg/m<sup>2</sup> so pokazale teratogenost in/ali toksičnost za plod. Zato

naj noseče ženske načeloma ne bi jemale zdravila Temodal. Če pa je uporaba v času nosečnosti nujna, morate bolnico opozoriti na možne nevarnosti

zdravila za plod. Ženskam v rodni dobi svetujemo, naj med zdravljenjem z zdravilom Temodal preprečijo zanositev. **Dojenje** Ni znano, ali se

temozolomid izloča v materino mleko, zato ženske, ki dojijo ne smejo jemati zdravila Temodal. **Neželeni učinki** V kliničnih preskušanjih so bili

najpogostejši neželeni učinki, povezani z zdravljenjem, prebavne motnje, natančneje slabost (43 %) in bruhanje (36 %). Oba učinka sta bila ponavadi

1. ali 2. stopnje (od 0 do 5 epizod bruhanja v 24 urah) in sta prenehala sama, ali pa ju je bilo mogoče hitro obvladati s standardnim antiemetičnim

zdravljenjem. Incidenca hude slabosti in bruhanja je bila 4 %. Laboratorijski izvidi: Trombocitopenija in. nevtropenija 3. in. 4. stopnje sta se pojavili

pri 19 % in. 17 % bolnikov, zdravljenih zaradi malignega glioma. Zaradi njih je bila potrebna hospitalizacija in/ali prekinitve zdravljenja z zdravilom

Temodal pri 8 % in. 4 % bolnikov. Mielosupresija je bila predvidljiva (ponavadi se je pojavila v prvih nekaj ciklusih in je bila najrazvirnejša med 21. in

28. dnevem), okrevanje pa je bilo hitro, ponavadi v 1 do 2 tednih. Opazili niso nobenih dokazov kumulativne mielosupresije. Trombocitopenija lahko

poveča tveganje za pojav krvavitev, nevtropenija ali levkopenija pa tveganje za okužbe. **Imetnik dovoljenja za promet** SP Europe 73, rue de Stalle

B-1180 Bruxelles Belgija. **Način in režim izdaje** Zdravilo se izdaja samo na recept, uporablja pa se pod posebnim nadzorom zdravnika specialista

ali od njega pooblaščenega zdravnika. **Datum priprave informacije** oktober 2007.

Dunajska 22, 1000 Ljubljana  
tel: 01 300 10 70  
fax: 01 300 10 80

 Schering-Plough

**Temodal**®  
temozolomid



# Resnični napredek

Pri na novo odkritem glioblastomu multiforme in malignih gliomih, ki se ponovijo ali napredujejo.



## Poenostavljeno zdravljenje

Z dvema novima jakostima  
**140 mg in 180 mg Temodal**

- Možnost prejemanja manjšega števila kapsul
- Boljša sprejemljivost in sodelovanje bolnika
- Natančno odmerjanje
- Barvne kapsule za enostavnejšo dnevno uporabo



Dunajska 22, 1000 Ljubljana  
tel: 01 300 10 70  
fax: 01 300 10 80

 Schering-Plough

**Temodal**<sup>®</sup>   
temozolomid



# Že desetletje prinašamo rešitve v Vaš laboratorij!

Za področja:

- bioznanosti **SYNGENE, INVITROGEN:**  
**DYNAL, ZYMED, MOLECULAR PROBES, CALTAG**
- diagnostike **MINERVA, MEDAC, BIOTEK**
- gojenja celičnih kultur **INVITROGEN-GIBCO,**  
**TPP, GREINER in SANYO**
- merjenja absorbance, fluorescence in luminiscence **BIOTEK**
- pipetiranja **BIOHIT in BIOTEK**
- laboratorijske opreme **SANYO**
- čiste vode za laboratorije **ELGA LABWATER**
- HPLC in GC kolon, vial in filtrov **PHENOMENEX in**  
**CHROMACOL/NATIONAL SCIENTIFIC**

**KEMOMED**  
*Prinašamo  
rešitve*

A therapeutic advance in second-line  
NSCLC and first-line pancreatic cancer

Prolongs your patients life<sup>1,2</sup>



Tarceva is indicated for:

- Treatment of patients with locally advanced or metastatic non-small cell lung cancer after failure of at least one prior chemotherapy regimen.
- Tarceva in combination with gemcitabine is indicated for the treatment of patients with metastatic pancreatic cancer.

For additional information please consult your local Roche office.

References:

1. Shepherd FA, Rodrigues Pereira J, Ciuleanu T et al. Erlotinib in previously treated non-small-cell lung cancer. *N Engl J Med*. 2005 Jul 14;353(2):123-32.
2. Moore MJ, Goldstein D, Hamm J et al. Erlotinib plus gemcitabine compared with gemcitabine alone in patients with advanced pancreatic cancer: a phase III trial of the National Cancer Institute of Canada Clinical Trials Group. *J Clin Oncol*. 2007 May 20;25(15):1960-6.

 **Tarceva**<sup>®</sup>  
erlotinib HCl



Roche farmacevtska družba d.o.o.  
Vodovodna cesta 109  
1000 Ljubljana  
[www.roche.si](http://www.roche.si)

**NOVO**

# NAVELBINE®

vinorelbin

Koncentrat za raztopino za infundiranje 10 mg/ml, 50 mg/5ml

Novost za zdravljenje: nedrobnoceličnega raka pljuč in napredovelega raka dojke



Izkušnje z  
več kot  
1 mio bolnikov  
po svetu

*Zdravljenje po meri bolnika!*

- Odlična učinkovitost v kombinaciji s cisplatinom ali kot monoterapija za bolnike, ki niso primerni za polikemoterapijo
- Dobra prenosljivost:
  - blaga alopecija
  - zelo nizka stopnja emetogenosti (< 10 %)
  - ni kardiotsičnosti
  - ni nevrotoksičnosti
- Premedikacija ni potrebna
- Sinergistično delovanje s tarčnim zdravilom trastuzumab

Pred predpisovanjem zdravila Navelbine® preberite povzetek temeljnih značilnosti, ki ga dobite pri naših strokovnih sodelavcih.



Pierre Fabre  
Médicament



M E D I S | [www.medis.si](http://www.medis.si) | [onkologija@medis.si](mailto:onkologija@medis.si)

## Editorial policy

**Editorial policy** of the journal *Radiology and Oncology* is to publish original scientific papers, professional papers, review articles, case reports and varia (editorials, reviews, short communications, professional information, book reviews, letters, etc.) pertinent to diagnostic and interventional radiology, computerized tomography, magnetic resonance, ultrasound, nuclear medicine, radiotherapy, clinical and experimental oncology, radiobiology, radiophysics and radiation protection. The Editorial Board requires that the paper has not been published or submitted for publication elsewhere: the authors are responsible for all statements in their papers. Accepted articles become the property of the journal and therefore cannot be published elsewhere without written permission from the editorial board. Papers concerning the work on humans, must comply with the principles of the declaration of Helsinki (1964). The approval of the ethical committee must then be stated on the manuscript. Papers with questionable justification will be rejected.

**Manuscript** written in English should be submitted to the Editorial Office in triplicate (the original and two copies), including the illustrations: *Radiology and Oncology*, Institute of Oncology, Zaloska 2, SI-1000 Ljubljana, Slovenia; (Phone: +386 (0)1 5879 369, Tel./Fax: +386 (0)1 5879 434, E-mail: gsera@onko-i.si). Authors are also asked to submit their manuscripts electronically, either by E-mail or on CD rom. The type of computer and word-processing package should be specified (Word for Windows is preferred).

All articles are subjected to editorial review and review by independent referee

selected by the editorial board. Manuscripts which do not comply with the technical requirements stated herein will be returned to the authors for correction before peer-review. Rejected manuscripts are generally returned to authors, however, the journal cannot be held responsible for their loss. The editorial board reserves the right to ask authors to make appropriate changes in the contents as well as grammatical and stylistic corrections when necessary. The expenses of additional editorial work and requests for reprints will be charged to the authors.

**General instructions** • Radiology and Oncology will consider manuscripts prepared according to the Vancouver Agreement (*N Engl J Med* 1991; **324**: 424-8, *BMJ* 1991; **302**: 6772; *JAMA* 1997; **277**: 927-34.). Type the manuscript double spaced on one side with a 4 cm margin at the top and left hand side of the sheet. Write the paper in grammatically and stylistically correct language. Avoid abbreviations unless previously explained. The technical data should conform to the SI system. The manuscript, including the references may not exceed 20 typewritten pages, and the number of figures and tables is limited to 8. If appropriate, organize the text so that it includes: Introduction, Material and methods, Results and Discussion. Exceptionally, the results and discussion can be combined in a single section. Start each section on a new page, and number each page consecutively with Arabic numerals.

*Title page* should include a concise and informative title, followed by the full name(s) of the author(s); the institutional affiliation of each author; the name and address of the corresponding author (includ-

ing telephone, fax and e-mail), and an abbreviated title. This should be followed by the *abstract page*, summarising in less than 200 words the reasons for the study, experimental approach, the major findings (with specific data if possible), and the principal conclusions, and providing 3-6 key words for indexing purposes. The text of the report should then proceed as follows:

*Introduction* should state the purpose of the article and summarize the rationale for the study or observation, citing only the essential references and stating the aim of the study.

*Material and methods* should provide enough information to enable experiments to be repeated. New methods should be described in detail. Reports on human and animal subjects should include a statement that ethical approval of the study was obtained.

*Results* should be presented clearly and concisely without repeating the data in the tables and figures. Emphasis should be on clear and precise presentation of results and their significance in relation to the aim of the investigation.

*Discussion* should explain the results rather than simply repeating them and interpret their significance and draw conclusions. It should review the results of the study in the light of previously published work.

**Illustrations and tables** must be numbered and referred to in the text, with appropriate location indicated in the text margin. Illustrations must be labelled on the back with the author's name, figure number and orientation, and should be accompanied by a descriptive legend on a separate page. Line drawings should be supplied in a form suitable for high-quality reproduction. Photographs should be glossy prints of high quality with as much

contrast as the subject allows. They should be cropped as close as possible to the area of interest. In photographs mask the identities of the patients. Tables should be typed double spaced, with descriptive title and, if appropriate, units of numerical measurements included in column heading.

**References** must be numbered in the order in which they appear in the text and their corresponding numbers quoted in the text. Authors are responsible for the accuracy of their references. References to the Abstracts and Letters to the Editor must be identified as such. Citation of papers in preparation, or submitted for publication, unpublished observations, and personal communications should not be included in the reference list. If essential, such material may be incorporated in the appropriate place in the text. References follow the style of Index Medicus. All authors should be listed when their number does not exceed six; when there are seven or more authors, the first six listed are followed by "et al". The following are some examples of references from articles, books and book chapters:

Dent RAG, Cole P. *In vitro* maturation of monocytes in squamous carcinoma of the lung. *Br J Cancer* 1981; **43**: 486-95.

Chapman S, Nakielny R. *A guide to radiological procedures*. London: Bailliere Tindall; 1986.

Evans R, Alexander P. Mechanisms of extracellular killing of nucleated mammalian cells by macrophages. In: Nelson DS, editor. *Immunobiology of macrophage*. New York: Academic Press; 1976. p. 45-74.

**Page proofs** will be faxed or sent by E-mail to the corresponding author. It is their responsibility to check the proofs carefully and fax a list of essential corrections to the editorial office within 48 hours of receipt. If corrections are not received by the stated deadline, proof-reading will be carried out by the editors.



